

# Studies on the Role of Entanglement in Mixed-state Quantum Computation

by

**Animesh Datta**

B.Tech., Electrical Engineering (Minor in Physics),  
Indian Institute of Technology, Kanpur 2003

DISSERTATION

Submitted in Partial Fulfillment of the  
Requirements for the Degree of

Doctor of Philosophy  
Physics

The University of New Mexico

Albuquerque, New Mexico

August, 2008



# Dedication

*To Maa, for everything.*



# Acknowledgments

The most significant character in any doctoral career is that of the advisor. Carl Caves, my advisor, has been more. Working with and under him has been a brilliant and fascinating experience. His strategy of offering ample freedom in choosing problems and the pace of solving them, and collaborating on them has been his single greatest contribution to my research. Encouraging one-liners like ‘The truth shall set you free’ when I’ve gotten negative results and confidence boosters like ‘A lot of people say a lot of things’ have been priceless; so has been his dictum of writing papers with meticulous precision. His ability to guide and advise has been phenomenal and a source of constant inspiration.

The contribution of the other members of the Information Physics group have been no less. Both Ivan Deutsch and Andrew Landahl have always been enthusiastic and encouraging of my research, asking penetrating question in group meeting presentations and discussing such topics on the outside. I also thank them for being on my dissertation committee. Ivan is also to be thanked for teaching fabulous courses on quantum optics and atomic physics. I’m infinitely thankful to Anil Shaji for being my surrogate advisor, with whom I have discussed almost all my projects, and he’s always been there to put me right and prevented me from going awry so often. Other members of the group with whom I’ve collaborated have taught me a lot as well. Steve Flammia, with his random math problems and refusal ever to be frightened by formidable mathematics has been a motivating experience. Discussions with Sergio Boixo have also been fruitful.

Other student members of the group have been no less important. Seth has always been there to chat about a nagging physics, math or programming problem. I also thank Matt, Collin, Aaron, Pat, Kiran, Drew, Rene, Sohini, Brian, Carlos, Heather, Brigitte and Alex Tacla. Bryan Eastin and Iris have been crucial for the random chats, on physics and often, otherwise.

My research has benefited a lot from external collaborations and academic visits. For these, I must thank Howard Barnum, who made it possible for me to visit Los

Alamos National Laboratory for a summer and inspired me to think that no result was useless in research and Michael Nielsen who sponsored a visit to the University of Queensland. Once there, discussions with Guifre Vidal, Michael Nielsen, Andrew Doherty, Mark DeBurgh, Nick Menicucci, Sukhwinder Singh and others germinated ideas that have shaped my research. Chats with W. H. Zurek, Lorenza Viola, Rolando Somma and Leonid Gurvits from LANL, Kavan Modi and Caesar Rodriguez from UT, Austin and Alex Monras and Emilio Bagan from Barcelona, Robert Raussendorf, Sev, Caterina and Tzu at Waterloo have also been enlightening.

I am most indebted to Prof. K. R. Parthasarathy with whom I first discussed quantum computation and Prof. P. Ghose with whom I did my first research in quantum mechanics. Both are to be thanked for the immense patience they showed towards me.

At UNM, wonderful courses by Sudhakar Prasad on E&M, Colston Chandler on scattering theory, Paul Parris on non-equilibrium statistical mechanics and Cris Moore on quantum algorithms have been very valuable. Discussions on the nature and fate of life with Denis Seletskiy, Mark Mero, Dave McInnis, Doug Bradshaw and Birk have kept me going, as has the assistance of Mary DeWitt, Roxanne Littlefield, Jennie Peer, Alisa Gibson, Russ and last but not the least, the Mountain Dew vending machine.

Beyond that, infinite thanks are due to Mukesh for always cooking dinner, and Navin for eating it, and Mohit, Arnab, Shailesh, Brittany, Hari and Naresh bhai, Tom, Lisa, Riti, Deepti and Divya for wasting time with me.

From still farther beyond, from India, I'm indebted to my mother for her prolonged faith and support and Bubun for her love. Lastly, thanks beyond words for the love, support and patience of my Priceless, beloved Baby, without whom a lot of this would have lost its meaning.

# Studies on the Role of Entanglement in Mixed-state Quantum Computation

by

**Animesh Datta**

ABSTRACT OF DISSERTATION

Submitted in Partial Fulfillment of the  
Requirements for the Degree of

Doctor of Philosophy  
Physics

The University of New Mexico

Albuquerque, New Mexico

August, 2008

# Studies on the Role of Entanglement in Mixed-state Quantum Computation

by

**Animesh Datta**

B.Tech., Electrical Engineering (Minor in Physics),  
Indian Institute of Technology, Kanpur 2003

Ph.D., Physics, University of New Mexico, 2018

## Abstract

In this thesis, I look at the role of quantum entanglement in mixed-state quantum computation. The model we consider is the DQC1 or ‘power of one qubit’ model. I show that there is minimal bipartite entanglement in a typical instance of the DQC1 circuit and even put an upper bound on the possible amount of entanglement. The upper bound does not scale with the size of the system, making it hard to attribute the exponential speedup in the DQC1 model to quantum entanglement. On the other hand, this limited amount of entanglement does not imply that the system is classically simulatable. This goes against the dictum that quantum evolutions involving states with limited amounts of entanglement can be simulated efficiently classically. A matrix product state (MPS) algorithm for a typical instance of the DQC1 system requires exponential classical resources. This exposes a gap between the amount of entanglement and the amount of purely nonclassical correlations in a quantum system.



This gap, I suggest, can be filled by quantum discord. An entropic measure of quantumness that tries to capture the quantum notion of a system being disturbed by a measurement, it is a true measure of purely nonclassical correlations. I calculate it in a typical instance of the DQC1 circuit and find that the amount of discord is a constant fraction of the maximum possible discord for a system of that size. This allows an interpretation of quantum discord as the resource that drives mixed-state quantum computation. I also study quantum discord as a quantity of independent interest. Its role in the phenomenon of entanglement distribution is studied through an easily comprehensible example.

This thesis also contains discussions on the relation between the complexity classes P, BQP and DQC1. Additional material is presented on the connections between the DQC1 model, Jones polynomials and statistical mechanics. The thesis concludes with a discussion of a few open problems related to the DQC1 model, the quantum discord and their scope in quantum information science.

# Contents

List of Figures	<b>xiii</b>
<b>1 Introduction</b>	<b>1</b>
1.1 List of Publications . . . . .	11
<b>2 Background</b>	<b>14</b>
2.1 Entanglement: Properties of negativity . . . . .	19
2.2 Beyond Entanglement: Quantum Discord . . . . .	22
2.2.1 Properties of Quantum Discord . . . . .	26
2.2.2 Discord for separable states . . . . .	39
2.3 Quantum discord in quantum communication . . . . .	41
<b>3 Entanglement in the DQC1 model</b>	<b>46</b>
3.1 Classical evaluation of the trace . . . . .	51
3.2 Entanglement in the DQC1 circuit . . . . .	55
3.3 The average negativity of a random unitary . . . . .	60

3.4	Bounds on the negativity . . . . .	63
3.4.1	The $s = 1, 2$ Bound . . . . .	67
3.4.2	The $s = 1, 2, 3$ Bound . . . . .	69
3.5	Conclusion . . . . .	73
<b>4</b>	<b>Classical simulation of quantum computation</b>	<b>75</b>
4.1	Tree Tensor Networks (TTN) . . . . .	78
4.2	DQC1 and Tree Tensor Networks (TTN) . . . . .	79
4.3	Exponential growth of Schmidt ranks . . . . .	80
4.4	A formal proof for the Haar-distributed case . . . . .	82
4.5	Conclusions . . . . .	88
<b>5</b>	<b>Quantum discord in the DQC1 model</b>	<b>89</b>
<b>6</b>	<b>Conclusion</b>	<b>96</b>
<b>A</b>	<b>DQC1 and Knot Theory</b>	<b>103</b>
A.1	Quadratically Signed Weight Enumerators . . . . .	103
A.2	Jones Polynomials . . . . .	105
<b>B</b>	<b>Proof of the Lemma</b>	<b>106</b>
<b>C</b>	<b>Negativity of a random pure state</b>	<b>107</b>
	<b>References</b>	<b>112</b>

# List of Figures

1.1	The ‘power of one qubit’ model . . . . .	3
1.2	DQC1 amongst physics, mathematics and computer science . . . . .	10
2.1	Polynomial hierarchy with P, BQP and DQC1 . . . . .	18
2.2	Quantum discord in a $2 \times 4$ bound entangled state . . . . .	36
3.1	The DQC1 circuit . . . . .	46
3.2	The DQC1 circuit with arbitrary polarization . . . . .	47
3.3	Structure of the unitary $U_4$ . . . . .	57
3.4	Mean of the negativity in a DQC1 circuit . . . . .	62
3.5	Variance in the negativity in a DQC1 circuit . . . . .	63
3.6	Mean negativity across different splits in a 9 qubit DQC1 circuit . . . . .	64
3.7	Various bounds on the negativity of the DQC1 circuit . . . . .	66
4.1	Schmidt rank of the DQC1 state for any equipartition . . . . .	82
5.1	Discord in the DQC1 circuit . . . . .	94

C.1 Negativity of random pure states . . . . . 111

# Chapter 1

## Introduction

*All great deeds, and all great thoughts have a ridiculous beginning. Great works are often born on a street corner or in a restaurant's revolving door.*

- Albert Camus

The field of quantum information science is largely propelled by the discovery of quantum algorithms that promise unprecedented advantages over the best known classical algorithms. The algorithms of Shor, Grover and others are of more than just academic interest. They possess the potential of affecting our way of life in the information age. It is thus of economic, industrial, in addition to scientific interest to comprehend the physical principles these algorithms operate upon. These novel algorithms harness the intrinsic structure of quantum mechanics, believed to be the fundamental law of nature. Yet, by itself, this is not enough to completely unravel the mysteries of quantum computation. Part of this stems from the intrinsic mystery of quantum mechanics as a physical theory and its counterintuitive predictions when compared to daily life classical mechanics. For the remainder, there are at present certain gaps in our understanding of the working of quantum algorithms. It is some

of these gaps that we look at in this dissertation and attempt to plug.

The ultimate aim of quantum information science is to build a functioning quantum computer. There have been spectacular advances in that direction. Multiple successful implementations of pure state algorithms in laboratories across the world have occurred. However, most of these schemes are limited by their lack of scalability. This is not entirely due to a lack of experimental capabilities. Quantum systems are intrinsically hard to isolate from their environment and manipulate. As the system gets bigger, the challenges mount. The higher the number of degrees of freedom, the higher the number of ways it can couple to the environment. Thus, if we are to build a functioning quantum computer, we must learn to operate with mixed states, the natural outcome of environmental decoherence. This has generically been tackled by quantum error correction, which aims at keeping quantum states as pure as possible through their quantum evolution. It was the notion of quantum error correction that first made the dream of a quantum computer realistic. Excellent techniques have since been devised to tackle an array of errors that might possibly plague a quantum computation, and this continues to be an active area of contemporary research. One needs to ensure that the error correcting part of the system is itself error-free, and most techniques of effective quantum error correction eventually rely on concatenation of several layers of error correction. The success of this scheme usually requisites the need to reduce errors below a threshold by successive layers of error correction, that is, fault tolerance for all operations. Though not entirely sisyphian<sup>1</sup>, it is undeniable that the exercise of quantum computation aggregated with error correction makes the whole endeavor more challenging.

A different approach would envisage a quantum computer using mixed states themselves. Their robustness against environmental decoherence and the reduction of some of the complications of quantum error correction is a worthy enough motiva-

---

<sup>1</sup>Sisyphus, of Greek mythology, was punished by being cursed to roll a large boulder up a hill, only to watch it roll down again, and to repeat this throughout eternity. The same character lends his name to the Sisyphus method of laser cooling of atoms.

tion. Additionally, one might be interested in the computational potential of mixed quantum states by themselves. This is where the gaps in our theoretical understanding about quantum algorithms arrests our progress. Though some attempts have been made, most of which rely on distilling pure states out of them, e.g., magic state distillation [10], mixed-state quantum computation by itself is particularly poorly understood. In this thesis, our endeavor will be to address this situation.

In 1998, E. Knill and R. Laflamme presented the first intrinsically mixed-state scheme of quantum computation [55]. It was dubbed the ‘power of one qubit’ or DQC1 (deterministic quantum computation with one pure qubit) model, as it required only one pure qubit for its operation. The setup for this scheme is as follows: The top qubit is first acted upon by a Hadamard gate, given by

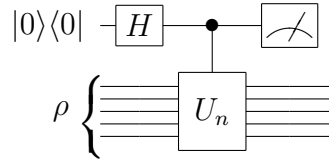


Figure 1.1: The DQC1 circuit

$$H = \frac{1}{\sqrt{2}} \begin{pmatrix} 1 & 1 \\ 1 & -1 \end{pmatrix},$$

which effects the transformations

$$|0\rangle \xrightarrow{H} \frac{|0\rangle + |1\rangle}{\sqrt{2}} \quad \text{and} \quad |1\rangle \xrightarrow{H} \frac{|0\rangle - |1\rangle}{\sqrt{2}}.$$

The state of the system before the controlled unitary is

$$\frac{1}{2} (|0\rangle\langle 0| + |0\rangle\langle 1| + |1\rangle\langle 0| + |1\rangle\langle 1|) \otimes \rho.$$

Next the controlled gate means that the unitary  $U_n$  acts on the lower set of  $n$  qubits in the state  $\rho$  if and only if the top (control) qubit is in the state  $|1\rangle$ . Otherwise it does not and  $I_n$  is applied. After this gate, the state of the system is

$$\Xi = \frac{1}{2} (|0\rangle\langle 0| \otimes \rho + |0\rangle\langle 1| \otimes \rho U_n^\dagger + |1\rangle\langle 0| \otimes U_n \rho + |1\rangle\langle 1| \otimes U_n \rho U_n^\dagger).$$



This is the final state of the system and can compactly be written as

$$\Xi = \frac{1}{2} \begin{pmatrix} \rho & \rho U_n^\dagger \\ U_n \rho & U_n \rho U_n^\dagger \end{pmatrix}.$$

Suppose now that we make a measurement of the top qubit in the  $X$  basis,  $X$  being the Pauli operator

$$X = \begin{pmatrix} 0 & 1 \\ 1 & 0 \end{pmatrix}.$$

We leave the  $n$  lower qubits untouched. The expectation of this measurement is given, quite simply, by

$$\langle X \rangle_\Xi = \text{tr}[(X \otimes I_n)\Xi] = \text{tr} \left[ \rho \left( \frac{U_n + U_n^\dagger}{2} \right) \right] = \text{Re}[\text{tr}(\rho U_n)].$$

A measurement in the  $Y$  basis similarly gives an expectation value of  $\text{Im}[\text{tr}(\rho U_n)]$ . This is, in effect, the DQC1 model of quantum computation.

Suppose now that we prepared  $\rho$  in a pure state  $\rho = |\Phi\rangle\langle\Phi|$  that was an eigenstate of  $U_n$  such that  $U_n |\Phi\rangle = e^{i\phi} |\Phi\rangle$ . Then

$$\langle X \rangle_\Xi = \cos \phi.$$

Then  $L$  measurements of the top qubit in the  $X$  basis would provide us with an estimate of  $\phi$ , via  $\cos \phi$  to within an accuracy of  $1/\sqrt{L}$ . This is, in effect, the phase estimation algorithm so commonly used in quantum algorithms. If, on the other hand,  $\rho = I_n/2^n$ , the completely mixed state, then  $L$  measurements will give us with an accuracy of  $1/\sqrt{L}$ , the quantity

$$\langle X \rangle_\Xi = \text{Re}[\text{tr}(U_n)]/2^n.$$

This is the real part of a quantity called the normalized trace of the unitary matrix  $U_n$ , and the scheme gives us an estimate for it with a fixed accuracy in a number of trials that does not scale with the size of the unitary matrix. Calculation of fidelity decay in quantum chaos, the evaluation of expectation values in condensed

matter physics and as shown very recently, even problems in quantum metrology, quadratically signed weight enumerators and estimation of Jones polynomials from knot theory and discrete quantum field theories can be reduced to the evaluation of normalized traces of particular unitary matrices.

As unitaries conserve the purity of a state,  $\text{tr}(\Xi^2) = \text{tr}(\rho^2)$ . For  $\rho = I_n/2^n$ , the states involved in the DQC1 model are thus very closed to being maximally mixed. Notwithstanding, this algorithm provides an exponential speedup over the best known classical algorithm. This shows that to harvest the benefits of exponential speedups in quantum computation, one does not necessarily need to work with pure states. To be able to harness this quantum advantage optimally in the face of a decoherent environment, one needs to understand the very simple DQC1 model better. Thus, the simple question I address in this thesis is the following- *Why does the DQC1 model work?* This, I will attempt to answer in the subsequent chapters and as we will see, the answer is not simple.

Quantum entanglement is the currency within the world of quantum information science. Over the last decade, it has come to be believed that entanglement is the resource that facilitates quantum advantages and speedups. This is based on evidence and knowledge that has been accrued since the early days of quantum information in the mid 1990's [48]. For instance, simulations have been done that study the rise and fall in the amount of entanglement in quantum evolutions that implement Shor's algorithm. The step having the maximum amount of entanglement is the so called 'quantum Fourier transform', which has come to be believed as the quantum soul of the whole algorithm. Quantum Fourier transform is a period finding technique, just like the conventional Fourier transform. The novelty, due to Shor, was to apply it over the field of integers, to find the period of the modular exponentiation function, to which integer factorization and discrete logarithm evaluation can be reduced [26]. Grover's search algorithm has also been studied from an entanglement perspective. It has been found that the quadratic speedup in the algorithm is directly related to

the flow of entanglement in the algorithm.

Preceding this line of work on quantum algorithms is the concept of quantum teleportation [62]. Quantum teleportation is the ability to transfer the quantum state of a system from one point in space to another by just classical communication and a quantum resource. In its simplest incarnation, a state of the form  $|\Psi\rangle = \alpha|0\rangle + \beta|1\rangle$  can be teleported from Alice to Bob by sending just two bits of classical information *if* they already share a maximally entangled Bell state, say,  $\frac{1}{\sqrt{2}}(|00\rangle + |11\rangle)$ . Note that  $|\Psi\rangle$  is completely denoted by three real parameters. This saving in the communication cost stems from the inherent power of quantum mechanics. It is this power that the field of quantum information science strives to harness for problems more realistic than teleportation. Motivated by this, measures of entanglement are often defined in terms of the number of Bell states that are needed to produce or can be extracted from a certain state by local operations and classical communications. In 2005, it was shown by Masanes that all entangled states (including bound entangled) can enhance the teleporting power of some quantum state [61].

Ever since the work on quantum teleportation, which is a genuinely quantum phenomenon, the research in quantum information science has been largely dominated by quantum entanglement. Evidence for this fact is the profuseness of papers beginning with the sentence – “Entanglement is a useful resource for quantum information and computation.” Tragically, this realization does not advance much the cause of quantum information science. An instance inspiring such an opinion is the existence of quantum systems in highly entangled states that are computationally no more powerful than classical ones. Such a class of states are the so-called stabilizer states. Though highly entangled, their dynamics can be efficiently simulated classically. The twist in the story, is however, a result by Jozsa and Linden [52] which shows that for any pure-state quantum computation to be exponentially faster than its classical counterpart, the extent of entanglement in the system must not be bounded by the system size.

It is in the light of these circumstances that I analyze the DQC1 model in Chapter 3. The findings are intriguing. I found the first example of a unitary matrix for which the DQC1 circuit showed a non-zero amount of entanglement. I then generalized this to create a family of unitaries which had the same behavior in terms of the entanglement content of the DQC1 state. In collaboration, I then looked for the presence of bipartite entanglement in typical instances of the DQC1 circuit. However, the amount of entanglement was small, in that the ratio of entanglement present to that maximally possible goes to zero in the limit of larger and larger systems. Since exponential speedups are determined asymptotically in the limit of large problem size, these results suggest that bipartite entanglement cannot be the reason behind the success of DQC1. I was also able to provide analytical upper bounds on the amount of entanglement (as measured by the negativity). This bound does not scale with size of the problem, and is the most crucial detriment in attributing the exponential speedup in the DQC1 model to entanglement. In the course of my studies into the entanglement of the DQC1 model, I was never able to find a unitary matrix which showed non-trivial negativity for  $\alpha$  (polarization of the top qubit) less than 0.5. This presents a problem of the most singular nature. For  $\alpha \leq 0.5$  the DQC1 state is at best bound entangled. The computational efficiency of the model, however, has no discontinuity at this value. If entanglement were behind the exponential speedup in the DQC1 model, it would imply that this particular entanglement cannot be exploited for any other task (as it is bound and therefore cannot be distilled to form Bell states). This certainly would be the most peculiar state of affairs !!

Another facet of the result by Jozsa and Linden is that quantum systems with small amounts of entanglement can be simulated classically. This is one of the reasons for believing entanglement to be a resource in the first place. This provided me with the impetus to study the classical simulatability of the DQC1 model. As presented in Chapter 4, I found that Matrix Product State (MPS) algorithms are incapable of simulating typical instances of the DQC1 system efficiently in spite of its having

a limited amount of entanglement. The degree of correlations, as measured by the rank of the operator Schmidt decomposition, scaled exponentially with the size of the system. This I first showed by numerical simulation. Then, in collaboration with Guifre Vidal, I was able to provide an analytical proof that the operator Schmidt rank did indeed scale exponentially with the problem size. MPS techniques are the most commonly used for simulating quantum systems with limited amounts of entanglement. My results, therefore, exclude a large family of algorithms from simulating the DQC1 model. Simultaneously, it shows the claim made at the beginning of this paragraph to be invalid in the case of mixed quantum systems.

The results of Chapters 3 and 4 leave us with a very uneasy realization. A typical instance of the DQC1 model has very little entanglement, and yet it cannot be simulated classically. The natural conclusion is that there must be more to quantum computation than just entanglement. This is the scenario I investigate in Chapter 5. I suggest that quantum discord<sup>2</sup>, a notion of quantum correlations more general than entanglement, is possibly that missing element which captures the power of a quantum computation completely. In particular, I show that across the most important split in the DQC1 circuit, which is shown to be separable in Chapter 3, there is a non-zero amount of discord. The analytic calculations done by me were for the set of random Haar-distributed unitaries. This set is, however, not efficiently implementable in terms of any gate set universal for quantum computation, but sets of pseudo-random unitaries exist which are efficiently implementable and have eigenvalue statistics that mimic that of the Haar-distributed unitaries. I used these for numerical confirmation of my analytic results. Finally, the ratio of this discord to the maximum possible does not vanish in the limit of large systems. Thus I present quantum discord as the potential resource behind quantum advantages in computation.

Quantum discord turns out to be an interesting and useful quantity in its own

---

<sup>2</sup>This quantity [63, 44] was brought to my attention by Anil Shaji.

right, with applications wider than just to mixed state quantum computation. I have preliminary evidence that it plays a role in quantum communication, too, at least in the phenomenon of distributing entanglement. The details of this inference and the role of discord in entanglement distribution is presented in Section 2.3.

In addition to studying the underpinnings of the DQC1 model, I have studied an interesting connection between the DQC1 model and knot theory. The DQC1 model is equivalent to approximately evaluating the Jones polynomial of the trace closure of a braid. Rather, this problem is actually complete for the complexity class DQC1. The problem of approximately evaluating the Jones polynomial of the *plat* closure of a braid is BQP-complete. It is believed that the class DQC1 actually lies in territory betwixt P and BQP, as shown in Fig 2.1. Since evaluation of the Jones polynomial is equivalent to evaluating the partition function of certain spin models like the Ising model, and different kind of braid closures correspond to different boundary conditions, this problem shows us a path for understanding the relations between complexity classes through physical models and theories like statistical mechanics. Thus, studying the DQC1 model and its correspondence to Jones polynomials promises to be a very fruitful one, and I discuss this in a little more detail in Appendix A.2.

The above explorations by no means exhaust the class of problems a mixed-state quantum computer or the DQC1 model can solve (See Fig 1.2 for some additional possibilities). One of the more exotic applications is through the quadratically signed weight enumerators (QSWEs). We will mention this as well in brief in Appendix A.1 and not go into any details of it in this thesis.

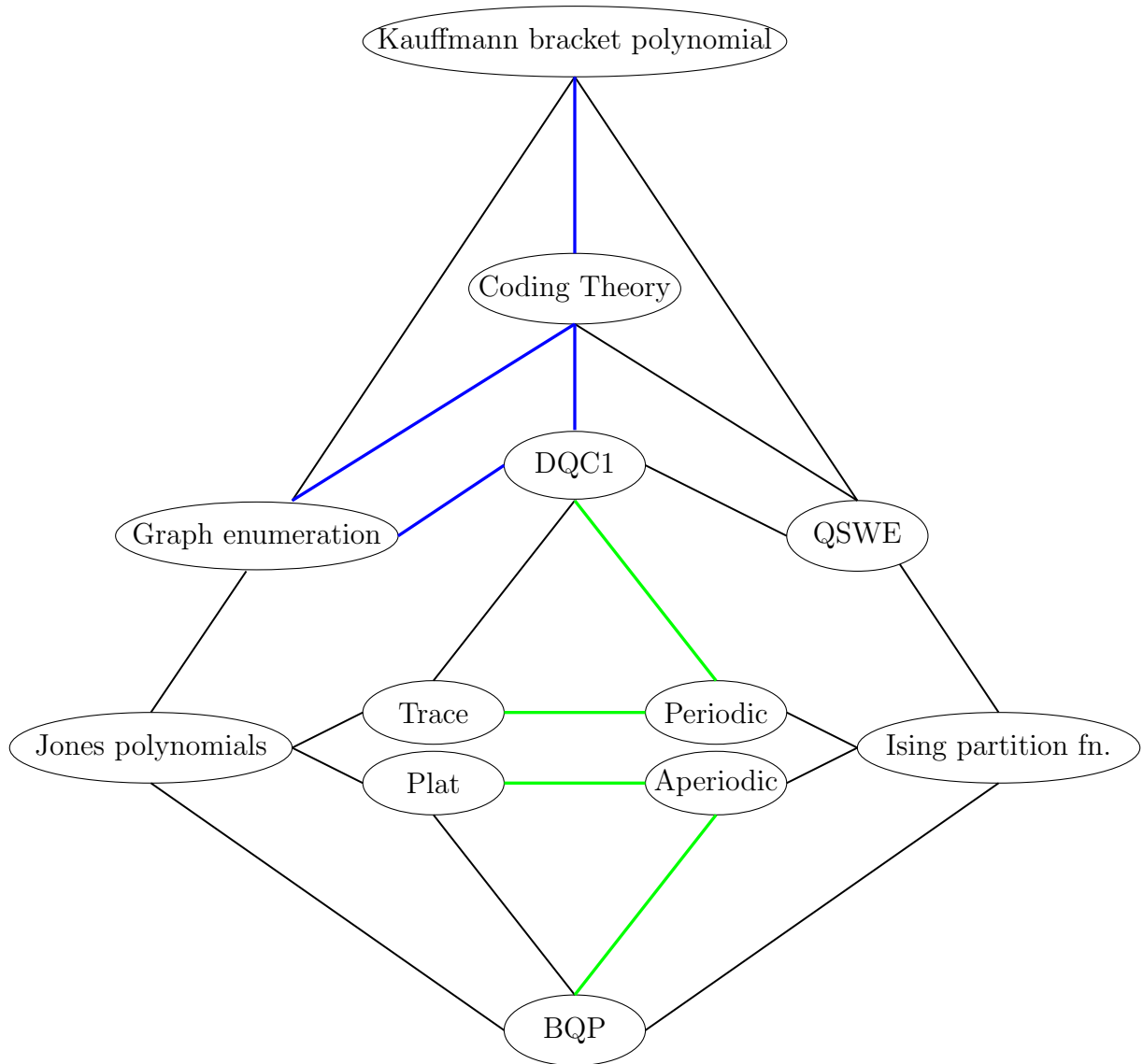


Figure 1.2: A schematic that displays the rich interdisciplinary nature of quantum computation in general, and DQC1 in particular. Black lines show the connections already known in the literature. Green lines are the connections first made in this thesis. The blue line show some of the possible connections that can be made and the potential for exploring the DQC1 model from several independent points of view. ‘Trace’ and ‘Plat’ refer to closures of braids whose Jones polynomials are of interest, while ‘Periodic’ and ‘Aperiodic’ refer to boundary conditions for Ising models. ‘Graph enumeration’ refers to the class of graph theoretic problems like the evaluation of the Tutte, the dichromatic, or the chromatic polynomial. The Kauffman bracket polynomial is a knot invariant which is a generalization of the Jones polynomial, and is related to partition functions of more esoteric statistical mechanical models like the vertex model and the IRF (interactions round a face) model. For further details, see Appendix A.

## 1.1 List of Publications

It is unlikely that any physics PhD thesis in this age of instant electronic collaboration is a collation of entirely original results. So it is with this dissertation. In addition to the background material taken from the literature, several new results presented in this dissertation were arrived at in collaboration with other researchers. Several of these have been published in refereed journals. This dissertation contains only my research on mixed-state quantum computation and the DQC1 model. In addition to this research, I have worked on two other topics during my graduate career at UNM, *viz*, quantum metrology and the abstract theory of entanglement. I provide below the list of my publications based on work done as a PhD student, classified according to which of the three topics they pertain to. For the papers on mixed-state quantum computation, I give which chapter each corresponds to in this dissertation.

### Mixed-State Quantum Computation

1. Quantum discord and the power of one qubit, [Animesh Datta](#), Anil Shaji, Carlton M. Caves, *Phys. Rev. Lett*, **100**, 050502 (2008). (Chapter 5)
2. Entanglement and the Power of One Qubit, [Animesh Datta](#), Steven T. Flammia, Carlton M. Caves, *Phys. Rev. A*, **72**, 042316 (2005). (Chapter 3)
3. Role of entanglement and correlations in mixed-state quantum computation, [Animesh Datta](#), Guifre Vidal, *Phys. Rev. A*, **75**, 042310 (2007). (Chapter 4)

### Quantum Metrology

4. Quantum Metrology: Dynamics vs Entanglement, Sergio Boixo, [Animesh Datta](#), Steven T. Flammia, Matthew J. Davis, Anil Shaji Carlton M. Caves, Submitted to *Physical Review Letters*.
5. Quantum-limited metrology with product states, Sergio Boixo, [Animesh Datta](#),



Steven T. Flammia, Anil Shaji, Emilio Bagan, Carlton M. Caves, *Phys. Rev. A*, **77**, 012317 (2008).

6. On Decoherence in Quantum Clock Synchronization, Sergio Boixo, Carlton M. Caves, [Animesh Datta](#), Anil Shaji, *Laser Physics: Special Issue on Quantum Information and Quantum Computation*, **16**, 1525 (2006).

### Quantum Entanglement

7. Doubly constrained bounds on the entanglement of formation, [Animesh Datta](#), Steven T. Flammia, Anil Shaji, Carlton M. Caves, arXiv:quant-ph/0608086.
8. Constrained bounds on measures of entanglement, [Animesh Datta](#), Steven T. Flammia, Anil Shaji, Carlton M. Caves, *Phys. Rev. A*, **75**, 062117 (2007)

The remainder of the Introduction explains in brief the results obtained in work not included in this dissertation.

The study of entanglement in a mixed quantum state led to some work on the general theory of quantum entanglement, which though not a part of this dissertation is listed below. This project considered entanglement measures constructed from two positive, but not completely positive, maps on density operators that were used as constraints in placing bounds on the entanglement of formation, the tangle, and the concurrence of  $4 \times N$  mixed states. The norm-based entanglement measures constructed from these two maps, called negativity and phi-negativity, respectively, lead to two sets of bounds on the entanglement of formation, the tangle, and the concurrence. These bounds were compared, and we identified the sets of  $4 \times N$  density operators for which the bounds from one constraint are better than the bounds from the other. Extensions of our results to bipartite states of higher dimensions and with more than two constraints were also discussed.

Another area of my research has been quantum metrology. The lure of beating the

shot-noise limit without using entanglement led my collaborators and myself to study various quantum clock synchronization protocols. We showed that the proposed schemes for beating the standard quantum limit without entanglement require as much resources as those using entanglement. We later turned to surpassing even the Heisenberg limit and proposed a scheme that involved product input states and measurements. Our results also provided evidence that the entanglement generated in the process was not responsible for the enhancement in precision. The next step involved proposing a demonstration of such a protocol using two-component Bose-Einstein condensates in  $^{87}\text{Rb}$ . This is the first realistic laboratory proposal of beating the  $1/n$  limit in metrology, certainly one using BECs

## Chapter 2

# Background

*Take nothing on its looks; take everything on evidence. There's no better rule.*

-Charles Dickens in *Great Expectations*

The intent of this chapter is to present research that is not entirely original, but nonetheless vital for the appreciation of the results appearing in the following chapters. Almost all of it can be found in the literature, and this will be pointed out at appropriate spots. This chapter will set the context and relevance of the DQC1 model. Subsequently we will outline the basics of entanglement theory and its relevance in quantum computation. Later we will present arguments and motivations for considering a quantity such as quantum discord and *its* relevance to quantum information science. There is some original research in this chapter, in the later parts of Sec 2.2. All of Sec 2.3 is original, dealing with quantum discord in quantum communication. Though not a central theme of this thesis, this role is vital to our understanding of quantum discord.

We begin this chapter with the requirements for a scalable quantum computation. We put the DQC1 model in perspective with the rest of quantum computation. We

discuss the relevance of the DQC1 model in several problems of physical importance and its place in computational complexity theory. We will briefly discuss the role of entanglement in all this and realize its shortcomings. Then we will move on to study a quantity that we think might be able to explain phenomena that entanglement fails at. This quantity, quantum discord, will be discussed in detail. We will explain how it is evaluated, and work out an example. Then we will study a phenomenon, called entanglement distribution, through a simple example and show, for the first time, the role of discord in its success.

Without further ado, let us begin by what are postulated to be the requirements for building a fully controllable and scalable quantum computer. Known as DiVincenzo's criteria [22], they are as follows:

1. Be scalable system in terms of well defined qubits (2-level quantum systems)
2. Be initializable into a simple quantum state such as  $|00 \cdots 000\rangle$
3. Have decoherence times long compared to gate operation times
4. Have a universal set of quantum gates
5. Permit high efficiency, single qubit measurements

However, fully controllable and scalable quantum computers are likely many years from realization. This motivates study and development of somewhat less ambitious quantum information processors, defined as devices that fail to satisfy one or more of DiVincenzo's five criteria for a quantum computer [22] listed above. An example of such a quantum information processor is a mixed-state quantum system, which fails to pass DiVincenzo's second requirement, that the system be prepared in an initial pure state.

The prime example of a mixed-state quantum information processor is provided by liquid-state NMR experiments in quantum information processing [49]. Current

NMR experiments, which operate with initial states that are highly mixed thermal states, use a technique called pseudo-pure-state synthesis to process the initial thermal state and thereby to simulate pure-state quantum information processing. This technique suffers from an exponential loss of signal strength as the number of qubits per molecule increases and thus is not scalable. There is a different technique for processing the initial thermal state, called algorithmic cooling [71], which pumps entropy from a subset of qubits into the remaining qubits, leaving the special subset in a pure state and the remaining qubits maximally mixed. Algorithmic cooling provides an in-principle method for making liquid-state NMR—or any qubit system that begins in a thermal state—scalable, in essence by providing an efficient algorithmic method for cooling a subset of the initially thermal qubits to a pure state, thereby satisfying DiVincenzo’s second criterion.

Knill and Laflamme [55] proposed a related mixed-state computational model, which they called DQC1, in which there is just one initial pure qubit, along with  $n$  qubits in the maximally mixed state. Although provably less powerful than a pure-state quantum computer [2], DQC1 can perform some computational tasks efficiently for which there are no known polynomial time classical algorithms. Knill and Laflamme referred to the power of this mixed-state computational model as the “power of one qubit.” In particular, a DQC1 quantum circuit can be used to evaluate, with fixed accuracy independent of  $n$ , the normalized trace,  $\text{tr}(U_n)/2^n$ , of any  $n$ -qubit unitary operator  $U_n$  that can be implemented efficiently in terms of quantum gates [55, 57]. In Sec. 3.1 we consider whether there might be efficient classical algorithms for estimating the normalized trace, and we conclude that this is unlikely.

The efficient quantum algorithm for estimating the normalized trace provides an exponential speedup over the best known classical algorithm for simulations of some quantum processes. It is known how to reduce the problem of measuring the average fidelity decay of a quantum map under small perturbations to that of

evaluating the normalized trace of a unitary matrix [66]. The DQC1 algorithm for this instance provides an exponential speedup. However, in testing the integrability of the classical limit of a quantum system, the same basic algorithm provides a square-root speedup [67]. Evaluating the local density of states, however, can be executed with an exponential advantage using only one pure qubit [29]. There has also been an attempt to exploit the DQC1 system in quantum metrology [8].

A very interesting application of the DQC1 model has been to topological quantum computation. It has been shown that the evaluation of the plat closure of the Jones polynomial of the same braid is BQP-complete [31, 32, 33]. An explicit quantum algorithm for this task was presented in 2006 [1] in the language of quantum circuits. This technique has now been extended to more general topological invariants like the HOMFLYPT polynomial and the Kauffman polynomial [82]. Recently, it was shown that the DQC1 model can be used to evaluate the Jones polynomial of the trace closure of a braid efficiently [51]. Indeed the problem of evaluating the Jones polynomial for the trace closure of a braid is complete for the complexity class DQC1. The notion of DQC1 as a quantum complexity class was developed in [74]. Since then, one of the important questions has been the relation of this class to other well known classes like P and BQP. As has already been shown, DQC1 is less powerful than BQP, a full scale pure state quantum computer [2]. Still, DQC1 can efficiently simulate classical circuits of logarithmic depth [2], a class known as NC1, which is contained in P, the class of problems that can be solved on a classical polynomial in polynomial time. On the other hand, as we show in Section 3.1, it is unlikely that DQC1 is contained in P. This leads to a very intriguing picture of the relative powers of these complexity classes in the polynomial hierarchy as shown in Fig 2.1.

This figure has a number of intriguing question lurking underneath. The least of these is a proof of the location of DQC1 in this figure. Also, if this figure is correct, as we believe at present, then DQC1 is really a class that lies between quantum and

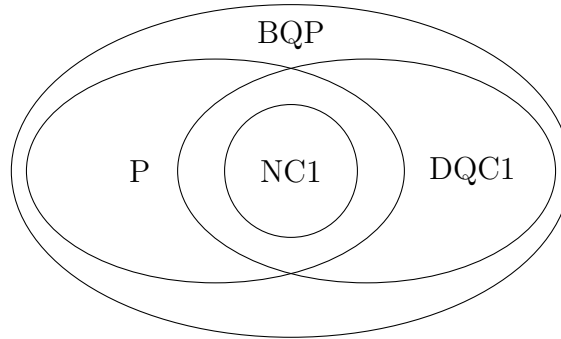


Figure 2.1: The relative hierarchy of the complexity classes P, BQP and DQC1.

classical computation. One would also like to understand the physical principle that governs this relative positioning. Such a sort of understanding will tell us of the particular aspects of nature that help us beat classical computers using quantum mechanics. We have been pursuing this program with some success. We describe this in Appendix [A](#).

Study of the power of one qubit is motivated partly by NMR experiments, but our primary motivation in this thesis is to investigate the role of entanglement in quantum computation, using DQC1 as a theoretical test bed for the investigation. For pure-state quantum computers, Jozsa and Linden [\[52\]](#) have shown that exponential speedup over a classical computer requires that entanglement not be restricted to blocks of qubits of fixed size as problem size increases. Entanglement whose extent increases with problem size is thus a necessary prerequisite for the exponential speedup achieved by a pure-state quantum computer. On the other hand, the Gottesman-Knill theorem [\[62\]](#) demonstrates that global entanglement is far from sufficient for exponential speedup. While this means that the role of entanglement is not entirely understood for pure-state quantum computers, far less is known about the role of entanglement in mixed-state quantum computers. When applied to mixed-state computation, the Jozsa-Linden proof does not show that entanglement is a requirement for exponential speedup. Indeed, prior to the work reported in this dissertation, it has not previously been shown that there is any entanglement in the DQC1 circuits

that provide an exponential speedup over classical algorithms.

Evidently, to invoke the above results, one must first calculate the entanglement in a quantum computation. This exercise of calculating the entanglement in a general quantum state is highly non-trivial. Indeed, even the simpler task of proving the separability of a general quantum state is NP-Hard [38]. For a general mixed quantum state, the task is further hardened by the lack of a unique measure of entanglement. This is partly due to the fact that entanglement, instead of being a physical notion, is a mathematical construct. Though it has been identified with physical tasks that can be thought of as operational interpretations of entanglement, this has not simplified the task of actually calculating the numerical value of entanglement. The computational task is not eased by the definition of mixed-state measures through convex-roof extensions of pure state measures, most commonly the von-Neumann entropy of the reduced density matrix. One exception is the negativity, which is formally easy to define and computationally feasible to calculate, a rare feature for an entanglement measure. It is this measure that we use in this thesis, after elaborating upon it in the next section. For an extensive review on the theory of entanglement, the reader is referred to the recent article by the Horodecki family [48].

## 2.1 Entanglement: Properties of negativity

In this section we briefly review properties of negativity as an entanglement measure, focusing on those properties that we need in the subsequent analysis (for a thorough discussion of negativity, see Ref. [80]).

Let  $A$  be an operator in the joint Hilbert space of two systems, system 1 of dimension  $d_1$  and system 2 of dimension  $d_2$ . The partial transpose of  $A$  with respect to an orthonormal basis of system 2 is defined by taking the transpose of the matrix elements of  $A$  with respect to the system-2 indices. A partial transpose can also be



defined with respect to any basis of system 1. Partial transposition preserves the trace, and it commutes with taking the adjoint.

The operator that results from partial transposition depends on which basis is used to define the transpose, but these different partial transposes are related by unitary transformations on the transposed system and thus have the same eigenvalues and singular values. Moreover, partial transposition on one of the systems is related to partial transposition on the other by an overall transposition, which also preserves eigenvalues and singular values. Despite the nonuniqueness of the partial transpose, we can talk meaningfully about its invariant properties, such as its eigenvalues and singular values. Similar considerations show that the eigenvalues and singular values are invariant under local unitary transformations.

The singular values of an operator  $O$  are the eigenvalues of  $\sqrt{O^\dagger O} \equiv |O|$  (or, equivalently, of  $\sqrt{OO^\dagger}$ ). Any operator has a polar decomposition  $O = T|O|$ , where  $T$  is a unitary operator. Writing  $|O| = W^\dagger S W$ , where  $W$  is the unitary that diagonalizes  $|O|$  and  $S$  is the diagonal matrix of singular values, we see that any operator can be written as  $O = V S W$ , where  $V = T W^\dagger$  and  $W$  are unitary operators.

We denote a partial transpose of  $A$  generically by  $\check{A}$ . We write the eigenvalues of  $\check{A}$  as  $\lambda_j(\check{A})$  and denote the singular values by  $s_j(\check{A})$ . If  $A$  is Hermitian, so is  $\check{A}$ , and the singular values of  $\check{A}$ , i.e., the eigenvalues of  $|\check{A}|$ , are the magnitudes of the eigenvalues, i.e.,  $s_j(\check{A}) = |\lambda_j(\check{A})|$ .

If a joint density operator  $\rho$  of systems 1 and 2 is separable, its partial transpose  $\check{\rho}$  is a positive operator. This gives the Peres-Horodecki entanglement criterion [64, 45]: if  $\check{\rho}$  has a negative eigenvalue, then  $\rho$  is entangled (the converse is not generally true). The magnitude of the sum of the negative eigenvalues of the partial transpose, denoted by

$$\mathcal{N}(\rho) \equiv - \sum_{\lambda_j(\check{\rho}) < 0} \lambda_j(\check{\rho}) , \quad (2.1)$$

is a measure of the amount of entanglement. Partial transposition preserves the trace, so  $\text{tr}(\check{\rho}) = 1$ , from which we get

$$1 + 2\mathcal{N}(\rho) = \sum_j |\lambda_j(\check{\rho})| = \text{tr}|\check{\rho}| \equiv \mathcal{M}(\rho) , \quad (2.2)$$

where  $\mathcal{M}(\rho)$  is a closely related entanglement measure. The quantity  $\mathcal{N}(\rho)$  was originally called the *negativity* [80]; we can distinguish the two measures by referring to  $\mathcal{M}(\rho)$  as the *multiplicative negativity*, a name that emphasizes one of its key properties and advantages over  $\mathcal{N}(\rho)$ . In this thesis, however, we use the multiplicative negativity exclusively and so refer to it simply as “the negativity”.

The negativity  $\mathcal{M}(\rho)$  equals one for separable states, and it is an entanglement monotone [80], meaning that (i) it is a convex function of density operators and (ii) it does not increase under local operations and classical communication. The negativity has the property of being multiplicative in the sense that the  $\mathcal{M}$  value for a state that is a product of states for many pairs of systems is the product of the  $\mathcal{M}$  values for each of the pairs. By the same token,  $\log \mathcal{M}(\rho)$ , called the *log-negativity*, is additive, but the logarithm destroys convexity so the log-negativity is not an entanglement monotone [80]. For another point of view on the monotonicity of the log-negativity, see Ref. [65].

The minimum value of the negativity is one, but we need to know the maximum value to calibrate our results. Convexity guarantees that the maximum value is attained on pure states. We can find the maximum [58] by considering the Schmidt decomposition of a joint pure state of systems 1 and 2,

$$|\psi\rangle = \sum_{j=1}^d \sqrt{\mu_j} |j, j\rangle , \quad (2.3)$$

where  $d = \min(d_1, d_2)$ . Taking the partial transpose of  $\rho$  relative to the Schmidt basis of system 2 gives

$$\check{\rho} = \sum_{j,k=1}^d \sqrt{\mu_j \mu_k} |j, k\rangle \langle k, j| , \quad (2.4)$$

with eigenvectors and eigenvalues

$$\begin{aligned} & |j, j\rangle, \quad \text{eigenvalue } \mu_j, \\ \frac{1}{\sqrt{2}}(|j, k\rangle \pm |k, j\rangle), \quad \text{eigenvalue } \pm\sqrt{\mu_j\mu_k}, \quad j < k. \end{aligned} \quad (2.5)$$

This gives a negativity

$$\mathcal{M}(\psi) = 1 + 2 \sum_{j < k} \sqrt{\mu_j\mu_k} = \sum_{j,k=1}^d \sqrt{\mu_j\mu_k} = \left( \sum_{j=1}^d \sqrt{\mu_j} \right)^2. \quad (2.6)$$

The concavity of the square root implies  $\sum_j \sqrt{\mu_j} \leq \sqrt{d}$ , with equality if and only if  $\mu_j = 1/d$  for all  $j$ , i.e.,  $|\psi\rangle$  is maximally entangled. We end up with

$$1 \leq \mathcal{M}(\rho) \leq d. \quad (2.7)$$

## 2.2 Beyond Entanglement: Quantum Discord

Characterizing and quantifying the information-processing capabilities offered by quantum phenomena like entanglement, superposition, and interference is one of the primary objectives of quantum information theory. Amongst these, entanglement has defined much of the research in quantum information science for almost a decade now. In spite of some progress [27, 52, 53], the precise role of entanglement in quantum information processing remains an open question [6, 9, 77, 54, 18]. It is quite well established that entanglement is essential for certain kinds of quantum-information tasks like teleportation and super-dense coding. In these cases, it is also known that the quantum enhancement must come from (pre-shared) entanglement between parts of the system. It is not known, however, if all information-processing tasks that can be done more efficiently with a quantum system than with a comparable classical system require entanglement as a resource. Indeed, there are several instances where we see a quantum advantage in the absence or near absence of entanglement. One

is quantum cryptography [5], where many protocols involve quantum states that are not entangled. These quantum cryptography protocols are provably more secure and thus better than the best known classical cryptographic techniques. This certainly cannot be attributed to entanglement. The second example we present is that of the DQC1 model, the theme of this dissertation. As this thesis shows, in Chapter 3, the system has very little entanglement - and even that little vanishes asymptotically - yet it provides an exponential speedup. These examples drive home one point: *all of quantum information science cannot be reduced to a study of quantum entanglement.*

This however leaves us in a lurch. What then explains all the quantum advantages? Certainly, it has something to do with the structure and inherent non-locality of quantum mechanics. Interestingly, it is known that non-locality and entanglement are not equivalent features [11]. Entanglement is the feature that having complete information about parts of a quantum system does not imply complete information of the whole system. This characterization goes all the way back to Schrödinger [69]. Not surprisingly, this is not the only characterization of a quantum system. There are other ones. For instance, the collapse of one part of a subsystem after a measurement of another is another feature unique to quantum systems. One can conceive of defining a quantity that captures this feature. Such a quantity is the quantum discord [63].

Quantum discord has been related to the superposition principle and the vanishing of discord shown to be a criterion for the preferred, effectively classical states of a system, i.e., the pointer states [63]. In addition, it has been used in analyzing the powers of a quantum Maxwell's demon [84] and also in the study of pure quantum states as a resource [46].

We start with a discussion of quantum discord, its definition and its relevance in quantum information theory. Consider the following two-qubit separable state

$$\rho = \frac{1}{4} \left[ (|+\rangle\langle+| \otimes |0\rangle\langle 0|) + (|-\rangle\langle-| \otimes |1\rangle\langle 1|) + (|0\rangle\langle 0| \otimes |-\rangle\langle-|) + (|1\rangle\langle 1| \otimes |+\rangle\langle+|) \right], \quad (2.8)$$

in which four nonorthogonal states of the first qubit are correlated with four nonorthogonal states of the second qubit. Such correlations cannot exist in any classical state of two bits. The extra correlations the quantum state can contain compared to an equivalent classical system with two bits could reasonably be called quantum correlations. Entanglement is certainly a kind of quantum correlation, but it is not the only kind. In other words, separable quantum states can have correlations that cannot be captured by a probability distribution defined over the states of an equivalent classical system.

Quantum discord attempts to quantify all quantum correlations including entanglement. It must be emphasized here that the discord supplements the measures of entanglement that can be defined on the system of interest. It aims to capture all the nonclassical correlations present in a system, those that can be identified as entanglement and then some more.

The information-theoretic measure of correlations between two systems  $A$  and  $B$  is the mutual information,  $\mathcal{I}(A : B) = H(A) + H(B) - H(A, B)$ . If  $A$  and  $B$  are classical systems whose state is described by a probability distribution  $p(A, B)$ , then  $H(\cdot)$  denotes the Shannon entropy,  $H(\mathbf{p}) \equiv -\sum_j p_j \log p_j$ , where  $\mathbf{p}$  is a probability vector. If  $A$  and  $B$  are quantum systems described by a combined density matrix  $\rho_{AB}$ , then  $H(\cdot)$  stands for the corresponding von Neumann entropy,  $H(\rho) \equiv -\text{tr}(\rho \log \rho)$ .

For classical probability distributions, Bayes's rule leads to an equivalent expression for the mutual information,  $\mathcal{I}(A : B) = H(B) - H(B|A)$ , where the conditional entropy  $H(B|A)$  is an average of Shannon entropies for  $B$ , conditioned on the alternatives for  $A$ . For quantum systems, we can regard this form for  $\mathcal{I}(A : B)$  as defining a conditional entropy, but it is not an average of von Neumann entropies and is not necessarily nonnegative [12].

Another way of generalizing the classical conditional entropy to the quantum case is to recognize that classically  $H(B|A)$  quantifies the ignorance about the system  $B$

that remains if we make measurements to determine  $A$ . When  $A$  is a quantum system, the amount of information we can extract about it depends on the choice of measurement. If we restrict to projective measurements (*a priori*, we could consider POVMs, but we will show later that rank one projectors suffice) described by a complete set of orthogonal projectors,  $\{\Pi_j\}$ , corresponding to outcomes  $j$ , then the state of  $B$  after a measurement is given by

$$\rho_{B|j} = \text{tr}_M(\Pi_j \rho_{AB} \Pi_j) / p_j, \quad p_j = \text{tr}_{A,B}(\rho_{AB} \Pi_j). \quad (2.9)$$

A quantum analogue of the conditional entropy can then be defined as  $\tilde{H}_{\{\Pi_j\}}(B|A) \equiv \sum_j p_j H(\rho_{B|j}) \geq 0$ . Since  $\rho_B = \sum_j p_j \rho_{B|j}$ , the concavity of von Neumann entropy implies that  $H(B) \geq \tilde{H}_{\{\Pi_j\}}(B|A)$ . We can now define an alternative quantum version of the mutual information,

$$\mathcal{J}_{\{\Pi_j\}}(A : B) \equiv H(B) - \tilde{H}_{\{\Pi_j\}}(B|A) \geq 0. \quad (2.10)$$

Performing projective measurements onto a complete set of orthogonal states of  $A$  effectively removes all nonclassical correlations between  $B$  and  $A$ . In the post-measurement state, mutually orthogonal states of  $A$  are correlated with at most as many states of  $B$ . It is easy to see that these sorts of correlations can be present in an equivalent classical system. If on the other hand, the system  $B$  is bigger than  $A$ , the correlations are certainly non-classical, or quantum.

The value of  $\mathcal{J}_{\{\Pi_j\}}(A : B)$  in Eq. (2.10) depends on the choice of  $\{\Pi_j\}$ . We want  $\mathcal{J}_{\{\Pi_j\}}(A : B)$  to quantify *all* the classical correlations in  $\rho_{AB}$ , so we maximize  $\mathcal{J}_{\{\Pi_j\}}(A : B)$  over all  $\{\Pi_j\}$  and define a measurement-independent mutual information  $\mathcal{J}(A : B) \equiv H(B) - \tilde{H}(B|A) \geq 0$ , where  $\tilde{H}(B|A) \equiv \min_{\{\Pi_j\}} \sum_j p_j H(\rho_{B|j})$  is a measurement-independent conditional information. Henderson and Vedral [44] investigated how  $\mathcal{J}(A : B)$  quantifies classical correlations. The criterion they postulated for a measure of classical correlations  $\mathcal{C}$  were [44]

1.  $\mathcal{C} = 0$  for product states

2.  $\mathcal{C}$  is invariant under local unitary transformations. This is because any change of basis should not affect the correlation between two subsystems.
3.  $\mathcal{C}$  is non-increasing under local operations. If the two subsystems evolve independently then the correlation between them cannot increase.
4.  $\mathcal{C} = H(\rho_A) = H(\rho_B)$  for pure states.

One can then define a measure of purely quantum correlations as the difference of the total correlations in a system and  $\mathcal{C}$ . Taking the quantum mutual information to be a measure of total correlations in a system, the purely quantum correlations can be measured by

$$\mathcal{D}(A, B) \equiv \mathcal{I}(A : B) - \mathcal{J}(A : B) = \tilde{H}(B|A) - H(B|A). \quad (2.11)$$

This quantity was first called quantum discord by Ollivier and Zurek in [63]. Another operational approach to identifying the nature of correlations is presented in [37]. The discord of the state (2.8) is  $\frac{3}{4} \log \frac{4}{3} = 0.311$ .

This thesis is the first to propound a role for quantum discord in quantum computation and information. It is, therefore, imperative that we present all the known properties of discord here. This is the content of the next section. We will present several properties of quantum discord, some of which are present in prior literature. We will provide appropriate indications at requisite spots.

### 2.2.1 Properties of Quantum Discord

The first property that we present is that the discord is nonnegative and is zero for states with only classical correlations [44, 63]. Thus a nonzero value of  $\mathcal{D}(A, B)$  indicates the presence of nonclassical correlations [63].

**Theorem 1.** *Quantum discord is always positive, i.e.,  $\mathcal{D}(A, B) \geq 0$ .*

*Proof:* Consider the joint state  $\rho_{AB}$  subject to one dimensional orthogonal measurements  $\Pi_j = |e_j\rangle\langle e_j|$  on  $B$ , extended to arbitrary (at most  $\dim(B)^2$ ) dimensions. Then

$$p_j \rho_{A|j} = \text{tr}_B(\rho_{AB}\Pi_j) = \langle e_j | \rho_{AB} | e_j \rangle, \quad p_j = \text{tr}_B(\rho_B\Pi_j) = \langle e_j | \rho_{AB} | e_j \rangle.$$

Note that the measurement is made on the system  $B$ , while in the definition of discord, it was on  $A$ . Discord is not symmetric under the exchange of the subsystems, but this is not a concern as we just as well have proved the result for  $\mathcal{D}(B, A)$ .

Suppose now that a system  $C$  interacts with  $B$  so as to make the desired measurement ( $U |e_j\rangle \otimes |0\rangle = |e_j\rangle \otimes |f_j\rangle$ ), leaving the state

$$\rho'_{ABC} = \sum_{j,k} \langle e_j | \rho_{AB} | e_k \rangle \otimes |e_j\rangle \langle e_k| \otimes |f_j\rangle \langle f_k|. \quad (2.12)$$

If the eigendecomposition of  $\rho_{AB} = \sum_l \lambda_l |r_l\rangle\langle r_l|$ , then

$$\begin{aligned} \rho'_{ABC} &= \sum_{j,k,l} \lambda_l \langle \mathbb{I}_A, e_j | r_l \rangle \langle r_l | \mathbb{I}_A, e_k \rangle \otimes |e_j\rangle \langle e_k| \otimes |f_j\rangle \langle f_k| \\ &= \sum_l \lambda_l |e_l, r_l, f_l\rangle \langle e_l, r_l, f_l| \end{aligned}$$

whereby

$$H(\rho'_{ABC}) = H(\rho_{AB}).$$

Also, from Eq. 2.12,

$$\rho'_{AB} = \sum_j p_j \rho_{A|j} \otimes |e_j\rangle\langle e_j|, \quad \text{so } H(\rho'_{AB}) = H(\mathbf{p}) + \sum_j p_j H(A|j), \quad (2.13a)$$

$$\rho'_{BC} = \sum_{j,k} |e_j\rangle\langle e_j| \rho_B |e_k\rangle\langle e_k| \otimes |f_j\rangle \langle f_k|, \quad \text{so } H(\rho'_{BC}) = H(\rho_B), \quad (2.13b)$$

$$\rho'_B = \sum_j p_j |e_j\rangle\langle e_j|, \quad \text{so } H(\rho'_B) = H(\mathbf{p}). \quad (2.13c)$$

Now use the strong subadditivity of the von-Neumann entropy which is

$$H(\rho'_{ABC}) + H(\rho'_B) \leq H(\rho'_{AB}) + H(\rho'_{BC}). \quad (2.14)$$



Eqs. 2.13 reduces this to

$$H(\rho_{AB}) + H(\mathbf{p}) \leq H(\mathbf{p}) + \sum_j p_j H(A|j) + H(\rho_B), \quad (2.15)$$

whereby

$$\tilde{H}_{\{\Pi_j\}}(A|B) \equiv \sum_j p_j H(A|j) \geq H(\rho_{AB}) - H(\rho_B) \equiv H(A|B). \quad (2.16)$$

This, being true for all measurements, also holds for the minimum. So

$$\mathcal{D}(A, B) = \min_{\{\Pi_j\}} \tilde{H}_{\{\Pi_j\}}(A|B) - H(A|B) \geq 0.$$

□

Having proved that the quantum discord is always nonnegative, it is worthwhile to seek the condition for it being zero. The reason is that the set of states with zero discord is exactly those which have no nonclassical correlations in it. This is the aim of the next theorem. It is evident that the condition for zero discord can be reduced to that of the equality in strong subadditivity in Eq 2.14. To that end, we will employ a result of Hayden *et al.* [42] which we present below for completeness.

**Lemma 1** ([42]). *A state  $\rho'_{ABC}$  on  $\mathcal{H}_A \otimes \mathcal{H}_B \otimes \mathcal{H}_C$  satisfies strong subadditivity (Eq. 2.14) with equality if and only if there is a decomposition of system  $B$  as*

$$\mathcal{H}_B = \bigoplus_j \mathcal{H}_{B_j^L} \otimes \mathcal{H}_{B_j^R}$$

into a direct sum of tensor products such that

$$\rho'_{ABC} = \bigoplus_j q_j \rho_{AB_j^L} \otimes \rho_{AB_j^R}$$

with states  $\rho_{AB_j^L}$  on  $\mathcal{H}_A \otimes \mathcal{H}_{B_j^L}$  and  $\rho_{AB_j^R}$  on  $\mathcal{H}_{B_j^R} \otimes \mathcal{H}_C$ , and a probability distribution  $\{q_j\}$ .

**Theorem 2.**  $\mathcal{D}(A, B) = 0$  if and only if the state  $\rho_{AB}$  is block diagonal in its own eigenbasis, that is

$$\rho_{AB} = \sum_j P_j \rho_{AB} P_j$$

where  $\rho_{AB} = \sum_j \tau_j P_j$ , with  $\{\tau\}$  a probability distribution.

*Proof:* The decomposition of the Hilbert space of  $B$  can be written as

$$\mathbb{I}_B = \sum_{\alpha} \Pi_{\alpha} = \sum_{\alpha} \Pi_{\alpha L} \otimes \Pi_{\alpha R},$$

and  $\Pi_{\alpha}\Pi_{\beta} = \delta_{\alpha\beta}\Pi_{\alpha}$ . In our case, the state  $\rho'_{ABC}$  is invariant under the exchange of  $B$  and  $C$  relative to the measurement basis, here denoted by  $|E_{\alpha j}\rangle$  and  $|F_{\alpha j}\rangle$ . Thus using Lemma 1, we conclude that it must have the form

$$\rho'_{ABC} = \sum_{\alpha} q_{\alpha} \rho_{A|\alpha} \otimes \rho_{BC}^{\alpha},$$

where  $\rho_{BC}^{\alpha} = \Pi_{\alpha} \rho_{BC}^{\alpha} \Pi_{\alpha}$ , with  $\Pi_{\alpha}$  being projectors of the form

$$\Pi_{\alpha} = \sum_j |E_{\alpha j}\rangle\langle E_{\alpha j}| \otimes |F_{\alpha j}\rangle\langle F_{\alpha j}|.$$

Thus

$$\rho_{BC}^{\alpha} = \sum_{j,k} \rho_{jk}^{\alpha} |E_{\alpha j}\rangle\langle E_{\alpha k}| \otimes |F_{\alpha j}\rangle\langle F_{\alpha k}|$$

and

$$\rho'_{AB} = \sum_{\alpha} q_{\alpha} \rho_{A|\alpha} \otimes \rho_B^{\alpha} = \sum_{\alpha,j} \rho_{jj}^{\alpha} q_{\alpha} \rho_{A|\alpha} \otimes |E_{\alpha j}\rangle\langle E_{\alpha j}|.$$

Undoing the measurement,  $U |e_j\rangle \otimes |0\rangle = |e_j\rangle \otimes |f_j\rangle$ , gives

$$\rho_{AB} = \langle 0_C | U^{\dagger} \rho'_{ABC} U | 0_C \rangle = \sum_{\alpha} q_{\alpha} \rho_{A|\alpha} \otimes \rho_B^{\alpha}.$$

Diagonalizing  $\rho_B^{\alpha} = \sum_j \lambda_j^{\alpha} |\lambda_j^{\alpha}\rangle\langle \lambda_j^{\alpha}|$ , we get

$$\rho_{AB} = \sum_{\alpha,j} \lambda_j^{\alpha} q_{\alpha} \rho_{A|\alpha} |\lambda_j^{\alpha}\rangle\langle \lambda_j^{\alpha}|.$$

Relabelling, we have that the discord is zero if and only if

$$\rho_{AB} = \sum_j p_j \rho_{A|j} \otimes |\lambda_j\rangle\langle \lambda_j| \tag{2.17}$$

in the basis that diagonalizes  $\rho_B$ . The  $\alpha$  subspaces take into account that if the states  $\rho_{A|j}$  are the same for different  $j$ , then we can attain zero discord by using any measurement in the subspace spanned by those values of  $j$ .

Diagonalising  $\rho_{A|j} = \sum_k \mu_{jk} |\mu_{jk}\rangle\langle\mu_{jk}|$ , we get that a state has zero discord if and only if

$$\rho_{AB} = \sum_{jk} p_j \mu_{jk} |\mu_{jk}, \lambda_j\rangle\langle\mu_{jk}, \lambda_j|. \quad (2.18)$$

Thus the eigenbasis of  $\rho_{AB}$  has a tree product structure  $|\mu_{jk}\rangle \otimes |\lambda_j\rangle$ . From Eq. 2.18, it is also evident that a state has zero discord if and only if it is block diagonal in its eigenbasis, that is,

$$\mathcal{D}(A, B) = 0 \quad \text{iff} \quad \rho_{AB} = \sum_j P_j \rho_{AB} P_j \quad (2.19)$$

with

$$P_j = \sum_k |\mu_{jk}, \lambda_j\rangle\langle\mu_{jk}, \lambda_j|.$$

which is the statement of the theorem.  $\square$

It is now a valid question to ask for the maximum possible value of discord. The next theorem addresses just this point.

**Theorem 3.** *The value of quantum discord is upper bounded by the von-Neumann entropy of the measured subsystem, i.e.,  $\mathcal{D}(A, B) \leq H(A)$ .*

*Proof:* Start with the eigendecomposition

$$\rho_{AB} = \sum_a p_a \Pi_a,$$

which yields

$$p_j \rho_{B|j} = \sum_a p_a p_{j|a} \rho_{B|a,j},$$

where

$$\rho_{B|a,j} = \text{tr}_A(\Pi_j \rho_B \Pi_a) / p_{j|a},$$

is a pure state of  $B$ . It follows from the pure-state decomposition

$$\rho_{B|j} = \sum_a p_{a|j} \rho_{B|a,j},$$

that  $H(\{a\}|j) \geq H(\rho_{B|j})$ . Thus

$$\begin{aligned}
 H(A, B) &= H(\{a\}) \geq H(\{a\}|j) \\
 &= \sum_j p_j H(\{a\}|j) \\
 &\geq \tilde{H}_{\{\Pi_j\}}(B|A) \\
 &\geq \tilde{H}(B|A),
 \end{aligned} \tag{2.20}$$

from which the marginal entropy  $H(A)$  follows as the upper bound on discord.  $\square$

When the joint state  $\rho_{AB}$  is pure,  $H(A, B)$  and  $\tilde{H}(B|A)$  are zero,  $H(B) = H(A) = -H(B|A)$ , and the discord is equal to its maximum value,  $H(A)$ , which is a measure of entanglement for bipartite pure states. In other words, for pure states all nonclassical correlations characterized by quantum discord can be identified as entanglement as measured by the marginal entropy.

Coming back to the question of mixed quantum states, we find that the actual evaluation of quantum discord involves the minimization of an entropic quantity over the set of all POVMs, as shown in Eq 2.11. This minimization, though perhaps easier than the one involved in the convex roof optimization needed for certain measures of entanglement, is nevertheless not trivial. Some simplification is in order as we show in the following two theorems.

**Theorem 4.** *The quantity  $\mathcal{D}(A, B) = H(B|A) - \tilde{H}_{\mathcal{E}}(B|A)$  is a concave function on the set of POVMs  $\mathcal{E}$ .*

*Proof:* We start by stating that for quantum states the von Neumann entropy is concave, that is,

$$H(\lambda\rho_1 + (1 - \lambda)\rho_2) \geq \lambda H(\rho_1) + (1 - \lambda)H(\rho_2) \tag{2.21}$$

for all  $0 \leq \lambda \leq 1$ . To study the concavity of the classical measure  $\tilde{H}(B|A)$ , let introduce Positive Operator Valued Measurements (POVMs) given by a set of quantum

operations

$$\mathcal{A}_j = \sum_{\alpha} A_{j\alpha} \odot A_{j\alpha}^{\dagger}, \quad (2.22)$$

with

$$\sum_{\alpha} A_{j\alpha}^{\dagger} A_{j\alpha} = E_j \quad \text{and} \quad \sum_j E_j = \mathbb{I}.$$

Not confusing the POVM elements  $A_{j\alpha}$  with the system  $A$  on which they are executed, the post-measurement state of  $B$  is

$$\begin{aligned} \rho_{B|j} &= \text{tr}_A(\mathcal{A}_j(\rho_{AB})) / p_j = \sum_{\alpha} \text{tr}_A(A_{j\alpha} \rho_{AB} A_{j\alpha}^{\dagger}) / p_j \\ &= \text{tr}_A(\rho_{AB} \sum_{\alpha} A_{j\alpha}^{\dagger} A_{j\alpha}) / p_j \\ &= \text{tr}_A(\rho_{AB} E_j) / p_j. \end{aligned} \quad (2.23)$$

The post-measurement state is thus completely determined by the POVM. Now let us call the POVM  $\mathcal{E} = \{E_j\}$  and define the functional  $F(\rho_B, \mathcal{E})$  as

$$F(\rho_B, \mathcal{E}) \equiv \tilde{H}(B|A) = \sum_j p_j H(\rho_{B|j}). \quad (2.24)$$

Let  $\mathcal{C}$  and  $\mathcal{D}$  be two POVMs and  $\mathcal{E} = \lambda \mathcal{C} + (1 - \lambda) \mathcal{D}$  their combination.  $\mathcal{E}$  is certainly a POVM since the set of POVMs is convex. This is, in effect, tantamount to

$$E_j = \lambda C_j + (1 - \lambda) D_j.$$

Then it is simple to show that

$$p_{E_j} \rho_{S|E_j} = \lambda p_{C_j} \rho_{B|C_j} + (1 - \lambda) p_{D_j} \rho_{B|D_j}, \quad p_{E_j} = \lambda p_{C_j} + (1 - \lambda) p_{D_j}.$$

Using these two relations and the fact that the von-Neumann entropy is concave, it can be seen that

$$\begin{aligned} F(\rho_B, \mathcal{E}) &= \sum_j p_{E_j} H(\rho_{B|E_j}) \\ &\geq \sum_j \lambda p_{C_j} H(\rho_{B|C_j}) + (1 - \lambda) p_{D_j} H(\rho_{B|D_j}) \\ &= \lambda F(\rho_B, \mathcal{C}) + (1 - \lambda) F(\rho_B, \mathcal{D}). \end{aligned} \quad (2.25)$$

This shows that the objective function which is to be minimized to obtain the discord is concave over the convex set of POVMs .  $\square$

Thus the minima that provides the value of discord will always be attained at the extremal points of the set of POVMs. The extreme points of the set of POVMs on a  $D$  dimensional system is no more than  $D^2$  dimensional; a necessary and sufficient condition for its extremality being that the eigenvectors of the POVM elements be linearly independent as operators [16]. It consists of projectors of all ranks. Fortunately, the next theorem will provide a considerable simplification.

**Theorem 5.** *The minimum of the quantity  $\mathcal{D}(A, B) = H(B|A) - \tilde{H}_{\mathcal{E}}(B|A)$  is always attained for a rank-1 POVM.*

*Proof:* We start by supposing a POVM on system  $A$ , whose elements can be fine-grained as

$$E_j = \sum_k E_{jk}.$$

Then

$$p_{jk}\rho_{B|jk} = \text{tr}_A(\rho_{AB}E_{jk}), \quad p_{jk} = \text{tr}(\rho_{AB}E_{jk}).$$

Evidently,  $\sum_k p_{jk} = p_j$  whereby we can define  $p_{k|j} = p_{jk}/p_j$ . Also,

$$\rho_{B|j} = \text{tr}_A(\rho_{AB}E_j)/p_j = \sum_k \frac{p_{jk}}{p_j} \text{tr}_A(\rho_{AB}E_{jk})/p_{jk} = \sum_k p_{k|j} \rho_{B|jk}. \quad (2.26)$$

Now,

$$\begin{aligned} \sum_j p_j H(\rho_{B|j}) &= \sum_j p_j H\left(\sum_k p_{k|j} \rho_{B|jk}\right) \\ &\geq \sum_{j,k} p_j p_{k|j} H(\rho_{B|jk}) \\ &= \sum_{j,k} p_{jk} H(\rho_{B|jk}). \end{aligned} \quad (2.27)$$

Since any POVM element can be written in terms of its eigendecomposition, the minimum conditional entropy, and therefore the discord is always attained on a rank-1 POVM.  $\square$

A rank-1 POVM is extremal if and only if its elements are linearly independent [16]. Even after these simplifications, the minimization over all rank one POVMs remains a hard task for general Hilbert spaces. We are not aware of the exact computational complexity of the problem, which might be formidable, but one can envisage casting this as a semi-definite program. This particular aspect is still under investigation by us. Accordingly, this thesis deals only with instances where the minimization is done over a two dimensional Hilbert space.

In light of the present scenario, we conclude the discussion on the evaluation of quantum discord by explicitly working out an example. The state we consider is the well known  $2 \times 4$  bound entangled state due to Horodecki [47], written in the standard product basis as

$$\rho = \frac{1}{1+7p} \begin{pmatrix} p & 0 & 0 & 0 & 0 & p & 0 & 0 \\ 0 & p & 0 & 0 & 0 & 0 & p & 0 \\ 0 & 0 & p & 0 & 0 & 0 & 0 & p \\ 0 & 0 & 0 & p & 0 & 0 & 0 & 0 \\ 0 & 0 & 0 & 0 & \frac{1+p}{2} & 0 & 0 & \frac{\sqrt{1-p^2}}{2} \\ p & 0 & 0 & 0 & 0 & p & 0 & 0 \\ 0 & p & 0 & 0 & 0 & 0 & p & 0 \\ 0 & 0 & p & 0 & \frac{\sqrt{1-p^2}}{2} & 0 & 0 & \frac{1+p}{2} \end{pmatrix} \quad \text{for } 0 \leq p \leq 1. \quad (2.28)$$

That this state is bound entangled for all  $0 \leq p \leq 1$  can be concluded from its positive partial transpose, and its entanglement is hidden in a very subtle way. The calculation of the discord begins with the evaluation of the von-Neumann entropy of  $\rho$ . Its spectrum is

$$\lambda = \left\{ 0, 0, 0, \frac{p}{1+7p}, \frac{2p}{1+7p}, \frac{2p}{1+7p}, \frac{1+9p+14p^2 - \sqrt{1+12p+23p^2-70p^3+98p^4}}{2(1+14p+49p^2)}, \frac{1+9p+14p^2 + \sqrt{1+12p+23p^2-70p^3+98p^4}}{2(1+14p+49p^2)} \right\}, \quad (2.29)$$

from which  $H(\rho) = H(\boldsymbol{\lambda}) = -\text{tr}(\boldsymbol{\lambda} \log(\boldsymbol{\lambda}))$ . The reduced density matrix of the smaller subsystem is

$$\rho_M = \text{tr}_S(\rho) = \begin{pmatrix} \frac{4p}{1+7p} & 0 \\ 0 & \frac{1+3p}{1+7p} \end{pmatrix}, \quad (2.30)$$

whose von-Neumann entropy is trivially obtained. As is clear by now, we have chosen to make our measurement on the 2 dimensional subsystem. These projectors are generally defined as

$$\Pi_1 = \frac{\mathbb{I}_2 + \mathbf{a} \cdot \boldsymbol{\sigma}}{2} \otimes \mathbb{I}_4, \quad \Pi_2 = \frac{\mathbb{I}_2 - \mathbf{a} \cdot \boldsymbol{\sigma}}{2} \otimes \mathbb{I}_4, \quad (2.31)$$

with  $a_1 = \sin \theta \cos \phi$ ,  $a_2 = \sin \theta \sin \phi$ ,  $a_3 = \cos \theta$ . Using these, we calculate

$$p_1 = \text{tr}(\Pi_1 \rho \Pi_1) = \frac{1 + 7p - \cos \theta + p \cos \theta}{2 + 14p}, \quad (2.32a)$$

$$p_2 = \text{tr}(\Pi_2 \rho \Pi_2) = \frac{1 + 7p + \cos \theta - p \cos \theta}{2 + 14p}, \quad (2.32b)$$

and

$$\rho_1 = \frac{\text{tr}_M(\Pi_1 \rho \Pi_1)}{p_1} = \frac{1}{4(1+7p)p_1} \times \begin{pmatrix} 1 + 3p - \cos \theta(1-p) & 2p \sin \theta e^{i\phi} & 0 & \sqrt{1-p^2}(1-\cos \theta) \\ 2p \sin \theta e^{-i\phi} & 4p & 2p \sin \theta e^{i\phi} & 0 \\ 0 & 2p \sin \theta e^{-i\phi} & 4p & 2p \sin \theta e^{i\phi} \\ \sqrt{1-p^2}(1-\cos \theta) & 0 & 2p \sin \theta e^{-i\phi} & 1 + 3p - \cos \theta(1-p) \end{pmatrix}, \quad (2.33)$$

$$\rho_2 = \frac{\text{tr}_M(\Pi_2 \rho \Pi_2)}{p_2} = \frac{1}{4(1+7p)p_2} \times \begin{pmatrix} 1 + 3p + \cos \theta(1-p) & -2p \sin \theta e^{i\phi} & 0 & \sqrt{1-p^2}(1+\cos \theta) \\ -2p \sin \theta e^{-i\phi} & 4p & -2p \sin \theta e^{i\phi} & 0 \\ 0 & -2p \sin \theta e^{-i\phi} & 4p & -2p \sin \theta e^{i\phi} \\ \sqrt{1-p^2}(1+\cos \theta) & 0 & -2p \sin \theta e^{-i\phi} & 1 + 3p + \cos \theta(1-p) \end{pmatrix}. \quad (2.34)$$



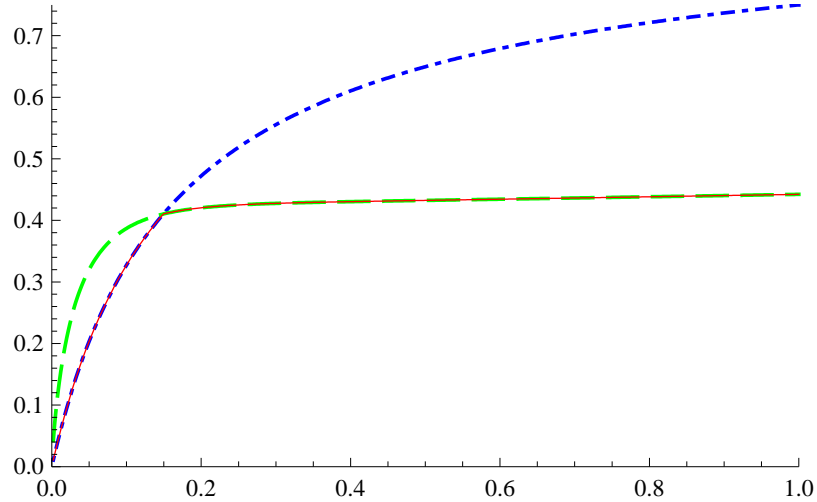


Figure 2.2: The green dashed line is the value of the discord when the projector (Eq 2.31) is parameterized by  $\theta = \pi/2, \phi = 0$ . The blue dot-dashed line is when the projector is given by  $\theta = 0, \phi = 0$ . The solid red line, which is the smaller of the two, is the quantum discord in the  $2 \times 4$  bound entangled Horodecki state of Eq 2.28 obtained by explicit numerical minimization. The expression for the discord is given by Eq 2.35. We see how the optimal projector changes from the former to the latter at  $p = 1/7$ . This exemplifies how the optimal measurement can change even for the same family of states and therefore is tricky to obtain analytically.

This state provides a very good example when optimizing over the POVM though seemingly tractable analytically, actually leads to erroneous conclusions. This is due to the fact that the optimal measurement that minimizes the conditional entropy changes with the value of  $p$ . We can however do it numerically without much ado. The value of discord in this case is

$$\mathcal{D} = H_2\left(\frac{4p}{1+7p}\right) + \text{tr}(\boldsymbol{\lambda} \log(\boldsymbol{\lambda})) + \min_{(\theta, \phi)} [p_1 H(\rho_1) + p_2 H(\rho_2)], \quad (2.35)$$

$H_2(\cdot)$  being the binary Shannon entropy. We plot the result of the numerical minimization as the green line in Fig 2.2. The plot was obtained in a couple of minutes on a 1.83 GHz Dell XPS laptop. In addition to demonstrating the feasibility of the minimization in small instances, Fig 2.2 shows one very important feature. This state is bound entangled, meaning it has entanglement that cannot be distilled [48].

Quantifying the amount of entanglement in a quantum state is generally hard, harder still for bound entangled states. As we have now shown, quantum discord can be used to quantify non-classical correlations in such states, which further makes discord a useful tool in the study of quantum states. Additionally, we are going to demonstrate an analytical technique that might be useful in the minimization as well its caveats. Let us now proceed towards that.

It is worthwhile to point out at the outset that the optimal measurements that give us the actual value of discord are *not* given by the eigenvectors of the reduced density matrices. Indeed, an independent measure of non-classicality has been proposed where measurements are made on both the subsystems, and that too in the eigenbasis of their respective subsystems [76]. In the minimization of quantum discord, the hard part is often using the explicit analytical expressions of the eigenvalues of the states in Eqs 2.33, 2.34. Here is a handy trick that is often helpful. Consider  $p = 1$ . In that case the Eqs 2.33, 2.34 simplify drastically to

$$\rho_1 = \begin{pmatrix} \frac{1}{4} & \frac{\sin \theta e^{i\phi}}{8} & 0 & 0 \\ \frac{\sin \theta e^{-i\phi}}{8} & \frac{1}{4} & \frac{\sin \theta e^{i\phi}}{8} & 0 \\ 0 & \frac{\sin \theta e^{-i\phi}}{8} & \frac{1}{4} & \frac{\sin \theta e^{i\phi}}{8} \\ 0 & 0 & \frac{\sin \theta e^{i\phi}}{8} & \frac{1}{4} \end{pmatrix}, \quad (2.36)$$

and

$$\rho_2 = \begin{pmatrix} \frac{1}{4} & -\frac{\sin \theta e^{i\phi}}{8} & 0 & 0 \\ -\frac{\sin \theta e^{-i\phi}}{8} & \frac{1}{4} & -\frac{\sin \theta e^{i\phi}}{8} & 0 \\ 0 & \frac{\sin \theta e^{-i\phi}}{8} & \frac{1}{4} & -\frac{\sin \theta e^{i\phi}}{8} \\ 0 & 0 & -\frac{\sin \theta e^{i\phi}}{8} & \frac{1}{4} \end{pmatrix}, \quad (2.37)$$

both of which have spectrum

$$\begin{aligned} \boldsymbol{\lambda}(\rho_1) &= \boldsymbol{\lambda}(\rho_1) \\ &= \left\{ \frac{4 - \sqrt{6 - 2\sqrt{5}} \sin \theta}{16}, \frac{4 + \sqrt{6 - 2\sqrt{5}} \sin \theta}{16}, \right. \\ &\quad \left. \frac{4 - \sqrt{6 + 2\sqrt{5}} \sin \theta}{16}, \frac{4 + \sqrt{6 + 2\sqrt{5}} \sin \theta}{16} \right\}. \end{aligned} \quad (2.38)$$

Simultaneously,  $p_1 = p_2 = 1/2$ . Then the conditional quantum entropy is just  $H(\boldsymbol{\lambda}(\rho_1))$ , the Shannon entropy of the vector in Eq 2.38, which is minimized when the distribution is most disparate, that is,  $\theta = \pi/2$ . We note that  $\phi$ , having dropped out of the problem, can be set to zero. We now have at least one point where we have carried out the minimization explicitly. One might now be tempted to believe that this point gives the minimum for all  $p$ , and we would have succeeded in the minimization without doing it explicitly. Fig 2.2 shows the catch. The red line is the expression for discord obtained when setting  $\theta = \pi/2, \phi = 0$ . We see that it matches with the actual minima for a range of  $p$ , but not all of it. The region where they diverge is  $p \in \{0, 1/7\}$ . Interestingly enough, in this region, the optimal choice of the projector is given by  $\theta = 0, \phi = 0$ . This is shown by the blue line, which we see lies exactly on top of the green line obtained by explicit numerical minimization in  $p \in \{0, 1/7\}$ .

To reemphasize the point made at the beginning of the last paragraph, we present the eigenvectors of  $\mathbf{E}(\rho_1)$  and  $\mathbf{E}(\rho_2)$  of  $\rho_1$  and  $\rho_2$  in Eqs. 2.36 and 2.37 respectively. For all values of  $\theta$  and  $\phi$ ,

$$\mathbf{E}(\rho_1) = \left\{ \left( \begin{array}{c} e^{3i\phi} \\ -\frac{\sqrt{5}-1}{2} e^{2i\phi} \\ -\frac{\sqrt{5}-1}{2} e^{i\phi} \\ 1 \end{array} \right), \left( \begin{array}{c} -e^{3i\phi} \\ -\frac{\sqrt{5}-1}{2} e^{2i\phi} \\ -\frac{\sqrt{5}-1}{2} e^{i\phi} \\ 1 \end{array} \right), \left( \begin{array}{c} -e^{3i\phi} \\ \frac{\sqrt{5}+1}{2} e^{2i\phi} \\ -\frac{\sqrt{5}+1}{2} e^{i\phi} \\ 1 \end{array} \right), \left( \begin{array}{c} e^{3i\phi} \\ \frac{\sqrt{5}+1}{2} e^{2i\phi} \\ \frac{\sqrt{5}+1}{2} e^{i\phi} \\ 1 \end{array} \right) \right\}, \quad (2.39)$$

and

$$\mathbf{E}(\rho_2) = \left\{ \left( \begin{array}{c} -e^{3i\phi} \\ -\frac{\sqrt{5}-1}{2}e^{2i\phi} \\ \frac{\sqrt{5}-1}{2}e^{i\phi} \\ 1 \end{array} \right), \left( \begin{array}{c} e^{3i\phi} \\ -\frac{\sqrt{5}-1}{2}e^{2i\phi} \\ -\frac{\sqrt{5}-1}{2}e^{i\phi} \\ 1 \end{array} \right), \left( \begin{array}{c} e^{3i\phi} \\ \frac{\sqrt{5}+1}{2}e^{2i\phi} \\ \frac{\sqrt{5}+1}{2}e^{i\phi} \\ 1 \end{array} \right), \left( \begin{array}{c} -e^{3i\phi} \\ \frac{\sqrt{5}+1}{2}e^{2i\phi} \\ -\frac{\sqrt{5}+1}{2}e^{i\phi} \\ 1 \end{array} \right) \right\}, \quad (2.40)$$

and the ordering of the eigenvectors correspond to the eigenvalues in Eq 2.38. As is evident, there is no  $\theta$  dependence in these vectors. Accordingly, it is no surprise that they cannot provide any information about the optimal measurement that appears in the calculation of discord.

As mentioned before, and reiterated by this example, there is a gap between discord and entanglement. Certainly, zero discord states are separable. The converse is, in general *not* true for mixed quantum states. In light of this, a valid question is whether there is a bound on the value of discord for separable states. This result can be used indirectly to detect an entangled state. In the following section we inquire about the value of quantum discord for separable states.

## 2.2.2 Discord for separable states

Let us consider a separable state

$$\rho_{AB} = \sum_i p_i \rho_i^A \otimes \rho_i^B,$$

whereby

$$\rho_A = \sum_i p_i \rho_i^A \quad \text{and} \quad \rho_B = \sum_i p_i \rho_i^B.$$

The quantum discord of a quantum state is defined as

$$\mathcal{D} = H(\rho_A) - H(\rho_{AB}) + \min_{\{\Pi_j\}} \sum_j q_j H(\rho_{B|j}),$$

where

$$\rho_{B|j} = \frac{\text{tr}_A(\Pi_j \rho_{AB} \Pi_j)}{q_j}, \quad q_j = \text{tr}_{A,B}(\rho_{AB} \Pi_j).$$

It is known that for a separable state

$$H(\rho_{AB}) \geq H(\rho_A) \quad \text{and} \quad H(\rho_{AB}) \geq H(\rho_B), \quad (2.41)$$

whereby

$$\begin{aligned} \mathcal{D} &= H(\rho_A) - H(\rho_{AB}) + \min_{\{\Pi_j\}} \sum_j q_j H(\rho_{B|j}) \\ &\leq \min_{\{\Pi_j\}} \sum_j q_j H(\rho_{B|j}) \\ &\leq \min_{\{\Pi_j\}} H\left(\sum_j q_j \rho_{B|j}\right), \end{aligned} \quad (2.42)$$

where the last inequality follows from the concavity of  $H$ . Now

$$\begin{aligned} \sum_j q_j \rho_{B|j} &= \sum_j \text{tr}_A(\Pi_j \rho_{AB} \Pi_j) = \sum_j \text{tr}_A(\Pi_j \rho_{AB}) \\ &= \text{tr}_A\left(\left(\sum_j \Pi_j\right) \rho_{AB}\right) = \rho_B. \end{aligned} \quad (2.43)$$

Therefore, we have,

$$\mathcal{D} \leq H(\rho_B).$$

Of course, one can choose not to invoke the separability condition first, and rather say that (since  $\mathcal{J} \geq 0$ )

$$\mathcal{D} \leq H(\rho_A) + H(\rho_B) - H(\rho_{AB}), \quad (2.44)$$

and then employ (2.41) to conclude

$$\mathcal{D} \leq \min(H(A), H(B), \mathcal{I}(A : B)), \quad (2.45)$$

which is probably a more sensible upper bound for separable states. This, in fact, leads to the conclusion that  $\mathcal{D} = 0$  for pure separable states.

## 2.3 Quantum discord in quantum communication

The centerpiece of this thesis is undoubtedly mixed-state quantum information. Nonetheless, we have an instance from quantum communication where quantum discord might have a role to play. We will not delve into a general analysis of this; rather we will point out the role of quantum discord through a simple example. We also thank W. H. Zurek for pointing out the problem.

The phenomenon we have in mind is the distribution of entanglement. The significance of this task cannot be overemphasized in quantum information science. To be able to entangle two distant particles is at the heart of quantum communication and computation. That this can be achieved via a third mediating particle which remains separable at all times from the other two was shown in [15]. Let us, in very brief, demonstrate this claim.

We start with a tripartite state  $\rho_{abc}$ , where  $a$  and  $b$  denote the systems of Alice and Bob, while  $c$  is the mediator particle or channel, which starts out in Alice's possession. In our particular example, taken from [15],

$$\rho_{abc} = \frac{1}{6} \sum_{k=0}^3 |\Psi_k, \Psi_{-k}, 0\rangle \langle \Psi_k, \Psi_{-k}, 0| + \frac{1}{6} \sum_{i=0}^1 |i, i, 1\rangle \langle i, i, 1|, \quad (2.46)$$

where

$$|\Psi_k\rangle = \frac{|0\rangle + e^{ik\pi/2} |1\rangle}{\sqrt{2}}.$$

This state is separable between all three parties as it is a convex combination of



Then the spectrum of the partial transpose of  $\sigma_{abc}$  with respect to  $a$  is

$$\left\{ -\frac{1}{6}, \frac{1}{6}, \frac{1}{6}, \frac{1}{6}, \frac{1}{6}, \frac{1}{6}, \frac{1}{6}, \frac{1}{6} \right\},$$

which has a negative eigenvalue. Hence, the  $a$ - $bc$  split actually contains entanglement.

Once Bob receives the particle, he does a CNOT between  $b$  and  $c$ , with the former as the control. The resulting state is

$$\tau_{abc} = \frac{1}{3} |\Phi^+\rangle \langle \Phi^+| \otimes |0\rangle \langle 0| + \frac{2}{3} \mathbb{I}_{ab} \otimes |1\rangle \langle 1|, \quad (2.50)$$

where  $|\Phi^+\rangle = (|00\rangle + |11\rangle)/\sqrt{2}$  is the maximally entangled state. In the standard product basis,

$$\tau_{abc} = \frac{1}{6} \begin{pmatrix} 1 & 0 & 0 & 0 & 0 & 0 & 1 & 0 \\ 0 & 1 & 0 & 0 & 0 & 0 & 0 & 0 \\ 0 & 0 & 0 & 0 & 0 & 0 & 0 & 0 \\ 0 & 0 & 0 & 1 & 0 & 0 & 0 & 0 \\ 0 & 0 & 0 & 0 & 0 & 0 & 0 & 0 \\ 0 & 0 & 0 & 0 & 0 & 1 & 0 & 0 \\ 1 & 0 & 0 & 0 & 0 & 0 & 1 & 0 \\ 0 & 0 & 0 & 0 & 0 & 0 & 0 & 1 \end{pmatrix}. \quad (2.51)$$

The particle  $c$  is still separable from the other two particles, which we have managed to get entangled. However, the  $a$ - $bc$  split and the  $b$ - $ac$  split have the same amount of entanglement as in the  $a$ - $bc$  split of  $\sigma_{abc}$ . One uses this entanglement to get a Bell state by measuring  $c$  in the standard basis. On average, we can thus use this 1 ebit of entanglement  $1/3$  of the time for any desired purpose.

Having demonstrated our claim, we now invest in a little introspection. If entanglement is to behave as a resource, one would expect some nature of conservation law to hold. At least, we should be able to argue that the entanglement we generated was a result of some form of expenditure. We performed two CNOT gates, which generates some entanglement in the intermediate states. However, we are at



a loss to take this any further due to a lack of our ability quantifying entanglement, particularly in entropy units. We will now show that quantum discord will provide a natural accounting of the resources and a more soothing resolution.

Let us consider measurements on  $c$ , as that is the most contentious party in our protocol. The projectors are

$$\Pi_1 = \mathbb{I}_{ab} \otimes \frac{\mathbb{I}_c + \boldsymbol{\alpha} \cdot \boldsymbol{\sigma}}{2}, \quad \Pi_2 = \mathbb{I}_{ab} \otimes \frac{\mathbb{I}_c - \boldsymbol{\alpha} \cdot \boldsymbol{\sigma}}{2}, \quad (2.52)$$

with  $\alpha_1 = \sin \theta \cos \phi$ ,  $\alpha_2 = \sin \theta \sin \phi$ ,  $\alpha_3 = \cos \theta$  as usual.

We will start with the state  $\rho_{abc}$ . A simple calculation shows

$$p_1 = \frac{3 + \cos \theta}{6}, \quad p_2 = \frac{3 - \cos \theta}{6},$$

and that the spectrum of the reduced operators are

$$\boldsymbol{\lambda}(\rho_{ab}^1) = \left\{ 0, 0, 0, 0, \frac{1}{2}, \frac{1 + \cos \theta}{2(3 + \cos \theta)}, \frac{1 + \cos \theta}{2(3 + \cos \theta)}, \frac{1 - \cos \theta}{2(3 + \cos \theta)} \right\}, \quad (2.53)$$

$$\boldsymbol{\lambda}(\rho_{ab}^2) = \left\{ 0, 0, 0, 0, \frac{1}{2}, \frac{1 + \cos \theta}{2(3 - \cos \theta)}, \frac{1 - \cos \theta}{2(3 - \cos \theta)}, \frac{1 - \cos \theta}{2(3 - \cos \theta)} \right\}. \quad (2.54)$$

We immediately see that the minimization in this case is a single variable affair ( $\phi$  having dropped out), and this quickly leads to (for  $\theta = 0$ )

$$\mathcal{D}(\rho_{abc}) = 0. \quad (2.55)$$

Next, let us calculate the discord for the state  $\sigma_{abc}$ . We find

$$p_1 = p_2 = \frac{1}{2},$$

and that the spectrum of the reduced operators is

$$\boldsymbol{\lambda}(\sigma_{ab}^1) = \boldsymbol{\lambda}(\sigma_{ab}^2) = \left\{ 0, 0, 0, 0, \frac{1}{3} \cos^2 \frac{\theta}{2}, \frac{1}{3} \sin^2 \frac{\theta}{2}, \frac{2 + \sin \theta}{6}, \frac{2 - \sin \theta}{6} \right\}. \quad (2.56)$$

Again, the minimization involves one variable, whose minimum is attained for  $\theta = 0$ , as

$$\mathcal{D}(\sigma_{abc}) = \frac{1}{3}. \quad (2.57)$$

Finally, a similar calculation for  $\tau_{abc}$  provides

$$\mathcal{D}(\tau_{abc}) = 0. \tag{2.58}$$

The three results, in Eqs 2.55, 2.57, 2.58 lead us to very striking conclusions, *viz.*,

1. The amount of discord generated is exactly equal to the average amount of entanglement we can extract in the next stage of the protocol.
2. The fact there is no discord at the end of the protocol is circumstantial evidence that the discord is somehow ‘converted’ into entanglement.

This might be construed to imply that discord is a more fundamental resource for quantum information than entanglement. In our view, however, further investigation is called for before such conclusions are drawn. Indeed, a genuine measure of tripartite entanglement may help clear up the resource nature of entanglement in the protocol. Another line of investigation would be to demonstrate the qualitative and/or quantitative role of discord in the general scheme of entanglement distribution [15], of which we presented just an example, or in other mixed-state protocols involving entanglement. A third line of research would be to arrive at an independent operational interpretational for quantum discord. An interpretation of this nature will demonstrate the power, utility and resourcefulness of quantum discord.

With these statements, we will move on to our study of mixed-state quantum computation in Chapters 3 and 4.

## Chapter 3

# Entanglement in the DQC1 model

*Why then, can one desire too much of a good thing ?*

-William Shakespeare in *As You Like It*

The purpose of this chapter is to investigate the existence of and amount of entanglement in the DQC1 circuit that is used to estimate the normalized trace. The DQC1 model consists of a *special qubit* (qubit 0) in the initial state  $|0\rangle\langle 0| = \frac{1}{2}(I_1 + Z)$ , where  $Z$  is a Pauli operator, along with  $n$  other qubits in the completely mixed state,  $I_n/2^n$ , which we call the *unpolarized qubits*. The circuit consists of a Hadamard gate on the special qubit followed by a controlled unitary on the remaining qubits [57]:

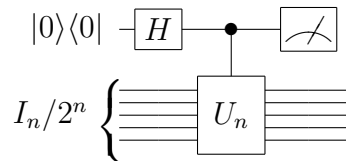


Figure 3.1: The DQC1 circuit

After these operations, the state of the  $n + 1$  qubits becomes

$$\rho_{n+1} = \frac{1}{2N} \left( |0\rangle\langle 0| \otimes I_n + |1\rangle\langle 1| \otimes I_n + |0\rangle\langle 1| \otimes U_n^\dagger + |1\rangle\langle 0| \otimes U_n \right) = \frac{1}{2N} \begin{pmatrix} I_n & U_n^\dagger \\ U_n & I_n \end{pmatrix}, \quad (3.1)$$

where  $N = 2^n$ . The information about the normalized trace of  $U_n$  is encoded in the expectation values of the Pauli operators  $X$  and  $Y$  of the special qubit, i.e.,  $\langle X \rangle = \text{Re}[\text{tr}(U_n)]/2^n$  and  $\langle Y \rangle = -\text{Im}[\text{tr}(U_n)]/2^n$ .

To read out the desired information, say, about the real part of the normalized trace, one runs the circuit repeatedly, each time measuring  $X$  on the special qubit at the output. The measurement results are drawn from a distribution whose mean is the real part of the normalized trace and whose variance is bounded above by 1. After  $L$  runs, one can estimate the real part of the normalized trace with an accuracy  $\epsilon \sim 1/\sqrt{L}$ . Thus, to achieve accuracy  $\epsilon$  requires that the circuit be run  $L \sim 1/\epsilon^2$  times. More precisely, what we mean by estimating with fixed accuracy is the following: let  $P_e$  be the probability that the estimate is farther from the true value than  $\epsilon$ ; then the required number of runs is  $L \sim \ln(1/P_e)/\epsilon^2$ . That the number of runs required to achieve a fixed accuracy does not scale with number of qubits and scales logarithmically with the error probability is what is meant by saying that the DQC1 circuit provides an efficient method for estimating the normalized trace.

Throughout much of our analysis, we use a generalization of the DQC1 circuit, in which the initial pure state of the special qubit is replaced by the mixed state  $\frac{1}{2}(I_1 + \alpha Z)$ , which has polarization  $\alpha$ , giving an overall initial state

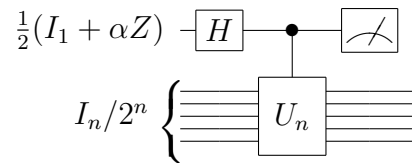


Figure 3.2: The DQC1 circuit with arbitrary polarization

$$\rho_i = \frac{1}{2N}(I_1 + \alpha Z) \otimes I_n = \frac{1}{2N} \left[ I_{n+1} + \alpha \begin{pmatrix} I_n & 0 \\ 0 & -I_n \end{pmatrix} \right]. \quad (3.2)$$

We generally assume that  $\alpha \geq 0$ , except where we explicitly note otherwise. After the circuit is run, the system state becomes

$$\rho_{n+1}(\alpha) = \frac{1}{2N} \left[ I_{n+1} + \alpha \begin{pmatrix} 0 & U_n^\dagger \\ U_n & 0 \end{pmatrix} \right] = \frac{1}{2N} \begin{pmatrix} I_n & \alpha U_n^\dagger \\ \alpha U_n & I_n \end{pmatrix}. \quad (3.3)$$

The effect of subunity polarization is to reduce the expectation values of  $\langle X \rangle$  and  $\langle Y \rangle$  by a factor of  $\alpha$ , thereby making it more difficult to estimate the normalized trace. Specifically, the number of runs required to estimate the normalized trace becomes  $L \sim \ln(1/P_e)/\alpha^2 \epsilon^2$ . Reduced polarization introduces an additional overhead, but as long as the special qubit has nonzero polarization, the model still provides an efficient estimation of the normalized trace. What we are dealing with is really the “power of even the tiniest fraction of a qubit.”

For  $n + 1$  qubits, *all* states contained in a ball of radius  $r_{n+1}$  centered at the completely mixed state are separable [9, 39] (distance is measured by the Hilbert-Schmidt norm). Unitary evolution leaves the distance from the completely mixed state fixed, so at all times during the circuit in Fig. (3.2), the system state is a fixed distance  $\sqrt{\text{tr}(\rho_i - I_{n+1}/2N)^2} = \alpha 2^{-(n+1)/2}$  from the completely mixed state. This suggests that with  $\alpha$  small enough, there might be an exponential speedup with demonstrably separable states. This suggestion doesn’t pan out, however, because the radius of the separable ball decreases exponentially faster than  $2^{-(n+1)/2}$ . The best known lower bound on  $r_n$  is  $2 \times 6^{-n/2}$  [40]; for the system state to be contained in a ball given by this lower bound, we need  $\alpha \leq 2 \times 3^{-(n+1)/2}$ . The exponential decrease of  $\alpha$  means that an exponentially increasing number of runs is required to estimate the normalized trace with fixed accuracy. More to the point, the possibility that the actual radius of the separable ball might decrease slowly enough to avoid an exponential number of runs is ruled out by the existence of a family of  $n$ -qubit entangled states found by Dür *et al.* [24], which establishes an upper bound on  $r_n$

that goes as  $2 \times 2^{-n}$  for large  $n$ , implying that  $\alpha \leq 2 \times 2^{-(n+1)/2}$  if the system state is to be in the ball given by the upper bound. These considerations do not demonstrate the impossibility of an exponential speedup using separable states, but they do rule out the possibility of finding such a speedup within the maximal separable ball about the completely mixed state.

We are thus motivated to look for entanglement in states of the form in Eq. (3.3), for at least some unitary operators  $U_n$ . Initial efforts in this direction are not encouraging. It is clear from the start that the marginal state of the  $n$  unpolarized qubits remains completely mixed, so these qubits are not entangled among themselves. Moreover, in the state in Eq. (3.3), as was shown in Ref. [66], the special qubit is unentangled with the  $n$  unpolarized qubits, no matter what  $U_n$  is used. To see this, one plugs the eigendecomposition of the unitary,  $U_n = \sum_j e^{i\phi_j} |e_j\rangle\langle e_j|$ , into the expression for  $\rho_{n+1}(\alpha)$ . This gives a separable decomposition

$$\rho_{n+1}(\alpha) = \frac{1}{2N} \sum_j (|a_j\rangle\langle a_j| + |b_j\rangle\langle b_j|) \otimes |e_j\rangle\langle e_j|, \quad (3.4)$$

where  $|a_j\rangle = \cos\theta|0\rangle + e^{i\phi_j} \sin\theta|1\rangle$  and  $|b_j\rangle = \sin\theta|0\rangle + e^{i\phi_j} \cos\theta|1\rangle$ , with  $\sin 2\theta = \alpha$ .

No entanglement of the special qubit with the rest and no entanglement among the rest—where then are we to find any entanglement? We look for entanglement relative to other divisions of the qubits into two parts. In such bipartite divisions the special qubit is grouped with a subset of the unpolarized qubits. To detect entanglement between the two parts, we use the Peres-Horodecki partial transpose criterion [64, 45], and we quantify whatever entanglement we find using a closely related entanglement monotone which we call the *multiplicative negativity* [80]. The Peres-Horodecki criterion and the multiplicative negativity do not reveal all entanglement—they can miss what is called bound entanglement—but we are nonetheless able to demonstrate the existence of entanglement in states of the form in Eq. (3.1) and Eq. (3.3). For convenience, we generally refer to the multiplicative negativity simply as the negativity. The reader should note, as we discuss in Sec. 2.1, that the

term “negativity” was originally applied to an entanglement measure that is closely related to, but different from the multiplicative negativity.

The amount of entanglement depends, of course, on the unitary operator  $U_n$  and on the bipartite division. We present three results in this regard. First, in Sec. 3.2, we construct a family of unitaries  $U_n$  such that for  $\alpha > 1/2$ ,  $\rho_{n+1}(\alpha)$  is entangled for all bipartite divisions that put the first and last unpolarized qubits in different parts, and we show that for all such divisions, the negativity is  $(2\alpha + 3)/4$  for  $\alpha \geq 1/2$  ( $5/4$  for  $\alpha = 1$ ), independent of  $n$ . Second, in Sec. 3.3, we present numerical evidence that the state  $\rho_{n+1}$  of Eq. (3.1) is entangled for typical unitaries, i.e., those created by random quantum circuits. For  $n+1 = 5, \dots, 10$ , we find average negativities between 1.155 and just above 1.16 for the splitting that puts  $\lfloor n/2 \rfloor$  of the unpolarized qubits with qubit 0. Third, in Sec. 3.4, we show that for all unitaries and all bipartite divisions of the  $n + 1$  qubits, the negativity of  $\rho_{n+1}(\alpha)$  is bounded above by the constant  $\sqrt{1 + \alpha^2}$  ( $\sqrt{2} \simeq 1.414$  for  $\alpha = 1$ ), independent of  $n$ . Thus, when  $n$  is large, the negativity achievable by the DQC1 circuit (3.1) becomes a vanishingly small fraction of the maximum negativity,  $\sim 2^{n/2}$ , for roughly equal bipartite divisions.

The layout of this chapter is as follows. In Sec. 3.1 we examine the classical problem of estimating the normalized trace of a unitary. In Sec. 2.1 we reviewed the pertinent properties of the negativity. We apply these to obtain our three key results in Secs. 3.2–3.4. We conclude in Sec. 3.5 and prove a brief Lemma in Appendix B. Throughout we use  $\check{A}$  to stand for the partial transpose of an operator  $A$  relative to a particular bipartite tensor-product structure, and we rely on context to make clear which bipartite division we are using at any particular point in this chapter.

### 3.1 Classical evaluation of the trace

Every fair judgement on the power of quantum computation to solve a mathematical problem must be made relative to the best known classical algorithm to solve the same. In that spirit, this section briefly outlines a classical method for estimating the trace of a unitary operator that can be implemented efficiently in terms of quantum gates, and we indicate why this appears to be a problem that is exponentially hard in the number of qubits.

The trace of a unitary matrix  $U_n \equiv U$  is the sum over the diagonal matrix elements of  $U$ :

$$\text{tr}(U) = \sum_{\mathbf{a}} \langle \mathbf{a} | U | \mathbf{a} \rangle . \quad (3.5)$$

Here  $\mathbf{a}$  is a bit string that specifies a computational-basis state of the  $n$  qubits. By factoring  $U$  into a product of elementary gates from a universal set and inserting a resolution of the identity between all the gates, we can write  $\text{tr}(U)$  as a sum over the amplitudes of Feynman paths. A difficulty with this approach is that the sum must be restricted to paths that begin and end in the same state. We can circumvent this difficulty by preceding and succeeding  $U$  with a Hadamard gate on all the qubits. This does not change the trace, but does allow us to write it as

$$\text{tr}(U) = \sum_{\mathbf{a}, \mathbf{b}, \mathbf{c}} \langle \mathbf{a} | H^{\otimes n} | \mathbf{b} \rangle \langle \mathbf{b} | U | \mathbf{c} \rangle \langle \mathbf{c} | H^{\otimes n} | \mathbf{a} \rangle = \frac{1}{2^n} \sum_{\mathbf{a}, \mathbf{b}, \mathbf{c}} (-1)^{\mathbf{a} \cdot (\mathbf{b} + \mathbf{c})} \langle \mathbf{b} | U | \mathbf{c} \rangle . \quad (3.6)$$

Now if we insert a resolution of the identity between the elementary gates, we get  $\text{tr}(U)$  written as an unrestricted sum over Feynman-path amplitudes, with an extra phase that depends on the initial and final states.

Following Dawson *et al.* [19], we consider two universal gate sets: (i) the Hadamard gate  $H$ , the  $\pi/4$  gate  $T$ , and the controlled-NOT gate and (ii)  $H$  and the Toffoli gate. With either of these gate sets, most of the Feynman paths have zero amplitude. Dawson *et al.* [19] introduced a convenient method, which we describe briefly now, for



including only those paths with nonzero amplitude. One associates with each wire in the quantum circuit a classical bit value corresponding to a computational basis state. The effect of an elementary gate is to change, deterministically or stochastically, the bit values at its input and to introduce a multiplicative amplitude. The two-qubit controlled-NOT gate changes the input control bit  $x$  and target bit  $y$  deterministically to output values  $x$  and  $y \oplus x$ , while introducing only unit amplitudes. Similarly, the three-qubit Toffoli gate changes the input control bits  $x$  and  $y$  and target bit  $z$  deterministically to  $x$ ,  $y$ , and  $z \oplus xy$ , while introducing only unit amplitudes. The  $T$  gate leaves the input bit value  $x$  unchanged and introduces a phase  $e^{ix\pi/4}$ . The Hadamard gate changes the input bit value  $x$  stochastically to an output value  $y$  and introduces an amplitude  $(-1)^{xy}/\sqrt{2}$ .

The classical bit values trace out the allowed Feynman paths, and the product of the amplitudes introduced at the gates gives the overall amplitude of the path. In our application of evaluating the trace (3.6), a path is specified by  $n$  input bit values (which are identical to the output bit values),  $n$  random bit values introduced by the initial Hadamard gates, and  $h$  random bit values introduced at the  $h$  Hadamard gates required for the implementation of  $U$ . This gives a total of  $2n + h$  bits to specify a path and thus  $2^{2n+h}$  allowed paths. We let  $\mathbf{x}$  denote collectively the  $2n + h$  path bits.

If we apply the gate rules to a Hadamard-Toffoli circuit, the only gate amplitudes we have to worry about are the  $\pm 1/\sqrt{2}$  amplitudes introduced at the Hadamard gates. There being no complex amplitudes, the trace cannot be complex. Indeed, for this reason, achieving universality with the  $H$ -Toffoli gate set requires the use of a simple encoding, and we assume for the purposes of our discussion that this encoding has already been taken into account. With all this in mind, we can write the trace (3.6) as a sum over the allowed paths,

$$\mathrm{tr}(U) = \frac{1}{2^{n+h/2}} \sum_{\mathbf{x}} (-1)^{\psi(\mathbf{x})} . \quad (3.7)$$

Here  $\psi(\mathbf{x})$  is a polynomial over  $\mathbb{Z}_2$ , specifically, the mod-2 sum of the products of input and output bit values at each of the Hadamard gates. The downside is that a string of Toffoli gates followed by a Hadamard can lead to a polynomial that is high order in the bit values. As pointed out by Dawson *et al.* [19], we can deal with this problem partially by putting a pair of Hadamards on the target qubit after each Toffoli gate, thus replacing the quadratic term in the output target bit with two new random variables and preventing the quadratic term from iterating to higher order terms in subsequent Toffoli gates. In doing so, we are left with a cubic term in  $\psi(\mathbf{x})$  from the amplitude of the first Hadamard. The upshot is that we can always make  $\psi(\mathbf{x})$  a cubic polynomial.

Notice now that we can rewrite the trace as

$$\mathrm{tr}(U) = \frac{1}{2^{n+h/2}} \left[ \binom{\text{number of } \mathbf{x} \text{ such that } \psi(\mathbf{x}) = 0}{\text{that } \psi(\mathbf{x}) = 0} - \binom{\text{number of } \mathbf{x} \text{ such that } \psi(\mathbf{x}) = 1}{\text{that } \psi(\mathbf{x}) = 1} \right], \quad (3.8)$$

thus reducing the problem of evaluating the trace exactly to counting the number of zeroes of the cubic polynomial  $\psi(\mathbf{x})$ . This is a standard problem from computational algebraic geometry, and it is known that counting the number of zeroes of a general cubic polynomial over any finite field is  $\#\mathbf{P}$  complete [25]. It is possible that the polynomials that arise from quantum circuits have some special structure that can be exploited to give an efficient algorithm for counting the number of zeroes, but in the absence of such structure, there is no efficient classical algorithm for computing the trace exactly unless the classical complexity hierarchy collapses and *all* problems in  $\#\mathbf{P}$  are efficiently solvable on a classical computer.

Of course, it is not our goal to compute the trace exactly, since the quantum circuit only provides an efficient method for estimating the normalized trace to fixed accuracy. This suggests that we should estimate the normalized trace by sampling the amplitudes of the allowed Feynman paths. The normalized trace,

$$\frac{\mathrm{tr}(U)}{2^n} = \frac{1}{2^{2n+h}} \sum_{\mathbf{x}} 2^{h/2} (-1)^{\psi(\mathbf{x})}, \quad (3.9)$$

which lies between  $-1$  and  $+1$ , can be regarded as the average of  $2^{2n+h}$  quantities whose magnitude,  $2^{h/2}$ , is exponentially large in the number of Hadamard gates. To estimate the average with fixed accuracy requires a number of samples that goes as  $2^h$ , implying that this is not an efficient method for estimating the normalized trace. The reason the method is not efficient is pure quantum mechanics, i.e., that the trace is a sum of amplitudes, not probabilities.

If we apply the gate rules to a Hadamard- $T$ -controlled-NOT circuit, the bit value on each wire in the circuit is a mod-2 sum of appropriate bit values in  $\mathbf{x}$ , but now we have to worry about the amplitudes introduced by the Hadamard and  $T$  gates. The trace (3.6) can be written as

$$\mathrm{tr}(U) = \frac{1}{2^{n+h/2}} \sum_{\mathbf{x}} e^{i(\pi/4)\chi(\mathbf{x})} (-1)^{\phi(\mathbf{x})}. \quad (3.10)$$

Here  $\phi(\mathbf{x})$  is a polynomial over  $\mathbb{Z}_2$ , obtained as the mod-2 sum of the products of input and output bit values at each of the Hadamard gates. Since the output value is a fresh binary variable and the input value is a mod-2 sum of bit values in  $\mathbf{x}$ ,  $\phi(\mathbf{x})$  is a purely quadratic polynomial over  $\mathbb{Z}_2$ . The function  $\chi(\mathbf{x})$  is a mod-8 sum of the input bit values to all of the  $T$  gates. Since these input bit values are mod-2 sums of bit values in  $\mathbf{x}$ ,  $\chi(\mathbf{x})$  is linear in bit values, but with an unfortunate mixture of mod-2 and mod-8 addition. We can get rid of this mixture by preceding each  $T$  gate with a pair of Hadamards, thus making the input to the every  $T$  gate a fresh binary variable. With this choice,  $\chi(\mathbf{x})$  becomes a mod-8 sum of appropriate bit values from  $\mathbf{x}$ .

We can rewrite the sum (3.10) in the following way:

$$\mathrm{tr}(U) = \frac{1}{2^{n+h/2}} \sum_{j=0}^7 e^{i\frac{\pi}{4}j} \left[ \left( \text{number of } \mathbf{x} \text{ such that } \begin{array}{l} \chi(\mathbf{x}) = j \text{ and } \phi(\mathbf{x}) = 0 \end{array} \right) - \left( \text{number of } \mathbf{x} \text{ such that } \begin{array}{l} \chi(\mathbf{x}) = j \text{ and } \phi(\mathbf{x}) = 1 \end{array} \right) \right]. \quad (3.11)$$

Thus the problem now reduces to finding simultaneous (binary) solutions to the purely quadratic  $\mathbb{Z}_2$  polynomial  $\phi(\mathbf{x})$  and the purely linear  $\mathbb{Z}_8$  polynomial  $\chi(\mathbf{x})$ . One

has to be careful here to note that we are only interested in binary solutions, so we are not solving  $\chi(\mathbf{x}) = j$  over all values in  $\mathbb{Z}_8$ . The number of solutions of a purely quadratic polynomial over  $\mathbb{Z}_2$  can be obtained trivially [25], but the constraint over  $\mathbb{Z}_8$  means that one must count the number of solutions over a mixture of a field and a ring. The complexity class for this problem is not known, but given the equivalence to counting the number of solutions of a cubic polynomial over  $\mathbb{Z}_2$ , it seems unlikely that there is an efficient classical algorithm. Moreover, an attempt to estimate the normalized trace by sampling allowed paths obviously suffers from the problem already identified above.

## 3.2 Entanglement in the DQC1 circuit

In this section we present our main results. As outlined earlier, we will use the negativity as measure of entanglement. The negativity is the sum of the singular values of  $\check{\rho}$ . For states of the form we are interested in, given by Eq. (3.3), the negativity is determined by the singular values of the partial transpose of the unitary operator  $U_n$ . To see this, consider any bipartite division of the qubits. Performing the partial transpose on the part that does not include the special qubit, we have

$$\check{\rho}_{n+1}(\alpha) = \frac{1}{2N} \begin{pmatrix} I_n & \alpha \check{U}_n^\dagger \\ \alpha \check{U}_n & I_n \end{pmatrix}, \quad (3.12)$$

where  $\check{U}_n$  is the partial transpose of  $U_n$  relative to the chosen bipartite division. Notice that if we make our division between the special qubit and all the rest, then  $\check{U}_n = U_n^T$  is a unitary operator, and  $\check{\rho}_{n+1}(\alpha)$  is the quantum state corresponding to using  $U_n^T$  in the circuit (3.2); this shows that for this division, the negativity is 1, consistent with our earlier conclusion that the special qubit is not entangled with the other qubits. For a general division, we know there are unitaries  $V$  and  $W$  such that  $\check{U}_n = VSW$ , where  $S$  is the diagonal matrix of singular values  $s_j(\check{U}_n)$ . This allows

us to write

$$\check{\rho}_{n+1}(\alpha) = \begin{pmatrix} W^\dagger & 0 \\ 0 & V \end{pmatrix} \frac{1}{2N} \begin{pmatrix} I_n & \alpha S \\ \alpha S & I_n \end{pmatrix} \begin{pmatrix} W & 0 \\ 0 & V^\dagger \end{pmatrix}, \quad (3.13)$$

showing that  $\check{\rho}_{n+1}(\alpha)$  is a unitary transformation away from the matrix in the middle and thus has the same eigenvalues. The block structure of the middle matrix makes it easy to find these eigenvalues, which are given by  $[1 \pm \alpha s_j(\check{U}_n)]/2N$ . This allows us to put the negativity in the form

$$\mathcal{M}(\rho_{n+1}(\alpha)) = \frac{1}{2N} \sum_{j=1}^N |1 + \alpha s_j(\check{U}_n)| + |1 - \alpha s_j(\check{U}_n)| = \frac{1}{N} \sum_{j=1}^N \max(|\alpha| s_j(\check{U}_n), 1), \quad (3.14)$$

which is valid for both positive and negative values of  $\alpha$ . An immediate consequence of Eq. (3.14) is that  $\mathcal{M}(\rho_{n+1}(\alpha)) = \mathcal{M}(\rho_{n+1}(-\alpha))$ , as one would expect. Since  $\rho_{n+1}(\alpha)$  is a mixture of  $\rho_{n+1}(+1) = \rho_{n+1}$  and  $\rho_{n+1}(-1)$ , convexity tells us immediately that  $\mathcal{M}(\rho_{n+1}(\alpha)) \leq \mathcal{M}(\rho_{n+1})$ , i.e., that a mixed input for the special qubit cannot increase the negativity over that for a pure input. More generally, we have that the negativity cannot decrease at any point as  $\alpha$  increases from 0 to 1.

As the first result of this section, we construct a family of unitaries  $U_n$  that produce global entanglement in the DQC1 circuit (3.1). For  $\alpha = 1$ , the negativity produced by this family is equal to  $5/4$ , independent of  $n$ , for all bipartite divisions that put the first and last unpolarized qubits in different parts. We conjecture that this is the maximum negativity that can be achieved in a circuit of the form (3.1).

Before the measurement, the output state of the circuit (3.2) is given by Eq. (3.3). To construct the unitaries  $U_n$ , we first introduce a two-qubit unitary matrix

$$U_2 \equiv \begin{pmatrix} A_1 & C_1 \\ D_1 & B_1 \end{pmatrix}, \quad (3.15)$$

where  $A_1$ ,  $B_1$ ,  $C_1$ , and  $D_1$  are single-qubit ( $2 \times 2$ ) matrices that must satisfy  $A_1^\dagger A_1 + D_1^\dagger D_1 = B_1^\dagger B_1 + C_1^\dagger C_1 = I_1$  and  $A_1^\dagger C_1 + D_1^\dagger B_1 = 0$  to ensure that  $U_2$  is unitary. The

$n$ -qubit unitary  $U_n$  is then defined by

$$\begin{aligned}
 U_n &\equiv \begin{pmatrix} I_{n-2} \otimes A_1 & X_{n-2} \otimes C_1 \\ X_{n-2} \otimes D_1 & I_{n-2} \otimes B_1 \end{pmatrix} \\
 &= |0\rangle\langle 0| \otimes I_{n-2} \otimes A_1 + |1\rangle\langle 1| \otimes I_{n-2} \otimes B_1 \\
 &\quad + |0\rangle\langle 1| \otimes X_{n-2} \otimes C_1 + |1\rangle\langle 0| \otimes X_{n-2} \otimes D_1 .
 \end{aligned} \tag{3.16}$$

Here we use  $X_1$ ,  $Y_1$ , and  $Z_1$  to denote single-qubit Pauli operators. A subscript  $k$  on the identity operator or a Pauli operator denotes a tensor product in which that operator acts on each of  $k$  qubits. If we adopt the convention that  $X_0 = I_0 = 1$ , then  $U_n$  reduces to  $U_2$  when  $n = 2$ . It is easy to design a quantum circuit that realizes  $U_n$ . The structure of the circuit is illustrated by the case of  $U_4$ : In general, the two-qubit

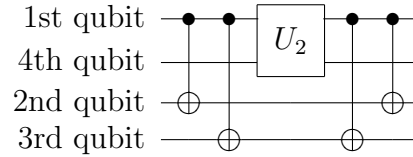


Figure 3.3: Unitary  $U_4$  that generates entanglement in DQC1 circuit for all  $n$

unitary  $U_2$ , acting on the first and last qubits, is bracketed by controlled-NOT gates from the first qubit, acting as control, to each of the other qubits, except the last, as targets.

Because  $I_1$  and  $X_1$  are invariant under transposition, it is clear from the form of  $U_n$  that in the state in Eq. (3.3), all qubits, except 0, 1, and  $n$ , are invariant under transposition. We can use this fact to find the negativity for all bipartite divisions. First consider any bipartite division that puts qubits 1 and  $n$  in the same part. There are two possibilities. If the special qubit is in the same part as qubits 1 and  $n$ , then partial transposition on the other part leaves  $\rho_{n+1}(\alpha)$  unchanged, so the negativity is 1. If the special qubit is not in the same part as 1 and  $n$ , then partial transposition on the part that includes 1 and  $n$  is the same as partial transposition of all the unpolarized qubits, a case we already know to have negativity equal to

1. We conclude that any bipartite division that puts 1 and  $n$  in the same part has negativity equal to 1.

Turn now to bipartite divisions that put qubits 1 and  $n$  in different parts. There are two cases to consider: (i) the special qubit is in the same part as qubit 1, and (ii) the special qubit is in the same part as qubit  $n$ . In case (i), partial transposition of the part that contains qubit  $n$  gives

$$\check{\rho}_{n+1}(\alpha) = \frac{1}{2N} \begin{pmatrix} I_n & \alpha \check{U}_n^\dagger \\ \alpha \check{U}_n & I_n \end{pmatrix} \quad \text{with} \quad \check{U}_n = \begin{pmatrix} I_{n-2} \otimes A_1^T & X_{n-2} \otimes C_1^T \\ X_{n-2} \otimes D_1^T & I_{n-2} \otimes B_1^T \end{pmatrix}. \quad (3.17)$$

The structure of  $\check{U}_n$  comes about due to the transposition over the last qubit in Eq. (3.16). In case (ii), partial transposition of the part that contains qubit 1 gives (here the transposition is over the first qubit in Eq. (3.16))

$$\check{\rho}_{n+1}(\alpha) = \frac{1}{2N} \begin{pmatrix} I_n & \alpha \check{U}_n^\dagger \\ \alpha \check{U}_n & I_n \end{pmatrix} \quad \text{with} \quad \check{U}_n = \begin{pmatrix} I_{n-2} \otimes A_1 & X_{n-2} \otimes D_1 \\ X_{n-2} \otimes C_1 & I_{n-2} \otimes B_1 \end{pmatrix}. \quad (3.18)$$

The basic structure of  $\check{\rho}_{n+1}(\alpha)$  is the same in both cases. Without changing the spectrum, we can reorder the rows and columns to block diagonalize  $\check{\rho}_{n+1}(\alpha)$  so that there are  $N/4$  blocks, each of which has the form

$$\frac{1}{2N} \begin{pmatrix} I_2 & \alpha \check{U}_2^\dagger \\ \alpha \check{U}_2 & I_2 \end{pmatrix} = \frac{4}{N} \check{\rho}_3(\alpha), \quad (3.19)$$

where  $\check{\rho}_3(\alpha)$  is the appropriate partial transpose of the three-qubit output state. Thus the spectrum of  $\check{\rho}_{n+1}(\alpha)$  is the same as the spectrum of  $\check{\rho}_3(\alpha)$ , except that each eigenvalue is reduced by a factor of  $4/N$ . In calculating the negativity, since each eigenvalue is  $(N/4)$ -fold degenerate, the reduction factor of  $4/N$  is cancelled by a degeneracy factor of  $N/4$ , leaving us with the fundamental result of our construction,

$$\mathcal{M}(\rho_{n+1}(\alpha)) = \mathcal{M}(\rho_3(\alpha)). \quad (3.20)$$

This applies to both cases of bipartite splittings that we are considering, showing that all divisions have the same negativity as the corresponding  $n = 2$  construction.

We now specialize to a particular choice of  $U_2$  given by

$$A_1 = \begin{pmatrix} 0 & 0 \\ 0 & 1 \end{pmatrix}, \quad B_1 = \begin{pmatrix} 1 & 0 \\ 0 & 0 \end{pmatrix}, \quad C_1 = \begin{pmatrix} 0 & 1 \\ 0 & 0 \end{pmatrix}, \quad \text{and} \quad D_1 = \begin{pmatrix} 0 & 0 \\ 1 & 0 \end{pmatrix}. \quad (3.21)$$

For this choice, the two cases of bipartite division lead to the same partial transpose.

The spectrum of

$$\check{\rho}_3(\alpha) = \frac{1}{8} \begin{pmatrix} I_1 & 0 & \alpha A_1 & \alpha D_1 \\ 0 & I_1 & \alpha C_1 & \alpha B_1 \\ \alpha A_1 & \alpha D_1 & I_1 & 0 \\ \alpha C_1 & \alpha B_1 & 0 & I_1 \end{pmatrix} \quad (3.22)$$

is

$$\text{Spec}(\check{\rho}_3(\alpha)) = \frac{1}{8}(1 + 2\alpha, 1, 1, 1, 1, 1, 1 - 2\alpha), \quad (3.23)$$

giving a negativity equal to 1 for  $\alpha \leq 1/2$  and a negativity

$$\mathcal{M}(\rho_{n+1}(\alpha)) = \mathcal{M}(\rho_3(\alpha)) = \frac{1}{4}(2\alpha + 3) \quad \text{for} \quad \alpha \geq 1/2. \quad (3.24)$$

This result shows definitively that the circuit can produce entanglement, at least for  $\alpha > 1/2$ . We stress that the negativity achieved by this family of unitaries is independent of  $n \geq 2$ .

For  $\alpha = 1$ , the negativity achieved by this family reduces to  $5/4$ . For large  $n$ , this amount of negativity is a vanishingly small fraction of the maximum possible negativity,  $\sim 2^{n/2}$ , for roughly equal divisions of the qubits. This raises the question whether it is possible for other unitaries to achieve larger negativities. A first idea might be to find two-qubit unitaries  $U_2$  that yield a higher negativity  $\mathcal{M}(\rho_3) = \mathcal{M}(\rho_{n+1})$  when plugged into the construction of this section, but the bounds we



find in Sec. 3.4 dispose of this notion, since they show that  $5/4$  is the maximum negativity that can be achieved for  $n = 2$ . Another approach would be to generalize the construction of this section in a way that is obvious from the circuit in Fig. (3.3), i.e., by starting with a  $k$ -qubit unitary in place of the two-qubit unitary of Fig. (3.3). Numerical investigation of the case  $k = 3$  has not turned up negativities larger than  $5/4$ . We conjecture that  $5/4$  is the maximum negativity that can be achieved by states of the form (3.1). Though we have not been able to prove this conjecture, we show in the next section that typical unitaries for  $n + 1 \leq 10$  achieve negativities less than  $5/4$  and in the following section that the negativity is rigorously bounded by  $\sqrt{2}$ .

We stress that we are not suggesting that the construction of this section, with  $U_2$  given by Eq. (3.21), achieves the maximum negativity for all values of  $\alpha$ , for that would mean that we believed that the negativity cannot exceed 1 for  $\alpha \leq 1/2$ , which we do not. Although we have not found entanglement for  $\alpha \leq 1/2$ , we suspect there are states with negativity greater than 1 as long as  $\alpha$  is large enough that  $\rho_{n+1}(\alpha)$  lies outside the separable ball around the maximally mixed state, i.e.,  $\alpha \geq 2^{(n+1)/2} r_{n+1}$ . The bound of Sec. 3.4 only says that  $\mathcal{M}(\rho_{n+1}(\alpha)) \leq \sqrt{1 + \alpha^2}$ , thus allowing negativities greater than 1 for all values of  $\alpha$  except  $\alpha = 0$ . Moreover, since the negativity does not detect bound entanglement, there could be entangled states that have a negativity equal to 1.

### 3.3 The average negativity of a random unitary

Having constructed a family of unitaries that yields a DQC1 state with negativity  $5/4$ , a natural question to ask is, “What is the negativity of a typical state produced by the circuit in Fig. (3.1)?” To address this question, we choose the unitary operator in the circuit in Fig. (3.1) at random and calculate the negativity. Of course, one must first define what it means for a unitary to be “typical” or “chosen at

random”. The natural measure for defining this is the Haar measure, which is the unique left-invariant measure for the group  $U(N)$  [13]. The resulting ensemble of unitaries is known as the Circular Unitary Ensemble, or CUE, and it is parameterized by the Hurwitz decomposition [68]. Although this is an exact parameterization, implementing it requires computational resources that grow exponentially in the size of the unitary [30]. To circumvent this, a pseudo-random distribution that requires resources growing polynomially in the size of the unitary was formulated and investigated in Ref. [30]. This is the distribution from which we draw our random unitaries, and we summarize the procedure for completeness.

We first define a random  $SU(2)$  unitary as

$$R(\theta, \phi, \chi) = \begin{pmatrix} e^{i\phi} \cos \theta & e^{i\chi} \sin \theta \\ -e^{-i\chi} \sin \theta & e^{-i\phi} \cos \theta \end{pmatrix}, \quad (3.25)$$

where  $\theta$  is chosen uniformly between 0 and  $\pi/2$ , and  $\phi$  and  $\chi$  are chosen uniformly between 0 and  $2\pi$ . A random unitary applied to each of the  $n$  qubits is then

$$R = \bigotimes_{i=1}^n R(\theta_i, \phi_i, \chi_i), \quad (3.26)$$

where a separate random number is generated for each variable at each value of  $i$ . Now define a mixing operator  $M$  in terms of nearest-neighbor  $Z \otimes Z$  couplings as

$$M = \exp \left( i \frac{\pi}{4} \sum_{j=1}^{n-1} Z^{(j)} \otimes Z^{(j+1)} \right). \quad (3.27)$$

The pseudo-random unitary is then given by

$$R_j M R_{j-1} \cdots M R_2 M R_1, \quad (3.28)$$

where  $j$  is a positive integer that depends on  $n$ , and each  $R_k$  is chosen randomly as described above. For a given  $n$ , the larger  $j$  is, the more accurately the pseudo-random unitary distribution resembles the actual CUE. From the results in Ref. [30],  $j = 40$  gives excellent agreement with the CUE for unitary operators on at least up to 10 qubits, so this is what we use in our calculations.

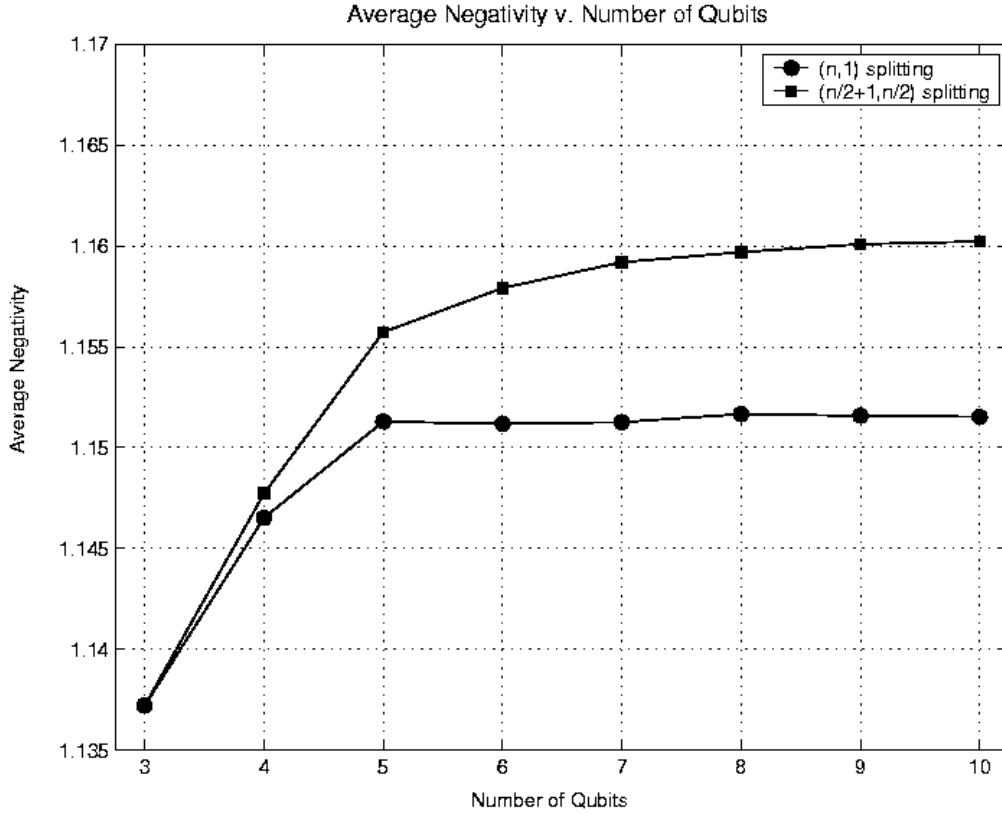


Figure 3.4: Average negativity of the state  $\rho_{n+1}$  of Eq. (3.1) ( $\alpha = 1$ ) for a randomly chosen unitary  $U_n$  for two different bipartite splittings,  $(n, 1)$  and  $(\lfloor n/2 \rfloor + 1, \lceil n/2 \rceil)$ . The  $(n, 1)$  splitting appears to reach an upper bound quickly, whereas the other splitting is still rising slowly at 10 qubits.

Due to boundary effects, not all bipartite splittings that put  $k$  unpolarized qubits in one part are equivalent. Nevertheless, we consider only bipartite divisions that split the qubits along horizontal lines placed at various points in the circuit of Eq. (3.1). We refer to the division that groups the last  $k$  qubits together as the  $(n + 1 - k, k)$  splitting. For  $\alpha = 1$ , we calculate the average negativity and standard deviation of a pseudo-random state  $\rho_{n+1}$  for two different bipartite splittings,  $(n, 1)$  and  $(\lfloor n/2 \rfloor + 1, \lceil n/2 \rceil)$ . These results are plotted in Figs. 3.4 and 3.5.

For  $n + 1 = 5, \dots, 10$ , the average negativity for the roughly equal splitting lies between 1.135 and just above 1.16. The standard deviation appears to converge

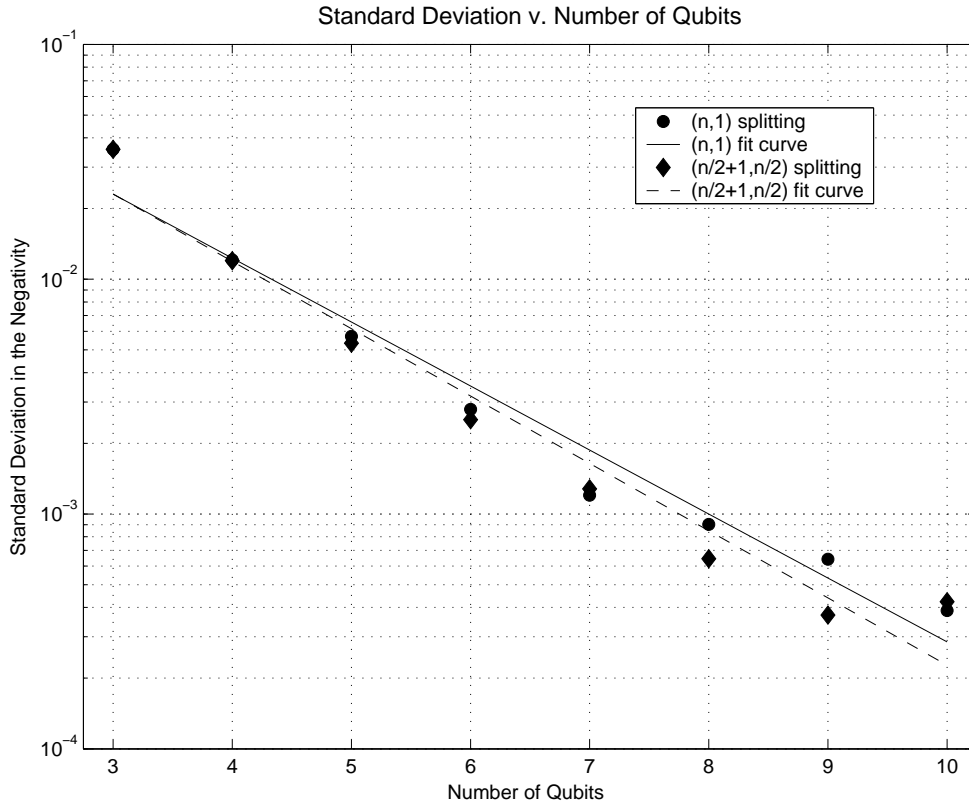


Figure 3.5: Semi-log plot of the standard deviation in the negativity of the randomly chosen state  $\rho_{n+1}$ . The fit curves show that the standard deviation is decaying exponentially, so that for large numbers of qubits, almost all unitaries give the same negativity.

exponentially to zero, as in Ref. [72], a behavior that is typical of asymptotically equivalent matrices. In addition, for  $9+1$  qubits, we calculate the average negativity and standard deviation for all nontrivial ( $k \neq n$ ) bipartite splittings  $(n+1-k, k)$ , and the results are shown in Fig. 3.6.

### 3.4 Bounds on the negativity

In this section, we return to allowing the special qubit in the circuit (3.2) to have initial polarization  $\alpha$ . Since the value of  $n$  is either clear from context or fixed, we

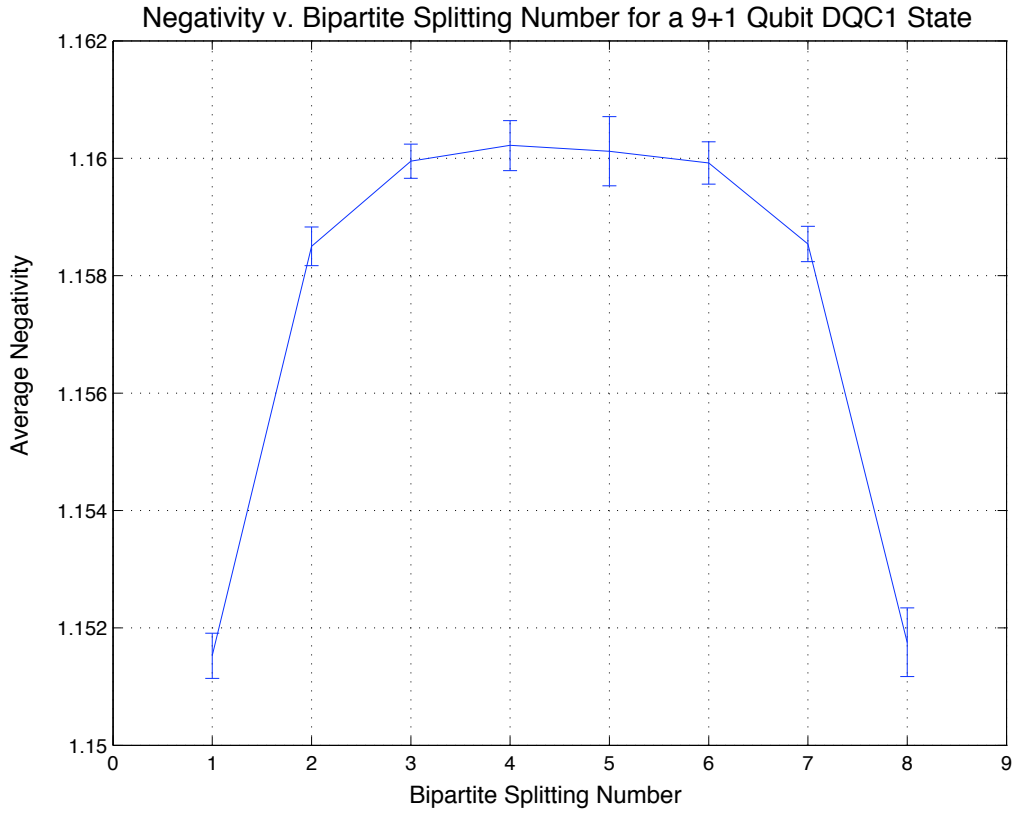


Figure 3.6: Average negativity of the state  $\rho_{10}$  of Eq. (3.1) ( $\alpha = 1$ ) for a randomly chosen unitary  $U_9$  as a function of bipartite splitting number  $k$  for bipartite splittings  $(10 - k, k)$ . The error bars give the standard deviations. The function attains a maximum when the bipartite split is made between half of the qubits on which the unitary acts.

reduce the notational clutter by denoting the state  $\rho_{n+1}(\alpha)$  of Eq. (3.3) as  $\rho_\alpha$ .

Given a particular bipartite division, the partial transpose of  $\rho_\alpha$  with respect to the part that does not include the special qubit is

$$\check{\rho}_\alpha = \frac{I_n + \alpha \check{C}}{2N} \quad \text{where} \quad \check{C} \equiv \begin{pmatrix} 0 & \check{U}_n^\dagger \\ \check{U}_n & 0 \end{pmatrix}. \quad (3.29)$$

Using the binomial theorem, we can expand  $\text{tr}(\check{\rho}_\alpha^s)$  in terms of  $\text{tr}(\check{C}^k)$ :

$$\text{tr}(\check{\rho}_\alpha^s) = \left(\frac{1}{2N}\right)^s \sum_{k=0}^s \binom{s}{k} \alpha^{k \text{tr}(\check{C}^k)}. \quad (3.30)$$

When  $k$  is odd,  $\check{C}^k$  is block off-diagonal, so its trace vanishes. When  $k$  is even, we have

$$\mathrm{tr}(\check{C}^k) = 2 \mathrm{tr}\left(\left(\check{U}_n \check{U}_n^\dagger\right)^{k/2}\right). \quad (3.31)$$

When  $k = 2$ , this simplifies to  $\mathrm{tr}(\check{C}^2) = 2\mathrm{tr}(\check{U}_n \check{U}_n^\dagger) = 2\mathrm{tr}(U_n U_n^\dagger) = 2N$ . The crucial step here follows immediately from the property  $\mathrm{tr}(\check{A}\check{B}) = \mathrm{tr}(AB)$ , which we prove as a Lemma in Appendix B. Note that in general  $\mathrm{tr}(\check{A}_1 \check{A}_2 \dots \check{A}_l) \neq \mathrm{tr}(A_1 A_2 \dots A_l)$  if  $l > 2$ , so we cannot give a similar general calculation of  $\mathrm{tr}(\check{\rho}_\alpha^s)$  for even  $s \geq 4$ , since it involves terms of this form.

Using Eq. (3.30), we can now obtain three independent constraint equations on the eigenvalues  $\lambda_j = \lambda_j(\check{\rho}_\alpha)$  of the partial transpose  $\check{\rho}_\alpha$ :

$$\sum_{j=1}^{2N} \lambda_j^s = \mathrm{tr}(\check{\rho}_\alpha^s) = \frac{1}{2^s N^{s-1}} [(1 + \alpha)^s + (1 - \alpha)^s], \quad s = 1, 2, 3. \quad (3.32)$$

Since the negativity is given by

$$\mathcal{M}(\rho_\alpha) = \sum_j |\lambda_j|, \quad (3.33)$$

we can find an upper bound on the negativity by maximizing  $\sum_j |\lambda_j|$  subject to the constraints (3.32). If we consider only the  $s = 1, 2$  constraints, we obtain a nontrivial upper bound on the negativity with little effort. We find that adding the constraint  $s = 3$  adds nothing asymptotically for large  $N$ , but for small  $N$  yields a tighter bound than we get from the  $s = 1, 2$  constraints, although this comes at the cost of considerably more effort. We emphasize that these bounds apply to all bipartite divisions and to all unitaries  $U_n$ . Notice that we have no reason to expect these bounds to be saturated, since the traces of higher powers of  $\check{\rho}_\alpha$  impose additional constraints that we are ignoring. The one exception is the case of three qubits, where the  $s = 1, 2, 3$  constraints are a complete set, and indeed, in this case, the  $s = 1, 2, 3$  bound is  $5/4$ , which is saturated by the unitary found in Sec. 3.2.

The remainder of this section is devoted to calculating the  $s = 1, 2$  and  $s = 1, 2, 3$  upper bounds. A graphical summary of our results for  $\alpha = 1$  is presented in Fig. 3.7.

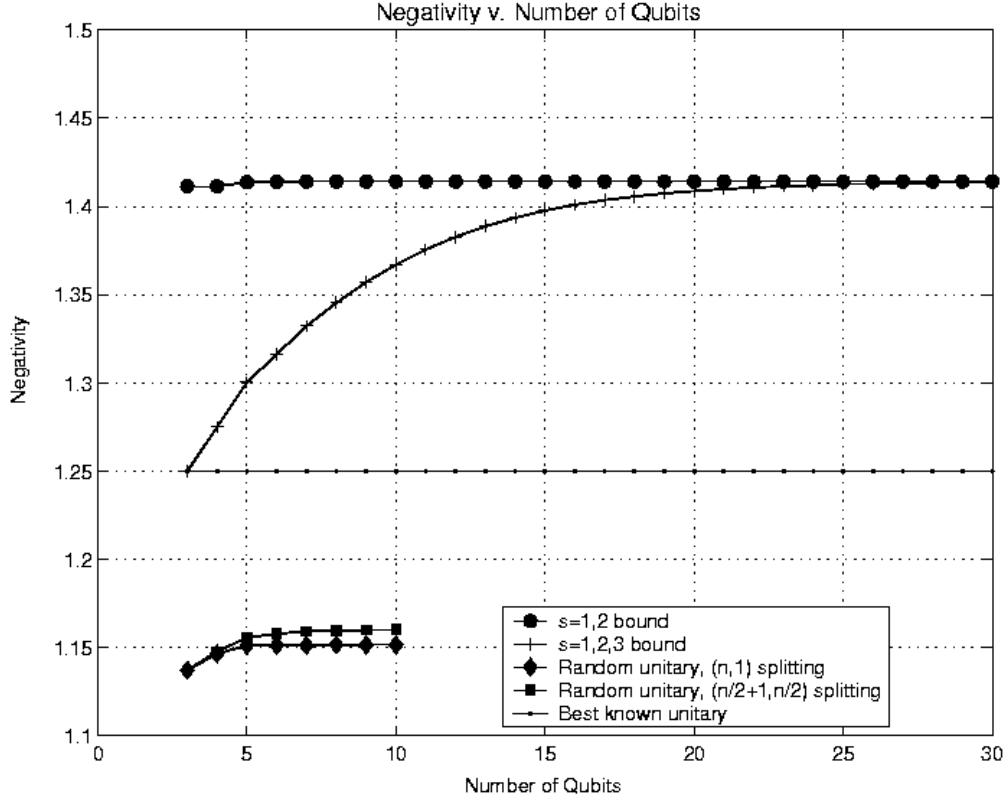


Figure 3.7: Plot of the bounds on the negativity of states of the form (3.1), i.e., for a pure-state input in the zeroth register ( $\alpha = 1$ ). The uppermost plot is the simple analytic bound  $\mathcal{M}_{1,2} = \sqrt{2}$ , obtained using the  $s = 1, 2$  constraint equations; the next largest plot is the numerically constructed  $s = 1, 2, 3$  bound. One can see that the  $s = 1, 2, 3$  bound asymptotes to the  $s = 1, 2$  bound. As noted in the text, these bounds are independent of the unitary  $U_n$  and the bipartite division. The flat line shows the negativity  $5/4$  for the state constructed in Sec. 3.2, currently the state of the form (3.1) with the largest demonstrated negativity; notice that for  $n + 1 = 3$ , this state attains the  $s = 1, 2, 3$  bound. The lowest two sets of data points display the expected negativities for a randomly chosen unitary using the bipartite splittings  $(n, 1)$  and  $(\lfloor n/2 \rfloor + 1, \lceil n/2 \rceil)$ , which were also plotted in Figs. 3.4 and 3.5.

### 3.4.1 The $s = 1, 2$ Bound

We can use Lagrange multipliers to reduce the problem to maximizing a function of one variable, but first we must deal with the absolute value in Eq. (3.33). To do so, we assume that  $t$  of the eigenvalues are negative and the  $2N - t$  others are nonnegative, where  $t$  becomes a parameter that must now be included in the maximization. We want to maximize

$$\mathcal{M}_{1,2} = - \sum_{i=1}^t \lambda_i + \sum_{j=t+1}^{2N} \lambda_j, \quad (3.34)$$

subject to the constraints

$$\sum_{k=1}^{2N} \lambda_k = 1 \quad \text{and} \quad \sum_{k=1}^{2N} \lambda_k^2 = \frac{1 + \alpha^2}{2N}. \quad (3.35)$$

The notation we adopt here for the indices is that  $i$  labels negative eigenvalues and  $j$  labels nonnegative eigenvalues, while  $k$  can label either. This serves to remind us of the sign of an eigenvalue just by looking at its index.

Introducing Lagrange multipliers  $\mu$  and  $\nu$ , the function we want to maximize is

$$f(\lambda_k, t) = - \sum_{i=1}^t \lambda_i + \sum_{j=t+1}^{2N} \lambda_j + \mu \left( \sum_{k=1}^{2N} \lambda_k - 1 \right) + \nu \left( \sum_{k=1}^{2N} \lambda_k^2 - \frac{1 + \alpha^2}{2N} \right). \quad (3.36)$$

Differentiating with respect to  $\lambda_i$  and then  $\lambda_j$ , we find

$$-1 + \mu + 2\nu\lambda_i = 0, \quad (3.37)$$

$$+1 + \mu + 2\nu\lambda_j = 0. \quad (3.38)$$

We immediately see that in the maximal solution, all the negative eigenvalues are equal, and all the nonnegative eigenvalues are equal. We can now reformulate the problem in the following way. If we call the two eigenvalues  $\lambda_-$  and  $\lambda_+$ , our new problem is to maximize

$$\mathcal{M}_{1,2} = \sum_k |\lambda_k| = -t\lambda_- + (2N - t)\lambda_+, \quad (3.39)$$



subject to the constraints

$$t\lambda_- + (2N - t)\lambda_+ = 1, \quad (3.40)$$

$$t\lambda_-^2 + (2N - t)\lambda_+^2 = \frac{1 + \alpha^2}{2N}. \quad (3.41)$$

We can now do the problem by solving the constraints for  $\lambda_-$  and  $\lambda_+$  in terms of  $t$ , plugging these results into  $\mathcal{M}_{1,2}$ , and then maximizing over  $t$ .

Before continuing, we note two things. First,  $t$  cannot be  $2N$ , for if it were, then all the eigenvalues would be negative, making it impossible to satisfy Eq. (3.40). Second, unless  $\alpha = 0$ ,  $t$  cannot be 0, for if it were, then all the eigenvalues would be equal to  $1/2N$  by Eq. (3.40), a situation Eq. (3.41) says can occur only if  $\alpha = 0$ . Since we are not really interested in the case  $\alpha = 0$ , for which  $\rho_\alpha$  is always the maximally mixed state, we assume  $\alpha > 0$  and  $0 < t < 2N$  in what follows.

Solving Eqs. (3.40) and (3.41) and plugging the solutions into Eq. (3.39), we get the two solutions

$$\mathcal{M}_{1,2} = \frac{N - t \pm \alpha\sqrt{t(2N - t)}}{N}. \quad (3.42)$$

We choose the positive branch, since it contains the maximum. Maximizing with respect to  $t$  treated as a continuous variable, we obtain the upper bound,

$$\mathcal{M}_{1,2} = \sqrt{1 + \alpha^2} \stackrel{\alpha \rightarrow 1}{\simeq} \sqrt{2} \simeq 1.414, \quad (3.43)$$

which occurs when the degeneracy parameter is given by

$$t = N \left( 1 - \frac{1}{\sqrt{1 + \alpha^2}} \right) \stackrel{\alpha \rightarrow 1}{\simeq} 0.292 N. \quad (3.44)$$

The numbers on the right are for the case  $\alpha = 1$ , corresponding to the special qubit starting in a pure state. Notice that the upper bound (3.43) allows a negativity greater than 1 for all  $\alpha$  except  $\alpha = 0$ .

Since we did not yet enforce the condition that  $t$  be a positive integer, the bound (3.43) can be made tighter for specific values of  $N$  and  $\alpha$  by calculating  $t$

and checking which of the two nearest integers yields a larger  $\mathcal{M}_{1,2}$ . Asymptotically, however, the ratio  $t/N$  can approach any real number, so this bound for continuous  $t$  is the same as the bound for integer  $t$  in the limit  $N \rightarrow \infty$ .

### 3.4.2 The $s = 1, 2, 3$ Bound

To deal with this case, we again make the assumption that  $t$  of the eigenvalues are negative and  $2N - t$  are nonnegative and thus write

$$\mathcal{M}_{1,2,3} = - \sum_{i=1}^t \lambda_i + \sum_{j=t+1}^{2N} \lambda_j, \quad (3.45)$$

as before. In addition to the constraints (3.35), we now have a third constraint

$$\sum_{k=1}^{2N} \lambda_k^3 = \frac{1 + 3\alpha^2}{4N^2}. \quad (3.46)$$

We specialize to the case  $\alpha = 1$  for the remainder of this subsection, because it is our main interest, and the algebra for the general case becomes difficult.

Introducing three Lagrange multipliers, we can write the function we want to maximize as

$$f(\lambda_k, t) = - \sum_{i=1}^t \lambda_i + \sum_{j=t+1}^{2N} \lambda_j + \mu \left( \sum_{k=1}^{2N} \lambda_k - 1 \right) + \nu \left( \sum_{k=1}^{2N} \lambda_k^2 - \frac{1}{N} \right) + \xi \left( \sum_{k=1}^{2N} \lambda_k^3 - \frac{1}{N^2} \right). \quad (3.47)$$

Differentiating with respect to  $\lambda_i$  and then  $\lambda_j$  gives

$$-1 + \mu + 2\nu\lambda_i + 3\xi\lambda_i^2 = 0, \quad (3.48)$$

$$+1 + \mu + 2\nu\lambda_j + 3\xi\lambda_j^2 = 0. \quad (3.49)$$

These equations being quadratic, we see that there are at most two distinct negative eigenvalues and at most two distinct nonnegative eigenvalues. Since the sum of the

two solutions of either of these equations is  $-2\nu/3\xi$ , however, we can immediately conclude either that one of the potentially nonnegative solutions is negative or that one of the potentially negative solutions is positive. Hence, we find that at least one of the four putative eigenvalues has the wrong sign, implying that there are at most three distinct eigenvalues, though we don't know whether one or two of them are negative.

Labelling the three eigenvalues by  $A$ ,  $B$ , and  $C$ , we can reduce the problem to solving the three constraint equations,

$$\begin{aligned} uA + vB + wC &= 1, \\ uA^2 + vB^2 + wC^2 &= 1/N, \\ uA^3 + vB^3 + wC^3 &= 1/N^2, \end{aligned} \tag{3.50}$$

for  $A$ ,  $B$ , and  $C$  and then maximizing  $\mathcal{M}_{1,2,3}$  over the degeneracy parameters  $u$ ,  $v$ , and  $w$ , which are nonnegative positive integers satisfying the further constraint

$$u + v + w = 2N. \tag{3.51}$$

We do not associate any particular sign with  $A$ ,  $B$ , and  $C$ ; the signs are determined by the solution of the equations.

One might hope that the symmetry of Eqs. (3.50) would allow for a simple analytic solution, but this appears not to be the case. In solving the three equations, one is inevitably led to a sixth-order polynomial in one of the variables, with the coefficients given as functions of  $u$ ,  $v$ , and  $w$ . Rather than try to solve this equation, which appears intractable, we elected to do a brute force optimization for any given value of  $2N$  by solving Eqs. (3.50) for each possible value of  $u$ ,  $v$ , and  $w$ . Picking the solution that has the largest negativity then yields the global maximum. We did this for each  $N$  up to  $2N = 78$ . The values of  $u$ ,  $v$ , and  $w$  that maximize the negativity

are always

$$u = \left\lceil N \left( 1 - \frac{1}{\sqrt{2}} \right) \right\rceil, \quad v = 1, \quad w = 2N - 1 - u, \quad (3.52)$$

where  $[x]$  denotes the integer nearest to  $x$ . The unique eigenvalue corresponding to  $v = 1$  is the largest positive eigenvalue,  $w$  is the degeneracy of another positive eigenvalue, and  $u$  is the degeneracy of the negative eigenvalue. Notice that the degeneracy of the negative eigenvalue is exactly what was found in the  $s = 1, 2$  case. Using the results (3.52) as a guide, we did a further numerical calculation of the maximum for larger values of  $N$ , by considering only the area around the degeneracy values given by Eq. (3.52). While this is not a certifiable global maximum, the perturbation expansion described below matches so well that the two are indistinguishable if they are plotted together for  $n + 1 > 7$ . This gives us confidence that the numerically determined upper bound  $\mathcal{M}_{1,2,3}$ , which we plot in Fig. 3.7, is indeed a global maximum for all  $N$ .

We have used the numerical work to help formulate a perturbation expansion that gives the first correction to the  $N \rightarrow \infty$  behavior of the  $s = 1, 2, 3$  bound. Defining  $x = 1/N$ , we rewrite the constraint equations (3.50) as

$$\begin{aligned} aA + bB + cC &= x, \\ aA^2 + bB^2 + cC^2 &= x^2, \\ aA^3 + bB^3 + cC^3 &= x^3, \end{aligned} \quad (3.53)$$

where  $a = u/N$ ,  $b = v/N$ , and  $c = w/N$ . We also have the constraint

$$a + b + c = 2. \quad (3.54)$$

As  $x$  is the variable that is asymptotically small, we seek an expansion in terms of it.

Our numerical work tells us that there are two positive eigenvalues, one of which is larger and nondegenerate. In formulating our perturbation expansion, we let  $B$

and  $C$  be the positive eigenvalues, with  $B$  being the larger one, having degeneracy  $v = b_1 \geq 1$ . We do not assume that  $b_1$  is 1, as the numerics show, but rather let the equations force us to that conclusion. With this assumption, the form of the constraints (3.53) shows that the variables have the following expansions to first order beyond the  $N \rightarrow \infty$  form:

$$\begin{aligned} a &= a_0 + a_1 x^{1/3}, \\ b &= b_1 x, \\ c &= c_0 + c_1 x^{1/3}, \end{aligned} \tag{3.55}$$

and

$$\begin{aligned} A &= A_0 x + A_1 x^{4/3}, \\ B &= B_1 x^{2/3}, \\ C &= C_0 x + C_1 x^{4/3}. \end{aligned} \tag{3.56}$$

We see that we are actually expanding in the quantity  $y = x^{1/3}$ . In terms of these variables, the negativity is given by

$$\begin{aligned} \mathcal{M}_{1,2,3} &= \frac{-aA + bB + cC}{x} \\ &= -a_0 A_0 + c_0 C_0 + (-a_0 A_1 - a_1 A_0 + c_0 C_1 + c_1 C_0) x^{1/3} + O(x^{2/3}), \end{aligned} \tag{3.57}$$

which we now endeavor to maximize.

Substituting Eqs. (3.55) and (3.56) into the constraints (3.53) and (3.54) and equating terms with equal exponents of  $x$ , we obtain, to zero order,

$$\begin{aligned} a_0 + c_0 &= 2, \\ a_0 A_0 + c_0 C_0 &= 1, \\ a_0 A_0^2 + c_0 C_0^2 &= 1. \end{aligned} \tag{3.58}$$

Solving for  $a_0$ ,  $c_0$ , and  $C_0$  in terms of  $A_0$  and substituting the results into the zero-order piece of  $\mathcal{M}_{1,2,3}$  gives

$$\mathcal{M}_{1,2,3} = \frac{1 - 4A_0 + 2A_0^2}{1 - 2A_0 + 2A_0^2}. \quad (3.59)$$

Maximizing Eq. (3.59) gives  $A_0^2 = 1/2$  and, hence,  $A_0 = -1/\sqrt{2}$ , since  $A$  is the negative eigenvalue. This leads to  $a_0 = 1 - 1/\sqrt{2}$ ,  $c_0 = 1 + 1/\sqrt{2}$ , and  $C_0 = 1/\sqrt{2}$ , and the resulting  $N \rightarrow \infty$  upper bound is  $\mathcal{M}_{1,2,3} = \sqrt{2}$ , as expected.

If we carry this process out to first order beyond the  $N \rightarrow \infty$  behavior, we obtain, after some algebraic manipulation,  $\mathcal{M}_{1,2,3} = \sqrt{2} - b_1^{1/3} x^{1/3} / 2^{7/6} + O(x^{2/3})$ . Maximizing this simply means making  $b_1$  as small as possible, i.e., choosing  $b_1 = 1$ , whence we obtain the following asymptotic expression for the  $s = 1, 2, 3$  upper bound:

$$\mathcal{M}_{1,2,3} = \sqrt{2} - \frac{1}{2^{7/6} N^{1/3}} + O\left(\frac{1}{N^{2/3}}\right). \quad (3.60)$$

This shows that the upper bound of  $\sqrt{2}$  is approached monotonically from below in the asymptotic regime. In addition, the procedure verifies that in the maximum solution, the largest positive eigenvalue is nondegenerate. For the case of qubits we have  $N = 2^n$ , implying that the approach to the  $N \rightarrow \infty$  bound is exponentially fast.

### 3.5 Conclusion

The mixed-state quantum circuit in Fig. (3.2) provides an efficient method for estimating the normalized trace of a unitary operator, a task that is thought to be exponentially hard on a classical computer. If one believes that global entanglement is the essential resource for the exponential speedup achieved by quantum computation, then the question begging to be answered is whether there is any entanglement in the circuit's output state in Eq. (3.3). The purpose of this chapter was to investigate this question.

A notable feature of the circuit in Fig. (3.2) is that it provides an efficient method for estimating the normalized trace no matter how small the initial polarization  $\alpha$  of the special qubit in the zeroth register, as long as that polarization is not zero. Since all the other qubits are initially completely unpolarized, we are led to characterize the computational power of this circuit as the “power of even the tiniest fraction of a qubit.” We provide preliminary results regarding the entanglement that can be achieved for  $\alpha < 1$ . Our results are consistent with, but certainly do not demonstrate the conclusion that separable states cannot provide an exponential speedup and that entanglement is possible no matter how small  $\alpha$  is. The question of entanglement for subunity polarization of the special qubit deserves further investigation.

Our key conclusions concern the case where the special qubit is initially pure ( $\alpha = 1$ ). We find that the circuit in Fig. (3.1) typically does produce global entanglement, but the amount of this entanglement is quite small. Using multiplicative negativity to measure the amount of entanglement, we show that as the number of qubits becomes large, the multiplicative negativity in the state in Eq. (3.1) is a vanishingly small fraction of the maximum possible multiplicative negativity for roughly equal splittings of the qubits. This hints that the key to computational speedup might be the global character of the entanglement, rather than the amount of the entanglement. In the spirit of the pioneering contribution of Wyler [83], what happier motto can we find for this state of affairs than *Multum ex Parvo*, or A Lot out of A Little.

## Chapter 4

# Classical simulation of quantum computation

*I looked for an answer to my question. But reason could not give me an answer—reason is incommensurable with the question.*

-Leo Tolstoy in *Anna Karenina*

Progress in our understanding of what makes quantum evolutions computationally more powerful than a classical computer has been scarce. A step forward, however, was achieved by identifying entanglement as a *necessary* resource for quantum computational speed-ups. Indeed, a speed-up is only possible if in a quantum computation, entanglement spreads over an adequately large number of qubits [52]. In addition, the amount of entanglement, as measured by the Schmidt rank of a certain set of bipartitions of the system, needs to grow sufficiently with the size of the computation [79]. Whenever either of these two conditions is not met, the quantum evolution can be efficiently simulated on a classical computer. These conditions (which are particular examples of subsequent, stronger classical simulation



results based on tree tensor networks (TTN) [75, 20]) are only necessary, and thus not sufficient, so that the presence of large amounts of entanglement spreading over many qubits does not guarantee a computational speed-up, as exemplified by the Gottesman-Knill theorem [62].

The above results refer exclusively to quantum computations with pure states. As shown in Chapter 3, the scenario for mixed-state quantum computation is rather different. The intriguing *deterministic quantum computation with one quantum bit* (DQC1 or ‘the power of one qubit’) [55] involves a highly mixed state that does not contain much entanglement [17] and yet it performs a task, the computation with fixed accuracy of the normalized trace of a unitary matrix, exponentially faster than any known classical algorithm. This also provides an exponential speedup over the best known classical algorithm for simulations of some quantum processes [66]. Thus, in the case of a mixed-state quantum computation, a large amount of entanglement does not seem to be necessary to obtain a speed-up with respect to classical computers.

A simple, unified explanation for the pure-state and mixed-state scenarios is possible [79] by noticing that the decisive ingredient in both cases is the presence of *correlations*. Indeed, let us consider the Schmidt decomposition of a vector  $|\Psi\rangle$ , given by

$$|\Psi\rangle = \sum_{i=1}^{\chi} \lambda_i |i_A\rangle \otimes |i_B\rangle, \quad (4.1)$$

where  $\langle i_A | j_A \rangle = \langle i_B | j_B \rangle = \delta_{ij}$  and  $\chi$  is the rank of the reduced density matrices  $\rho_A \equiv \text{tr}_B[|\psi\rangle\langle\psi|]$  and  $\rho_B \equiv \text{tr}_A[|\psi\rangle\langle\psi|]$ ; and the (operator) Schmidt decomposition of a density matrix  $\rho$  given by [85]

$$\rho = \sum_{i=1}^{\chi^\sharp} \lambda_i^\sharp O_{iA} \otimes O_{iB}, \quad (4.2)$$

where  $\text{tr}(O_{iA}^\dagger O_{jA}) = \text{tr}(O_{iB}^\dagger O_{jB}) = \delta_{ij}$ . The Schmidt ranks  $\chi$  and  $\chi^\sharp$  are a measure of correlations between parts  $A$  and  $B$ , with  $\chi^\sharp = \chi^2$  if  $\rho = |\Psi\rangle\langle\Psi|$ . Let the density

matrix  $\rho_t$  denote the evolving state of the quantum computer during a computation. Notice that  $\rho_t$  can represent both pure and mixed states. Then, as shown in Refs. [79] and [75, 20], the quantum computation can be efficiently simulated on a classical computer using a TTN decomposition if the Schmidt rank  $\chi^\sharp$  of  $\rho$  according to a certain set of bipartitions  $A : B$  of the qubits scales polynomially with the size of the computation. In other words, a necessary condition for a computational speed-up is that correlations, as measured by the Schmidt rank  $\chi^\sharp$ , grow super-polynomially in the number of qubits. In the case of pure states (where  $\chi = \sqrt{\chi^\sharp}$ ) these correlations are entirely due to entanglement, while for mixed states they may be quantum or classical.

Our endeavor in this chapter is to study the DQC1 model of quantum computation following the above line of thought. In particular, we elucidate whether DQC1 can be efficiently simulated with any classical algorithm, such as those in [79, 75, 20] (and, implicitly, in [52]), which exploit limits on the amount of correlations, in the sense of a small  $\chi^\sharp$  according to certain bipartitions of the qubits. We will argue here that the state  $\rho_t$  of a quantum computer implementing the DQC1 model displays an exponentially large  $\chi^\sharp$ , in spite of its containing only a small amount of entanglement [17]. We will conclude, therefore, that none of the simulation techniques mentioned above can be used to efficiently simulate ‘the power of one qubit’.

On the one hand, our result indicates that entanglement is not behind the (suspected) computational speed-up of DQC1. On the other hand, by showing the failure of a whole class of classical algorithms to efficiently simulate this mixed-state quantum computation, we reinforce the conjecture that DQC1 leads indeed to an exponential speed-up. We note, however, that our result does *not* rule out the possibility that this circuit could be simulated efficiently using some other classical algorithm.

Before we move on to the presentation of our results and conclusions, we will present a short review of tree tensor networks (TTN) for the sake of completeness and continuity. This will be the subject of the next section.

## 4.1 Tree Tensor Networks (TTN)

The discussion in this section is not original and a more detailed compilation can be found in [60]. For simplicity, let us deal with pure states of  $n$  qudits, denoted that by

$$|\Psi\rangle = \sum_{i_1=1}^d \cdots \sum_{i_n=1}^d c_{i_1 \dots i_n} |i_1\rangle \otimes \cdots \otimes |i_n\rangle. \quad (4.3)$$

This state is characterized by  $d^n$  complex amplitudes  $c_{i_1 \dots i_n}$ . We can think of all these coefficients as one entity, a rank- $n$  tensor. Such a tensor can be represented graphically, with vertices labelled by  $c$ , and connected by  $n$  open wires, each of which is labelled by a distinct index. One may represent a tensor *network* by starting with such graphical representation of its tensors, and then connecting wires corresponding to the same index. As quantum gates are performed on the state  $|\Psi\rangle$ , the graph (or the network) gets more involved.

In the quantum circuit model, result of the quantum computation is obtained by taking trace of the final state against measurement operators. In our present picture, this translates to contracting vertices of the tensor networks, that is, removing the edges between two vertices and replacing them by a single one. This operation is known as tensor contraction. The complexity of simulating a quantum computation thus reduces to that of simulating tensor contractions. For graphs which have small treewidths, this operation can be approximated classically with a high accuracy in polynomial time. Without going into its formal definition, the treewidth of a graph tells us how different it is from a tree. A tree has treewidth of 1. Single cycles of length at least 3 have a treewidth of 2.

For any graph  $G = (V, E)$ , the line graph  $G^*$  is defined as follows:  $V(G^*) \equiv E(G)$  and

$$E(G^*) \equiv \{\{e_1, e_2\} \subseteq E(G) : e_1 \neq e_2, \exists v \in V(G) \text{ such that } e_1 \text{ and } e_2 \text{ are incident on } v\}.$$

The contraction complexity of a graph  $G$ ,  $\text{cc}(G)$  is equal to the treewidth of the line graph  $G^*$ ,  $\text{tw}(G^*)$  [60]. Although determining the treewidth of a general graph is NP-hard [3], for trees it is trivial. For this simple case then,  $\text{cc}(G)$  is trivial. Additionally, if the graph underlying the quantum circuit is such that  $\text{tw}(G) = d$ , then the circuit can be simulated in time  $e^{O(d)}$ .

This is the inspiration for defining quantum circuits as tree tensor networks. The closer the underlying line graph for a quantum circuit is to a tree, easier it is to simulate the corresponding quantum circuit efficiently classically. This, not surprisingly then, is the motivation behind all the present simulation techniques of quantum computation like matrix product states (MPS), projected entangled-pair states (PEPS), Affleck-Kennedy-Leib-Tasaki (AKLT) states. If one is able to show that a certain quantum computation *cannot* be represented as a TTN, then a large class of techniques are excluded in providing an efficient classical simulation for it. This will be our line of approach in the rest of this chapter, with reference to the DQC1 model.

## 4.2 DQC1 and Tree Tensor Networks (TTN)

The DQC1 model, represented in Eq. (3.1), provides an estimate of the normalized trace  $\text{tr}(U_n)/2^n$  of a  $n$ -qubit unitary matrix  $U_n \in \mathbb{U}(2^n)$  with fixed accuracy efficiently [55]. This quantum circuit transforms the highly-mixed initial state  $\rho_0 \equiv |0\rangle\langle 0| \otimes I_n/2^n$  at time  $t = 0$  into the final state  $\rho_T$  at time  $t = T$ ,

$$\rho_T = \frac{1}{2^{n+1}} \begin{pmatrix} I_n & U_n^\dagger \\ U_n & I_n \end{pmatrix}, \quad (4.4)$$

through a series of intermediate states  $\rho_t$ ,  $t \in [0, T]$ . The simulation algorithms relevant in the present discussion [52, 79, 75, 20] require that  $\rho_t$  be efficiently represented with a TTN [75, 20] (or a more restrictive structure, such as a product of

$k$ -qubit states for fixed  $k$  [52] or a matrix product state [79]) at all times  $t \in [0, T]$ . Here we will show that the final state  $\rho_T$ , henceforth denoted simply by  $\rho$ , cannot be efficiently represented with a TTN. This already implies that none of the algorithms in [52, 79, 75, 20] can be used to efficiently simulate the DQC1 model.

Storing and manipulating a TTN requires computational space and time that grows linearly in the number of qubits  $n$  and as a small power of its rank  $q$ . The rank  $q$  of a TTN is the maximum Schmidt rank  $\chi_i^\sharp$  over all bipartitions  $A_i : B_i$  of the qubits according to a given tree graph whose leaves are the qubits of our system (see [75, 20] for details). The key observation of this chapter is that for a *typical* unitary matrix  $U_n$ , the density matrix  $\rho$  in Eq. (4.4) is such that any TTN decomposition has exponentially large rank  $q$ . By *typical*, here we mean a unitary matrix  $U_n$  efficiently generated through a (random) quantum circuit. That is,  $U_n$  is the product of  $\text{poly}(n)$  one-qubit and two-qubit gates. In the next section we present numerical results that unambiguously suggest that, indeed, *typical*  $U_n$  necessarily lead to TTN with exponentially large rank  $q$ .

We notice that the results of the next section do not exclude the possibility that the quantum computation in the DQC1 model can be efficiently simulated with a TTN for particular choices of  $U_n$ . For instance, if  $U_n$  factorizes into single-qubit gates, then  $\rho$  can be seen to be efficiently represented with a TTN of rank 3, and we can not rule out an efficient simulation of the power of one qubit for that case. Of course, this is to be expected, given that the trace of such  $U_n$  can be computed efficiently in the first place.

### 4.3 Exponential growth of Schmidt ranks

In this section we study the rank  $q$  of any TTN for the final state  $\rho$  of the DQC1 circuit, Eq. (4.4). We numerically determine that a lower bound to such a rank

grows exponentially with the number of qubits  $n$ .

The Schmidt rank  $\chi$  of a pure state  $|\rho_{\phi_A\psi_B}\rangle$  is

$$|\rho_{\phi_A\psi_B}\rangle \equiv \rho |\phi_A\rangle |\psi_B\rangle = \sum_{i=1}^{\chi^\sharp} \lambda_i^\sharp O_{iA} |\phi_A\rangle \otimes O_{iB} |\psi_B\rangle, \quad (4.5)$$

obtained by applying the density matrix  $\rho$  onto a product state  $|\phi_A\rangle |\psi_B\rangle$  is a lower bound on the operator Schmidt rank  $\chi^\sharp$  of  $\rho$ , i.e.,  $\chi^\sharp \geq \chi$ . For the purpose of our numerics, we consider the pure state  $U_n |0\rangle^{\otimes n}$ . We build  $U_n$  as a sequence of  $2n$  random two-qubit gates, applied to pairs of qubits, also chosen at random. The random two-qubit unitaries are generated using the mixing algorithm presented in [30]. Note that applying  $2n$  gates means that the resulting unitary is efficiently implementable, a situation for which the DQC1 model is valid. For an even number of qubits  $n$ , we calculate the smallest Schmidt rank  $\chi$  over all  $n/2 : n/2$  partitions of the qubits (similar results can be obtained for odd  $n$ ). The resulting numbers are plotted in Fig (4.1).

The above numerical results strongly suggest that the final state  $\rho$  in the DQC1 circuit has exponential Schmidt rank for a *typical* unitary  $U_n$ . We are not able to provide a formal proof of this fact. This is due to a general difficulty in describing properties of the set  $\mathbb{U}_{qc}(2^n)$  of unitary matrices that can be efficiently realized through a quantum computation. Instead, the discussion is much simpler for the set  $\mathbb{U}(2^n)$  of generic  $n$ -qubit unitary matrices, where it is possible to prove that  $\rho$  cannot be efficiently represented with a TTN for a Haar generated  $U_n \in \mathbb{U}(2^n)$ , as discussed in the next section. Notice that Ref. [28] shows that random (but efficient) quantum circuits generate random  $n$ -qubit gates  $U_n \in \mathbb{U}_{qc}(2^n)$  according to a measure that converges to the Haar measure in  $\mathbb{U}(2^n)$ . Combined with the theorem in the next section, this would constitute a formal proof of the otherwise numerically evident exponential growth of the rank  $q$  of any TTN for the DQC1 final state  $\rho$ .

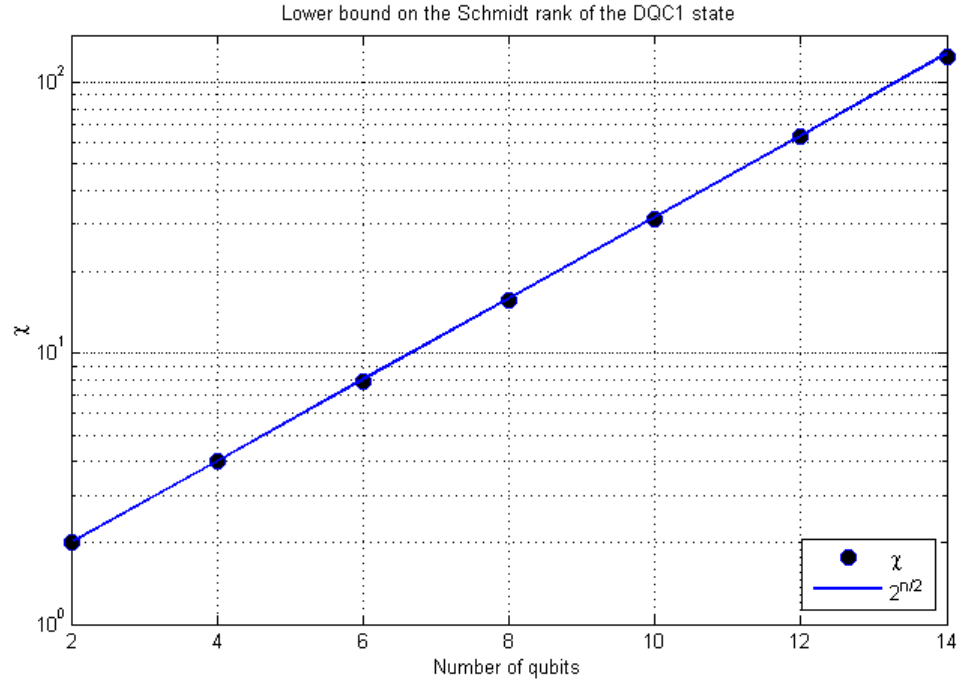


Figure 4.1: Lower bound for the operator Schmidt rank  $\chi^\sharp$  of the DQC1 state for any equipartition  $n/2 : n/2$ , as given by the Schmidt rank  $\chi$  of the pure state in Eq. (4.5). The dots are for even numbers of qubits, and the fit is the line  $2^{n/2}$ .  $\chi$  is calculated for a pure state obtained by applying  $2n$  random 2-qubit gates on the state  $|0\rangle^{\otimes n}$ . This is evidence that for a *typical* unitary  $U_n$ , the rank  $q$  of any TTN for the DQC1 state  $\rho$  in Eq. (4.4) grows exponentially with  $n$ .

## 4.4 A formal proof for the Haar-distributed case

Our objective in this section is to analyze the Schmidt rank  $\chi^\sharp$  of the density matrix  $\rho$  in Eq. (4.4) for certain bipartitions of the  $n + 1$  qubits, assuming that  $U_n \in \mathbb{U}(2^n)$  is Haar-distributed. As an aside, we calculate the negativity of a random pure state in Appendix C.

It is not difficult to deduce that for any tree of the  $n + 1$  qubits, there exists at least one edge that splits the tree in two parts  $A$  and  $B$ , with  $n_A$  and  $n_B$  qubits, where  $n_0 = \min(n_A, n_B)$  fulfills  $n/5 \leq n_0 \leq 2n/5$ . In other words, if a rank- $q$  TTN

exists for the  $\rho$  in Eq. (4.4), then there is a bipartition of the  $n + 1$  qubits with  $n_0$  qubits on either  $A$  or  $B$  and such that the Schmidt rank  $\chi^\# \leq q$ . Theorem 6, our main technical result, shows that if  $U_n$  is chosen randomly according to the Haar measure, then the Schmidt rank of any such bipartition fulfills  $\chi^\# \geq O(2^{n_0})$ . Therefore for a randomly generated  $U_n \in \mathbb{U}(2^n)$ , a TTN for  $\rho$  has rank  $q$  (and computational cost) exponential in  $n$ , and none of the techniques of [52, 79, 75, 20] can simulate the outcome of the DQC1 model efficiently.

Consider now any bipartition  $A : B$  of the  $n + 1$  qubits, where  $A$  and  $B$  contain  $n_A$  and  $n_B$  qubits, with the minimum  $n_0$  of those restricted by  $n/5 \leq n_0 \leq 2n/5$ . Without loss of generality we can assume that the top qubit lies in  $A$ . Actually, we can also assume that  $A$  contains the top  $n_A$  qubits. Indeed, suppose  $A$  does not have the  $n_A$  top qubits. Then we can use a permutation  $P_n$  on all the  $n$  qubits to bring the  $n_A$  qubits of  $A$  to the top  $n_A$  positions. This will certainly modify  $\rho$ , but since

$$\begin{pmatrix} P_n & 0 \\ 0 & P_n \end{pmatrix} \begin{pmatrix} I_n & U_n^\dagger \\ U_n & I_n \end{pmatrix} \begin{pmatrix} P_n^T & 0 \\ 0 & P_n^T \end{pmatrix} = \begin{pmatrix} I_n & V_n^\dagger \\ V_n & I_n \end{pmatrix}, \quad (4.6)$$

where  $V_n = P_n U_n P_n^T$  is another Haar-distributed unitary, we obtain that the new density matrix is of the same form as  $\rho$ . Finally, in order to ease the notation, we will assume that  $n_A = n_0$  (identical results can be derived for  $n_B = n_0$ ). Thus  $n/5 \leq n_A \leq 2n/5$ .

We note that

$$\begin{pmatrix} I_n & U_n^\dagger \\ U_n & I_n \end{pmatrix} = \mathbb{I}_2 \otimes \mathbb{I}_n + \begin{pmatrix} 0 & 1 \\ 0 & 0 \end{pmatrix} \otimes U_n^\dagger + \begin{pmatrix} 0 & 0 \\ 1 & 0 \end{pmatrix} \otimes U_n, \quad (4.7)$$

so that if we multiply  $\rho$  by the product state

$$|\phi_{\vec{\alpha}}\rangle \equiv |t, i, j\rangle \equiv |t, i_A\rangle |j_B\rangle, \quad (4.8)$$

where  $\vec{\alpha} \equiv (t, i, j)$ ,  $t = 0, 1$ ;  $i = 1, \dots, d_A$ ;  $j = 1, \dots, d_B$ , we obtain  $|\psi_{\vec{\alpha}}\rangle \equiv \rho |\phi_{\vec{\alpha}}\rangle$  where

$$|\psi_{\vec{\alpha}}\rangle = \begin{cases} \frac{1}{2^{n+1}}(|0, i, j\rangle + |1\rangle \otimes U_n |i, j\rangle) & \text{if } t = 0 \\ \frac{1}{2^{n+1}}(|1, i, j\rangle + |0\rangle \otimes U_n^\dagger |i, j\rangle) & \text{if } t = 1. \end{cases} \quad (4.9)$$



This also justifies our choice of the pure state used in the numerical calculations in the previous section.

Let us consider now the reduced density matrix

$$\begin{aligned}\sigma_{\bar{\alpha}}^B &\equiv \text{tr}_A[|\psi_{\bar{\alpha}}\rangle\langle\psi_{\bar{\alpha}}|] \\ &= \frac{1}{2^{n+1}} (|j\rangle\langle j| + \text{tr}_A[U_n |i, j\rangle\langle i, j| U_n^\dagger])\end{aligned}\tag{4.10}$$

for  $t = 0$  (for  $t = 1$ ,  $U_n$  and  $U_n^\dagger$  need to be exchanged). For a unitary matrix  $U_n$  randomly chosen according to the Haar measure on  $U(n)$ ,  $U_n |i, j\rangle$  is a random pure state on  $A \otimes B$ . Here, and henceforth  $A$  is the space of the first  $n_A$  qubits without the top qubit. It follows from [43] that the operator

$$Q = \text{tr}_A[U_n |i, j\rangle\langle i, j| U_n^\dagger]\tag{4.11}$$

has rank  $d_A$ . Therefore the rank of  $\sigma_{\bar{\alpha}}^B$  (equivalently, the Schmidt rank  $\chi$  of  $|\psi_{\bar{\alpha}}\rangle$ ) is at least  $2^{n_0}$ . From Eq. (4.5) we conclude that the Schmidt rank of  $\rho$  fulfills  $\chi^\sharp \geq 2^{n_0} \geq 2^{n/5}$ . We can now collate these results into

**Theorem 6.** *Let  $U_n$  be an  $n$ -qubit unitary transformation chosen randomly according to the Haar measure on  $U(2^n)$ , and let  $A : B$  denote a bipartition of  $n + 1$  qubits into  $n_A$  and  $n_B$  qubits, where  $n_0 \equiv \min(n_A, n_B)$ . Then  $n/5 \leq n_0 \leq 2n/5$  and the Schmidt decomposition of  $\rho$  in Eq. (4.4) according to bipartition  $A : B$  fulfills  $\chi^\sharp \geq 2^{n/5}$ .*

We have seen that we cannot efficiently simulate DQC1 with an algorithm that relies on having a TTN for  $\rho$  with low rank  $q$ . However, in order to make this result robust, we need to also show that  $\rho$  cannot be well approximated by another  $\tilde{\rho}$  accepting an efficient TTN. This is what we do next.

We now explore the robustness of the statement of Theorem 6. To this end, we consider the Schmidt rank  $\tilde{\chi}^\sharp$  for a density matrix  $\tilde{\rho}$  that approximates  $\rho$  according to a fidelity  $F(O_1, O_2)$  defined in terms of the natural inner product on the space of

linear operators,

$$F(O_1, O_2) \equiv \text{tr}(O_1^\dagger O_2) / \sqrt{\text{tr}(O_1^\dagger O_1)} \sqrt{\text{tr}(O_2^\dagger O_2)},$$

where  $F = 1$  if and only if  $O_1 = O_2$  and  $F = |\langle \psi_1 | \psi_2 \rangle|^2$  for projectors  $O_i = P_{\psi_i}$  on pure states  $|\psi_i\rangle$ . We will show that if  $\tilde{\rho}$  is close to  $\rho$ , then  $\tilde{\chi}^\sharp$  for a bipartition as in Theorem 1 is also exponential. To prove this, we will require a few lemmas which we now present.

**Lemma 2.** *Let  $|\Psi\rangle$  be a bipartite vector with  $\chi$  terms in its Schmidt decomposition,*

$$|\Psi\rangle = N_\Psi \sum_{i=1}^{\chi} \lambda_i |i_A\rangle |i_B\rangle, \quad \lambda_i \geq \lambda_{i+1} \geq 0, \quad \sum_{i=1}^{\chi} \lambda_i^2 = 1,$$

where  $N_\Psi \equiv \sqrt{\langle \Psi | \Psi \rangle}$ , and let  $|\Phi\rangle$  be a bipartite vector with norm  $N_\Phi$  and Schmidt rank  $\chi'$ , where  $\chi' \leq \chi$ . Then,

$$\max_{|\Phi\rangle} |\langle \Psi | \Phi \rangle| = N_\Psi N_\Phi \sqrt{\sum_{i=1}^{\chi'} \lambda_i^2}. \quad (4.12)$$

*Proof:* Let  $\mu_i$  denote the Schmidt coefficients of  $|\Phi\rangle$ . It follows from Lemma 1 in [78] that  $\max_{|\Phi\rangle} |\langle \Psi | \Phi \rangle| = N_\Psi N_\Phi \sum_{i=1}^{\chi'} \lambda_i \mu_i$ , and the maximization over  $\mu_i$  is done next. A straightforward application of the method of Lagrange multipliers provides us with  $\mu_i = c\lambda_i$ ,  $i = 1, 2, \dots, \chi'$  for some constant  $c$ . Since  $\sum_{i=1}^{\chi'} \mu_i^2 = 1 = c^2 \sum_{i=1}^{\chi'} \lambda_i^2$ ,  $c = 1/\sqrt{\sum_{i=1}^{\chi'} \lambda_i^2}$ . Thus,

$$\max_{|\Phi\rangle} |\langle \Psi | \Phi \rangle| = c N_\Psi N_\Phi \sum_{i=1}^{\chi'} \lambda_i^2,$$

and the result follows.  $\square$

We will also use two basic results related to majorization theory. Recall that, by definition, a decreasingly ordered probability distribution  $\vec{p} = (p_1, p_2, \dots, p_d)$ , where  $p_\alpha \geq p_{\alpha+1} \geq 0$ ,  $\sum_\alpha p_\alpha = 1$ , is *majorized* by another such probability distribution  $\vec{q}$ ,

denoted  $\vec{p} \prec \vec{q}$ , if  $\vec{q}$  is more ordered or concentrated than  $\vec{p}$  (equivalently,  $\vec{p}$  is flatter or more mixed than  $\vec{q}$ ) in the sense that the following inequalities are fulfilled:

$$\sum_{\alpha=1}^k p_{\alpha} \leq \sum_{\alpha=1}^k q_{\alpha} \quad \forall k = 1, \dots, d \quad (4.13)$$

with equality for  $k = d$ . The following result can be found in Exercise II.1.15 of [7]:

**Lemma 3.** *Let  $\rho_{\vec{x}}$  and  $\rho_{\vec{y}}$  be density matrices with eigenvalues given by probability distributions  $\vec{x}$  and  $\vec{y}$ . Let  $\sigma(M)$  denote the decreasingly ordered eigenvalues of hermitian operator  $M$ . Then*

$$\sigma(\rho_{\vec{x}} + \rho_{\vec{y}}) \prec \vec{x} + \vec{y}.$$

The next result follows by direct inspection.

**Lemma 4.** *Let coefficients  $\delta_i$ ,  $1 \leq i \leq d$ , be such that  $-\delta \leq \delta_i \leq \delta$  for some positive  $\delta \leq 1$  and  $\sum_i \delta_i = 1$ , and consider the probability distribution  $\vec{p}(\{\delta_i\})$ ,*

$$\vec{p}(\{\delta_i\}) \equiv \left( \frac{1}{2} + \frac{1 + \delta_1}{2d}, \frac{1 + \delta_2}{2d}, \dots, \frac{1 + \delta_d}{2d} \right).$$

Then

$$\vec{p}(\{\delta_i\}) \prec \vec{p}(\{\delta_i^*\}),$$

where

$$\delta_i^* \equiv \begin{cases} \delta & i \leq d/2 \\ -\delta & i > d/2, \end{cases}$$

and we assume  $d$  to be even.

Finally, we need a result from [43]:

**Lemma 5.** *With probability very close to 1,*

$$\begin{aligned} & \Pr \left[ (1 - \delta) \frac{\Upsilon}{d_A} \leq Q \leq (1 + \delta) \frac{\Upsilon}{d_A} \right] \\ & \geq 1 - \left( \frac{10 d_A}{\delta} \right)^{2d_A} 2^{(-d_B \delta^2 / 14 \ln 2)} \\ & \geq 1 - O \left( \frac{1}{\exp(\delta^2 \exp(n))} \right), \end{aligned} \quad (4.14)$$

where  $d_A = 2^{n_A} = 2^{n_0}$  and  $d_B = 2^{n_B} = 2^{n-n_0+1}$ , and the operator  $Q$  defined in Eq. (4.11) is within a ball of radius  $\delta$  of a (unnormalized) projector  $\Upsilon/d_A$  of rank  $d_A$  [provided  $d_B$  is a large multiple of  $d_A \log d_A/\delta^2$  [43], which is satisfied for large  $n$ , given that  $n/5 \leq n_0 \leq 2n/5$ ].

Our second theorem uses the fact that the Schmidt decomposition of  $\rho$  does not only have exponentially many coefficients, but that these are roughly of the same size.

**Theorem 7.** *Let  $\rho$ ,  $U_n$ , and  $A:B$  be defined as in Theorem 6. If  $F(\rho, \tilde{\rho}) \geq 1 - \epsilon$ , then with probability  $p(\delta, n) = 1 - O(\exp(-\delta^2 \exp(n)))$ , the Schmidt rank for  $\tilde{\rho}$  according to bipartition  $A:B$  satisfies  $\tilde{\chi}^\sharp \geq (1 - 4\epsilon - \delta)2^{n/5}$ .*

*Proof:* For any product vector of Eq. (4.8) we have

$$\begin{aligned} |\langle tij | \rho \tilde{\rho} | tij \rangle| &\leq N_{\tilde{\alpha}} \tilde{N}_{\tilde{\alpha}} \sqrt{\sum_{k=1}^{\tilde{\chi}^\sharp} (\lambda_k^{ij})^2} \\ &\leq N_{\tilde{\alpha}} \tilde{N}_{\tilde{\alpha}} g(\tilde{\chi}^\sharp/d_A), \end{aligned} \quad (4.15)$$

where

$$g(x) \equiv \sqrt{\frac{1 + (1 + \delta)x}{2}}, \quad (4.16)$$

and  $N_{\tilde{\alpha}} \equiv \sqrt{\langle tij | \rho^2 | tij \rangle}$ ,  $\tilde{N}_{\tilde{\alpha}} \equiv \sqrt{\langle tij | \tilde{\rho}^2 | tij \rangle}$ . The first inequality in (4.15) follows from Lemma 1, whereas the second one follows from the fact that the spectrum  $\vec{p}$  of

$$\rho_B \equiv (N_{\tilde{\alpha}})^{-2} \text{tr}_A[\rho | tij \rangle \langle tij | \rho] = \frac{1}{2}(|j \rangle \langle j| + Q),$$

where  $Q$  has all its  $d_A$  non-zero eigenvalues  $q_i$  in the interval  $2^{-n_0}(1 - \delta) \leq q_i \leq$

$2^{-n_0}(1 + \delta)$ , is majorized by  $\vec{p}(\{\delta_i^*\})$ , as follows from Lemmas 2 and 3. Then,

$$\begin{aligned}
1 - \epsilon &\leq \frac{\text{tr} \rho \tilde{\rho}}{\sqrt{\text{tr} \rho^2} \sqrt{\text{tr} \tilde{\rho}^2}} \\
&= \frac{\sum_{\vec{\alpha}} \langle \vec{\alpha} | \rho \tilde{\rho} | \vec{\alpha} \rangle}{\sqrt{\sum_{\vec{\alpha}'} \langle \vec{\alpha}' | \rho^2 | \vec{\alpha}' \rangle \sum_{\vec{\alpha}''} \langle \vec{\alpha}'' | \tilde{\rho}^2 | \vec{\alpha}'' \rangle}} \\
&\leq g(\tilde{\chi}^\# / d_A) \frac{\sum_{\vec{\alpha}} N_{\vec{\alpha}} \tilde{N}_{\vec{\alpha}}}{\sqrt{\sum_{\vec{\alpha}'} (N_{\vec{\alpha}'})^2 \sum_{\vec{\alpha}''} (\tilde{N}_{\vec{\alpha}'})^2}} \\
&\leq g(\tilde{\chi}^\# / d_A),
\end{aligned}$$

where in the last step we have used the Cauchy-Schwarz inequality,  $|\langle x | y \rangle| \leq \sqrt{\langle x | x \rangle} \sqrt{\langle y | y \rangle}$ . The result of the theorem follows from  $g(\tilde{\chi}^\# / 2^{n_0}) \geq 1 - \epsilon$ .  $\square$

## 4.5 Conclusions

The results in this chapter show that the algorithms of [52, 79, 75, 20] are unable to efficiently simulate a DQC1 circuit. The efficiency of a quantum simulation using these algorithms relies on the possibility of efficiently decomposing the state  $\rho$  of the quantum computer using a TTN. We have seen that for the final state of the DQC1 circuit no efficient TTN exists.

It is also interesting to note that the numerics and Theorems 1 and 2 in this chapter can be generalized for any fixed polarization  $\tau$  ( $0 < \tau \leq 1$ ) of the initial state  $\tau|0\rangle\langle 0| + (1 - \tau)\mathbb{I}/2$  of the top qubit of the circuit in Eq (3.1), implying that the algorithms of [52, 79, 75, 20] are also unable to efficiently simulate the power of even the  *tiniest*  fraction of a qubit.

## Chapter 5

# Quantum discord in the DQC1 model

*We are coming now rather into the region of guesswork! Say, rather, into the region where we balance probabilities and choose the most likely. It is the scientific use of imagination, but we always have some material basis on which to start our speculation.*

*-Arthur Conan Doyle in *The Hound of the Baskervilles**

We have seen in the last two chapters (Chapters 3, 4) that the DQC1 model presents to us a very intriguing challenge. It is a mixed-state quantum computation scheme [55] that has very little entanglement [17], yet it cannot be simulated by matrix product state techniques [18]. This suggests that entanglement cannot be the sole resource that drives mixed-state quantum computation. Although in pure state quantum computation entanglement can be shown to be an essential resource [52, 79], mixed-state quantum computation is a different story. It is evident that there is a gap in the resource based accounting for quantum computational speedups. It

is this gap that we hope to fill with the quantum discord [63].

Quantum discord, introduced by Ollivier and Zurek [63], captures the nonclassical correlations, including but not limited to entanglement, that can exist between parts of a quantum system. Some details about quantum discord are presented in Sec 2.2. One way of studying the quantum nature of a computational process is to investigate the nonclassical correlations in the quantum state at various stages during the computation. We investigate the effectiveness of discord in characterizing the performance of the model of quantum information processing introduced by Knill and Laflamme in [55], which is often referred to as the *power of one qubit*, or DQC1. In this model, information processing is performed with a collection of qubits in the completely mixed state coupled to a single control qubit that has some nonzero purity. Such a device can perform efficiently certain computational tasks for which there is no known efficient method using classical information processors.

In this thesis, thus far we have seen how discord can be used to characterize the nonclassical nature of the correlations in quantum states and studied its role and place in quantum information theory. We now apply these ideas to the DQC1 or *power-of-one-qubit* model [55] of mixed-state quantum computation, which accomplishes the task of evaluating the normalized trace of a unitary matrix efficiently. The quantum circuit corresponding to this model has a collection of  $n$  qubits in the completely mixed state,  $I_n/2^n$ , coupled to a single pure control qubit. A generalized version of this quantum circuit, with the control qubit having sub-unity polarization is shown below in Fig 3.1. This circuit evaluates the normalized trace of  $U_n$ ,  $\tau = \text{tr}(U_n)/2^n$ , with a polynomial overhead going as  $1/\alpha^2$ .

The problem of evaluating  $\tau$  is believed to be hard classically. Quantum mechanically, the circuit provides an estimate of  $\tau$  up to a constant accuracy in a number of trials that does not scale exponentially with  $n$ . It does so by making  $X$  and  $Y$  measurements on the top qubit. The averages of the obtained binary values provide estimates for  $\tau_R \equiv \text{Re}(\tau)$  and  $\tau_I \equiv \text{Im}(\tau)$ . The top qubit is completely separable

from the bottom mixed qubits at all times. The final state has vanishingly small entanglement, as measured by the negativity [17] across any split that groups the top qubit with some of the mixed qubits. Nonetheless, there is evidence that the quantum computation performed by this model cannot be simulated efficiently using classical computation [18].

The DQC1 circuit transforms the highly-mixed initial state  $\rho_0 \equiv |0\rangle\langle 0| \otimes I_n/2^n$  into the final state  $\rho_{n+1}$  given by Eq 3.1. Within this model the only place to look for nonclassical correlations is in this state.

Everything about the DQC1 setup, including the measurements on the control qubit, suggests a bipartite split between the control qubit  $M$  and the mixed qubits  $S$ . Relative to this split, we turn to computing the quantum discord for the state  $\rho_{SM} = \rho_{n+1}$ . The joint state  $\rho_{n+1}$  has eigenvalue spectrum

$$\lambda(\rho_{n+1}) = \frac{1}{2^{n+1}} \left( \underbrace{1 - \alpha, \dots, 1 - \alpha}_{2^n \text{ times}}, \underbrace{1 + \alpha, \dots, 1 + \alpha}_{2^n \text{ times}} \right),$$

which gives a joint entropy  $H(S, M) = n + H_2[(1 - \alpha)/2]$ , where  $H_2[\cdot]$  is the binary Shannon entropy. The marginal density matrix for the control qubit at the end of the computation is

$$\rho_M = \frac{1}{2} \begin{pmatrix} 1 & \alpha \tau^* \\ \alpha \tau & 1 \end{pmatrix}, \quad (5.1)$$

which has eigenvalues  $(1 \pm \alpha|\tau|)/2$  and entropy  $H(M) = H_2[(1 - \alpha|\tau|)/2]$ .

The evaluation of the quantum conditional entropy involves a minimization over all possible one-qubit projective measurements. The projectors are given by  $\Pi_{\pm} = \frac{1}{2}(I_1 \pm \mathbf{a} \cdot \boldsymbol{\sigma})$ , with  $\mathbf{a} \cdot \mathbf{a} = a_1^2 + a_2^2 + a_3^2 = 1$ . The post-measurement states are

$$\rho_{S|\pm} = \frac{1}{p_{\pm} 2^{n+1}} \left( I_n \pm \alpha \frac{a_1 - ia_2}{2} U_n \pm \alpha \frac{a_1 + ia_2}{2} U_n^{\dagger} \right), \quad (5.2)$$

occurring with outcome probabilities  $p_{\pm} = [1 \pm \alpha(a_1 \tau_R + a_2 \tau_I)]/2$ . The post-measurement states are independent of  $a_3$ , so without loss of generality, let  $a_3 = 0$ ,  $a_1 = \cos \phi$ , and



$a_2 = \sin \phi$ . The corresponding post-measurement states are

$$\rho_{S|\pm} = \frac{1}{p_{\pm} 2^{n+1}} \left( I_n \pm \alpha \frac{e^{-i\phi} U_n + e^{i\phi} U_n^\dagger}{2} \right). \quad (5.3)$$

To find the discord of the state at the end of the computation, we need the spectrum of  $\rho_{S|\pm}$  so that we can compute  $H(\rho_{S|\pm})$ . The eigenvalues of any unitary operator  $U_n$  are phases of the form  $e^{i\theta_k}$ , so we have

$$\lambda_k \left( \frac{e^{-i\phi} U_n + e^{i\phi} U_n^\dagger}{2} \right) = \cos(\theta_k - \phi), \quad k = 1, \dots, 2^n, \quad (5.4)$$

and

$$\lambda_k(\rho_{S|\pm}) = \frac{1}{2^n} \frac{1 \pm \alpha \cos(\theta_k - \phi)}{1 \pm \alpha(\tau_R \cos \phi + \tau_I \sin \phi)} \equiv q_{k\pm}. \quad (5.5)$$

We also have  $\tau_R = 2^{-n} \sum_k \cos \theta_k$  and  $\tau_I = 2^{-n} \sum_k \sin \theta_k$ . All this gives  $H(\rho_{S|\pm}) = H(\mathbf{q}_{\pm})$  and thus

$$\begin{aligned} \tilde{H}_{\Pi_{\pm}} &= p_+ H(\rho_{S|+}) + p_- H(\rho_{S|-}) \\ &= \frac{1}{2} [H(\mathbf{q}_+) + H(\mathbf{q}_-)] + \frac{\alpha}{2} (\tau_R \cos \phi + \tau_I \sin \phi) [H(\mathbf{q}_+) - H(\mathbf{q}_-)]. \end{aligned} \quad (5.6)$$

We now use the fact that we are interested in the behavior of the quantum discord of the DQC1 state for a typical unitary. By typical, we mean a unitary chosen randomly according to the (left and right invariant) Haar measure on  $\mathbb{U}(2^n)$ . For such a unitary, it is known that the phases  $\theta_k$  are almost uniformly distributed on the unit circle with large probability [21]. Thus for typical unitaries  $\sum_k e^{i\theta_k}$  is close to zero. Hence both  $\tau_R$  and  $\tau_I$  are small, and we can ignore the second term on the right-hand side in Eq. (5.6). In addition, the phases  $\theta_k$  can be taken to be placed at (with large probability) the  $2^n$ th roots of unity, i.e.,  $\theta_k = 2\pi k/2^n$ . It follows that the spectra  $\lambda_k(\rho_{S|\pm})$  are independent of  $\phi$ . Hence the entropies we are interested in computing are also independent of  $\phi$ , and we can set  $\phi$  to zero without loss of generality. This choice for  $\phi$  corresponds to measuring the pure qubit  $M$  along  $X$ .

The  $X$  measurement gives the real part of the normalized trace of  $U_n$ , and it is one of the two measurements discussed in the original proposal by Knill and Laflamme. Setting  $\phi = \pi/2$  yields the other measurement, along  $Y$ , which gives the imaginary part of the normalized trace of  $U_n$ .

In the limit of large  $n$ , we can simplify Eq. (5.6) as follows:

$$\begin{aligned}
\tilde{H} &= \frac{1}{2}[H(\mathbf{q}_+) + H(\mathbf{q}_-)] \\
&= -\frac{1}{2^{n+1}} \sum_{k=1}^{2^n} \left[ (1 + \alpha \cos \theta_k) \log \left( \frac{1 + \alpha \cos \theta_k}{2^n} \right) \right. \\
&\quad \left. + (1 - \alpha \cos \theta_k) \log \left( \frac{1 - \alpha \cos \theta_k}{2^n} \right) \right] \\
&= n - \frac{1}{2^{n+1}} \sum_{k=1}^{2^n} \left[ \log(1 - \alpha^2 \cos^2 \theta_k) + \alpha \cos \theta_k \log \left( \frac{1 + \alpha \cos \theta_k}{1 - \alpha \cos \theta_k} \right) \right]. \quad (5.7)
\end{aligned}$$

Furthermore, when  $n$  is large, we can replace the sum in the above equation with an integral to obtain

$$\begin{aligned}
\tilde{H} &= n - \frac{1}{4\pi} \left[ \int_0^{2\pi} \log(1 - \alpha^2 \cos^2 x) dx + \alpha \int_0^{2\pi} \cos x \log \left( \frac{1 + \alpha \cos x}{1 - \alpha \cos x} \right) dx \right] \\
&= n + 1 - \log \left( 1 + \sqrt{1 - \alpha^2} \right) - \left( 1 - \sqrt{1 - \alpha^2} \right) \log e. \quad (5.8)
\end{aligned}$$

Note that when the sums are replaced by integrals,  $H(\mathbf{q}_+) - H(\mathbf{q}_-) = 0$ , providing further justification for ignoring the second term in Eq. (5.6).

When  $|\tau|$  is small,  $H(M) \simeq 1$ , and the quantum discord for the DQC1 state is then given by the simple expression

$$\mathcal{D}_{\text{DQC1}} = 2 - H_2\left(\frac{1 - \alpha}{2}\right) - \log \left( 1 + \sqrt{1 - \alpha^2} \right) - \left( 1 - \sqrt{1 - \alpha^2} \right) \log e. \quad (5.9)$$

Note that the above expression for the discord, valid for large  $n$ , is independent of  $n$ . Figure 5.1 compares the discord from Eq. (5.9) with the average discord in a DQC1 circuit having five qubits in the mixed state ( $n = 5$ ) coupled to a control qubit

with purity  $\alpha$ . The average is taken over 500 instances of pseudo-random unitary matrices, generated using the efficient algorithm presented in [30]. The convergence of this ensemble to the Haar measure on the unitary group is shown in [28]. We see that in spite of the approximations made in obtaining Eq. (5.9), the analytic expression provides a very good estimate of the discord even when  $n$  is as low as five.

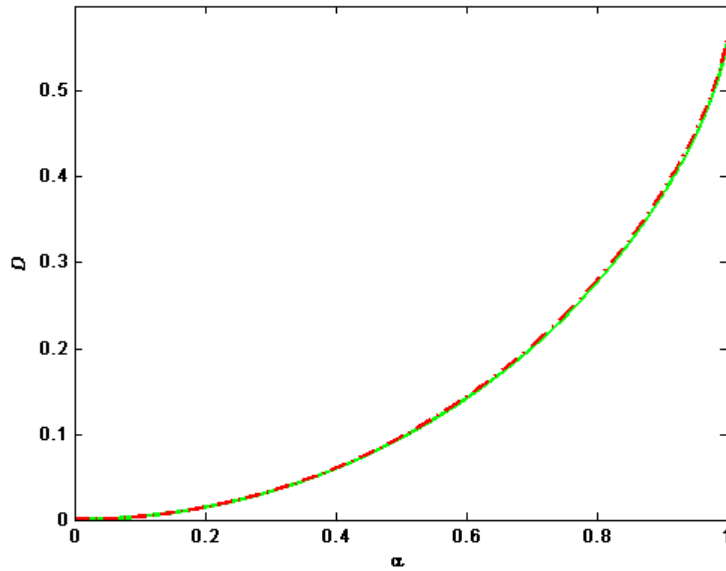


Figure 5.1: The dashed (red) line shows the average discord in a DQC1 circuit with five qubits in the mixed state ( $n = 5$ ) coupled to a qubit with purity  $\alpha$ . The average is taken over 500 instances of pseudo-random unitary matrices. The discord is shown as a function of the purity of the control qubit. The solid (green) line shows the analytical expression in Eq. (5.9), which grows monotonically from 0 at  $\alpha = 0$  (completely mixed control qubit) to  $2 - \log e = 0.5573$  at  $\alpha = 1$  (pure control qubit). These values of discord should be compared with a maximum possible discord of 1 when  $M$  is a single qubit.

There is no entanglement between the control qubit and the mixed qubits in the DQC1 circuit at any point in the computation, yet there are nonclassical correlations, as measured by the discord, between the two parts at the end of the computation

for any  $\alpha > 0$ . Other bipartite splittings of  $\rho_{n+1}$  can exhibit entanglement, but it was shown in [17] that the partial transpose criterion failed to detect entanglement in  $\rho_{n+1}$  for  $\alpha \leq 1/2$ . In this domain, several other tests for entanglement, including the first level of the scheme of Doherty *et al.* [23], which is based on semi-definite programming, also failed to detect entanglement. The above expression is thus the first signature of nonclassical correlations in the DQC1 circuit for  $\alpha \leq 1/2$ .

In conclusion, we calculated the discord in the DQC1 circuit and showed that nonclassical correlations are present in the state at the end of the computation even if there is no detectable entanglement. Thus for some purposes, quantum discord might be a better figure of merit for characterizing the quantum resources available to a quantum information processor. We present evidence of the presence of nonclassical correlations in the DQC1 circuit when  $\alpha \leq 1/2$ . For qubits quantum discord is known to be a true measure of nonclassical correlations [41]. This suggests that nonclassical correlations other than entanglement, as quantified by the discord, might explain the (sometimes exponential) speed-up in the DQC1 circuit and perhaps the speedup in other quantum computational circuits. For pure states, discord becomes a measure of entanglement. Therefore, using discord to connect quantum resources to the advantages offered by quantum information processors has the additional advantage that it works well for both pure- and mixed-state quantum computation.

# Chapter 6

## Conclusion

*If you want a happy ending, that depends, of course, on where you stop your story.*

-Orson Welles

The intent of this chapter is eponymous. The attempt will be to present the results of this thesis in a well-rounded manner, put them all in the perspective of a ‘big picture’, and end with a few suggestions for open problems.

A one line conclusion of this thesis would be the following:

*There is more to quantum information science than just entanglement.*

However, this statement needs qualifications. I presented evidence that entanglement fails to explain exponential speedups in mixed-state quantum computation, at least in the DQC1 model of Knill and Laflamme, the reason being that the amount of entanglement in the system is minimal, not scaling with the system size. This was the content of Chapter 3. Then I showed that this lack of entanglement does not mean that the system is classically simulatable. This is important as the simulation techniques that have their roots in renormalization group theory are very powerful

and among the most versatile in many-body physics. Thus Chapter 4 leaves us with a deep foreboding about the role of entanglement in mixed-state quantum computation and the criterion for classical simulatability of quantum systems that involve entanglement. In Chapter 5, I was able to show that there is a non-trivial amount of quantum discord in the DQC1 circuit. It is thus possible that quantum discord is the resource that drives mixed-state quantum computation.

Quantum discord can be thought of as a generalization of entanglement. For pure states, they are identical. For mixed quantum states, discord captures non-classical correlations beyond entanglement. As I have presented in Section 2.3, the scope of quantum discord is wider than just mixed-state quantum computation. I discussed the role of discord in distribution of entanglement without investing any entanglement.

Every PhD thesis is a compilation of results and solutions to problems that often seem disparate. Yet, it is rarely the case that these problems are not steps towards comprehending a fundamental problem in the field of study. In my case, the results dealt with the DQC1 model, its entanglement content, its classical simulatability or resource behind its exponentially enhanced operation. I also proposed quantum discord as a substitute for entanglement for the role of the resource in mixed-state quantum computation. I also studied how discord seems to be relevant in other information processing tasks and the major part that the DQC1 model can play in bringing together different areas of physics, mathematics and computer science. The fundamental problem I have attempted to attack is the following:

*Is entanglement a key resource for computational power?*

This is what I would call the ‘big picture.’ Jozsa and Linden have spoken most lucidly on this. The answer to this proceeds as follows: The significance of entanglement for pure-state computations is derived from the fact that unentangled pure states of  $n$  qubits have a description involving only  $poly(n)$  parameters (in contrast to  $O(2^n)$

parameters for a general pure state). But this special property of unentangled states (of having a ‘small descriptions’) is contingent on a particular mathematical description, as amplitudes in the computational basis. If we were to adopt some other choice of mathematical description for quantum states (and their evolution), then, although it will be mathematically equivalent to the amplitude description, there will be a different class of states which will now have a polynomially sized description; i.e. two formulations of a theory which are mathematically equivalent (and hence equally logically valid) need not have their corresponding mathematical descriptions of elements of the theory being interconvertible by a polynomially bounded computation. With this in mind we see that the significance of entanglement as a resource for quantum computation is not an intrinsic property of quantum physics itself, but is tied to a particular additional (arbitrary) choice of mathematical formalism for the theory.

Thus, suppose that instead of the amplitude description we choose some other mathematical description  $\mathcal{D}$  of quantum states (and gates). Indeed, there is a rich variety of possible alternative descriptions. Then there will be an associated property of states,  $prop(\mathcal{D})$ , which guarantees that the  $\mathcal{D}$ -description of the quantum computational process grows only polynomially with the number of qubits (e.g. if  $\mathcal{D}$  is the amplitude description, then  $prop(\mathcal{D})$  is just the notion of entanglement). Thus, just as for entanglement, we can equally well claim that  $prop(\mathcal{D})$  for any  $\mathcal{D}$  is an essential resource for quantum-computational speed-up! Entanglement itself appears to have no special status here.

Explicit examples of  $prop(\mathcal{D})$  would include the dimension of the Hilbert space in which the state resides, the purity of a quantum state or the stabilizer formalism and even quantum discord. Thus, in a fundamental sense, the power of quantum computation over classical computation ought to be derived simultaneously from all possible classical mathematical formalisms for representing quantum theory, not any single such formalism and associated quality (such as entanglement), i.e. we have

arrived at the enigmatic prospect of needing a representation of quantum physics that does not single out any particular choice of mathematical formalism.

We now seem to have realized the fundamental problem we ought to be tackling is perhaps too hard to solve. Yet, this should not be a detriment, but rather a challenge to be at least working on the right problem, hard or not. In this thesis, my attempt has been to start chipping at a small corner of this massive monolith. The sculpture is far from being done, but the work has begun.

As is with any work of scientific research, there always remain fairly immediate questions whose answers hold the possibility of further enlightening the topic at hand. This thesis is no exception. There remain open questions that could have been addressed in the course of my research. It is my belief that given enough time and effort, these could be resolved. Some of these concern the DQC1 model, others the nature and properties of quantum discord. As the last segment of this thesis, I sketch some of these prospective problems:

1. **DQC1 and knot theory:** Evaluation of the Jones polynomial of the trace closure of a braid is DQC1 complete. Knot invariants are related to partition functions of the Ising model, and this can be used to find a physical interpretation of the complexity class DQC1. As a continuation of the discussion in Section 2.2, the actual task would be to cast the complexity of approximating partition functions with different boundary conditions as graph theoretic problems whose complexity is well studied.
2. **Classical simulation of quantum systems:** In Chapter 4, I found that the DQC1 system is not efficiently simulatable classically using matrix product states (MPS) which had successfully simulated other quantum systems with little entanglement [77, 85]. It is known that pair entangled projected states (PEPS) can simulate any quantum computation efficiently [70]. My next aim in this regard is to study the simulatability of the DQC1 model using some



intermediate simulation scheme, lying between MPS and PEPS, and if possible, find a measurement-based quantum computation system that emulates DQC1. This will tell us more about the limits of quantum computation and the boundaries of classical computation.

3. **DQC1 and discrete Wigner functions:** Quantum computational speedup has been related to the positivity of discrete Wigner functions [34]. Such Wigner functions  $W$  can be defined so that the only pure states having non-negative  $W$  for all such functions are stabilizer states. Also, the unitaries preserving non-negativity of  $W$  for all definitions of  $W$  in the class form a subgroup of the Clifford group. This means pure states with non-negative  $W$  and their associated unitary dynamics are classical in the sense of admitting an efficient classical simulation scheme using the stabilizer formalism [14]. It is not hard to calculate discrete Wigner functions for mixed states. The hindrance in drawing conclusions similar to the pure state case arises from the non-uniqueness of discrete Wigner functions as they now are defined [35]. One must minimize over all such definitions to draw conclusions about the non-negativity of Wigner functions as is done in [14]. Further thought in this direction might be worthwhile and provide new insights into the power of the DQC1 model.
4. **Computation of quantum discord:** The minimization involved in the computation of quantum discord is non-trivial. It is a minimization of an entropic quantity over the set of POVMS. This quantity can be recast as the Holevo quantity in quantum information theory. We know that the computation of Holevo capacity in general is NP-Hard [4], but the quantum conditional entropy is a very special case. An interesting question would therefore be the complexity of calculating the quantum conditional entropy. More practically, attempts to reduce the minimization to a convex optimization technique, like semi-definite or semi-infinite programming, would be helpful and worthwhile.
5. **Quantum discord in quantum communication:** Beyond the results of

Section 2.3, the most important contribution would be to prove the role of discord in the general protocol of entanglement distribution. The protocol is given in [15], but the challenge is that the general protocol involves a mediating particle which is higher than two dimensional, making the explicit evaluation of discord challenging. In this context, the previous task is related to this one.

The above list is by no means exhaustive. The endeavor has been to present a few problems that I myself have been interested in. These might lead us to understanding certain aspects of the DQC1 model and quantum discord. It is likely that their study would lead to more open problems. All these and many more challenging and profound questions can arise in the study of mixed-state quantum computation and quantum discord.

# Appendices

# Appendix A

## DQC1 and Knot Theory

### A.1 Quadratically Signed Weight Enumerators

A general quadratically signed weight enumerator is of the form

$$S(A, B, x, y) = \sum_{b:Ab=0} (-1)^{b^T B b} x^{|b|} y^{n-|b|},$$

where  $A$  and  $B$  are be matrices over  $\mathbb{Z}_2$  with  $B$  of dimension  $n$  by  $n$  and  $A$  of dimension  $m$  by  $n$ . The variable  $b$  in the summand ranges over column vectors in  $\mathbb{Z}_2$  of dimension  $n$ ,  $b^T$  denotes the transpose of  $b$ ,  $|b|$  is the weight of  $b$  (the number of ones in the vector  $b$ ), and all calculations involving  $A$ ,  $B$  and  $b$  are modulo 2. The absolute value of  $S(A, B, x, y)$  is bounded by  $(|x| + |y|)^n$ . In general, one can consider the computational problem of evaluating these sums. In particular, it is known that for integers  $k, l$ , evaluating  $S(A, B, k, l)$  exactly is  $\#\mathbf{P}$  complete. Now, let  $A$  be square, of size  $n$  by  $n$ , and let  $\overleftarrow{A}$  denote the lower triangular part of  $A$ , which is the matrix obtained from  $A$  by setting to zero all the entries on or above the diagonal. Let  $diag(A)$  denote the diagonal matrix whose diagonal is the same as that of  $A$  and  $\mathbb{I}$  denote the identity matrix. For matrices  $C$  and  $D$  with the same number of columns, let  $[C; D]$  denote the matrix obtained by placing  $C$  above  $D$ .

Then, the following two theorems hold:

**Theorem 8.** *Given  $\text{diag}(A) = \mathbb{I}$ ,  $k, l$  positive integers, and the promise that  $|S(A, \overleftarrow{A}, k, l)| \geq (k^2 + l^2)^{n/2}/2$ , determining the sign of  $S(A, \overleftarrow{A}, k, l)$  is BQP-complete.*

**Theorem 9.** *Given  $\text{diag}(A) = \mathbb{I}$ ,  $k, l$  positive integers, and the promise that  $|S([A; A^T], \overleftarrow{A}, k, l)| \geq (k^2 + l^2)^{n/2}/2$ , the sign of  $S([A; A^T], \overleftarrow{A}, k, l)$  can be efficiently determined by the DQC1 model.*

In these two problems, the integers  $k$  and  $l$  can be restricted to 4 and 3, respectively, without affecting their hardness with respect to polynomial reductions (using classical deterministic algorithms). Note that in the second one, the question of DQC1 completeness is still open.

Lidar has made the first connection between QSWEs and partition functions of spin models on certain classes of graphs. In that case,  $A$  denotes the adjacency matrix of the relevant graph. Though these classes are highly restricted at the present, attempts at broadening their scope are ongoing. Through the connection to QSWEs, DQC1 can be applied to analyze problems in coding theory, like weight generating functions of binary codes. Studying the complexity of such problems will certainly give us a better understanding of the complexity classes P, BQP, and DQC1 and their relative inclusions. QSWEs relate the DQC1 model to Ising model partition functions in a way entirely independent from that to be outlined in Section A.2. On the other hand, as shown in Fig 1.2, the DQC1 model can be employed to tackle problems in graph and knot theory, disciplines that have provided scores of problems for theoretical computer science in general and quantum computation in particular. Identifying problems that are DQC1 complete and studying them in relation to BQP, P and NP complete graph and knot theoretic problems might unravel the underlying mathematical structures that separate P, BQP, DQC1. Such an understanding might illuminate greatly the mathematical framework behind the power of quantum computation, just as studying the complexity of partition functions might unravel

the physical foundations for that power. The diagram in Fig 1.2 outlines prospective avenues for exploring such problems in the context of mixed-state quantum computation, and has the potential of opening up whole new paradigms in mixed-state quantum computation research.

## A.2 Jones Polynomials

It has been known for quite some time that evaluating the partition functions of certain spin models, like the Ising model, is related to knot invariants, in particular, the Jones polynomial [81]. This is independent of the connections arrived at via Kauffman brackets and QSWEs [59, 56] as we discussed in Appendix A. The difference between trace and plat closure is in the way the ends of the braids are joined to make a knot. This has a counterpart in the physical world. Plat closures correspond to open boundary conditions, while trace closures correspond to periodic boundary conditions [50]. The partition function of a system depends on its boundary conditions. Therefore, one would expect that its evaluation would behave analogously. Of course, when we talk of evaluation, we actually mean approximation to its true value with a reasonable accuracy. The notion of ‘reasonable accuracy’ is a fairly technical one. Put simply, we aim for an approximation whose error scales only polynomially with the problem size. The exact evaluation of partition function of the Ising model on a general graph is  $\#\mathbf{P}$ -hard even when all the interactions are unity and there are no external magnetic fields [81]. We believe that the exact evaluation of the normalized trace of a unitary is  $\#\mathbf{P}$ -complete (See Section 3.1). As the DQC1 model provides a polynomial algorithm for an approximate solution to this hard problem, it might be possible to approximate partition functions through the DQC1 algorithm and uncover physical reasons for the success of the power of one qubit model.

# Appendix B

## Proof of the Lemma

**Lemma:**  $\text{tr}(\check{A}\check{B}) = \text{tr}(AB)$ .

**Proof:** Define two operators  $A$  and  $B$  by

$$A = \sum_{i,j,k,l} a_{ij,kl} |ij\rangle\langle kl| , \quad B = \sum_{m,n,p,q} b_{mn,pq} |mn\rangle\langle pq| . \quad (\text{B.1})$$

Taking the partial transpose with respect to the second subsystem, we find

$$\check{A} = \sum_{i,j,k,l} a_{ij,kl} |il\rangle\langle kj| , \quad \check{B} = \sum_{m,n,p,q} b_{mn,pq} |mq\rangle\langle pn| . \quad (\text{B.2})$$

Calculating the quantities of interest, we find that they are indeed equal.

$$\text{tr}(\check{A}\check{B}) = \sum_{\substack{i,j,k,l, \\ m,n,p,q}} a_{ij,kl} b_{mn,pq} \langle pn|il\rangle \langle kj|mq\rangle = \sum_{i,j,k,l} a_{ij,kl} b_{kl,ij} , \quad (\text{B.3})$$

$$\text{tr}(AB) = \sum_{\substack{i,j,k,l, \\ m,n,p,q}} a_{ij,kl} b_{mn,pq} \langle pq|ij\rangle \langle kl|mn\rangle = \sum_{i,j,k,l} a_{ij,kl} b_{kl,ij} . \quad (\text{B.4})$$

## Appendix C

### Negativity of a random pure state

An eigenvector of a random  $n$ -qubit unitary can be considered to be a random pure state in the Hilbert space of  $n$ -qubits,  $\mathcal{H}$ . Any such state can be Schmidt decomposed for a given bipartition  $\mathcal{H}_A \otimes \mathcal{H}_B$  with dimensions  $\mu$  and  $\nu$  ( $\mu \leq \nu$ ) and the distribution of the Schmidt coefficients is given by (for  $\mu = \nu$ )

$$P(\mathbf{p})d\mathbf{p} = N\delta(1 - \sum_{i=1}^{\mu} p_i) \prod_{1 \leq i < j \leq \mu} (p_i - p_j)^2 \prod_{k=1}^{\mu} d\mathbf{p}_k. \quad (\text{C.1})$$

Since the negativity for pure states is

$$\mathcal{N} = \left( \sum_{i=1}^{\mu} \sqrt{p_i} \right)^2 = 1 + \sum_{\substack{i,j=1 \\ i \neq j}}^{\mu} \sqrt{p_i p_j} \quad (\text{C.2})$$

$$\langle \mathcal{N} \rangle = 1 + \int \sum_{\substack{i,j=1 \\ i \neq j}}^{\mu} \sqrt{p_i p_j} P(\mathbf{p}) d\mathbf{p}. \quad (\text{C.3})$$

At this point, it helps to change variables such that  $p_i = r q_i$  which removes the hurdle of integrating over the probability simplex, whereby

$$Q(\mathbf{q})d\mathbf{q} \equiv \prod_{1 \leq i < j \leq \mu} (q_i - q_j)^2 \prod_{k=1}^{\mu} e^{-q_k} dq_k = N e^{-r} r^{\mu\nu-1} P(\mathbf{p}) d\mathbf{p} dr. \quad (\text{C.4})$$



The new variables  $q_i$  take on values independently in the range  $[0, \infty)$ . Integrating over all the values of the new variables, we find that the normalization constant is given by  $N = \bar{Q}/\Gamma(\mu\nu)$ , where  $\bar{Q} \equiv \int Q(\mathbf{q})d\mathbf{q}$ . Similarly, we find that

$$\int \sqrt{q_i q_j} Q(\mathbf{q}) d\mathbf{q} = \bar{Q} \frac{\Gamma(\mu^2 + 1)}{\Gamma(\mu^2)} \int \sqrt{p_i p_j} P(\mathbf{p}) d\mathbf{p}. \quad (\text{C.5})$$

Notice that the first product in Eq. (C.4) is the square of the Van der Monde determinant [72, 73]

$$\Delta(\mathbf{q}) \equiv \prod_{1 \leq i < j \leq \mu} (q_i - q_j) = \begin{vmatrix} 1 & \dots & 1 \\ q_1 & \dots & q_\mu \\ \vdots & \ddots & \vdots \\ q_1^{\mu-1} & \dots & q_\mu^{\mu-1} \end{vmatrix} = \begin{vmatrix} r_0^\alpha(q_1) & \dots & r_0^\alpha(q_\mu) \\ r_1^\alpha(q_1) & \dots & r_1^\alpha(q_\mu) \\ \vdots & \ddots & \vdots \\ r_{\mu-1}^\alpha(q_1) & \dots & r_{\mu-1}^\alpha(q_\mu) \end{vmatrix}. \quad (\text{C.6})$$

The second determinant in Eq. (C.6) follows from the basic property of invariance after adding a multiple of one row to another, with  $\alpha \equiv \nu - \mu$  and the polynomials  $r_k^\alpha(q) \equiv k! L_k^\alpha(q)$  judiciously chosen to be rescaled Laguerre polynomials [36], satisfying the recursion relation

$$r_k^\alpha(q) = r_k^{\alpha+1}(q) - k r_{k-1}^{\alpha+1}(q) = \sum_{i=0}^j (-1)^i \binom{j}{i} k(k-1) \dots (k-i+1) r_{k-i}^{\alpha+j}(q), \quad (\text{C.7})$$

and having the orthogonality property

$$\int_0^\infty dq e^{-q} q^\alpha r_k^\alpha(q) r_l^\alpha(q) = \Gamma(k+1) \Gamma(\alpha+k+1) \delta_{kl}. \quad (\text{C.8})$$

These facts in hand, we can evaluate

$$\begin{aligned}
 \bar{Q} &= \int \Delta(\mathbf{q})^2 \prod_{k=1}^{\mu} e^{-q_k} q_k^{\alpha} dq_k \\
 &= \sum_{\substack{i_1, \dots, i_{\mu} \\ j_1, \dots, j_{\mu}}} \epsilon_{i_1 \dots i_{\mu}} \epsilon_{j_1 \dots j_{\mu}} \prod_{k=1}^{\mu} \int dq_k e^{-q_k} q_k^{\alpha} r_{i_k-1}^{\alpha}(q_k) r_{j_k-1}^{\alpha}(q_k) \\
 &= \sum_{i_1, \dots, i_{\mu}} \epsilon_{i_1 \dots i_{\mu}}^2 \prod_{k=1}^{\mu} \Gamma(i_k) \Gamma(\alpha + i_k) \\
 &= \mu! \prod_{k=1}^{\mu} \Gamma(k) \Gamma(\alpha + k). \tag{C.9}
 \end{aligned}$$

For  $\mu = \nu$ ,  $\alpha = 0$  and we can simplify the algebra considerably. Under these conditions,

$$\sum_{\substack{i, j=1 \\ i \neq j}}^{\mu} \int \sqrt{q_i q_j} Q(\mathbf{q}) d\mathbf{q} = \bar{Q} \sum_{k, l=0}^{\mu-1} \left[ I_{kk}^{(1/2)} I_{ll}^{(1/2)} - \left( I_{kl}^{(1/2)} \right)^2 \right], \tag{C.10}$$

where

$$I_{kl}^{(1/2)} \equiv \int_0^{\infty} e^{-q} \sqrt{q} L_k(q) L_l(q) dq. \tag{C.11}$$

We thus have

$$\langle \mathcal{N} \rangle = 1 + \frac{1}{\mu^2} \sum_{k, l=0}^{\mu-1} \left[ I_{kk}^{(1/2)} I_{ll}^{(1/2)} - \left( I_{kl}^{(1/2)} \right)^2 \right], \tag{C.12}$$

except that the integral needs to be evaluated. For that, we use the generating function for Laguerre polynomials<sup>1</sup> [36]

$$(1 - z)^{-1} e^{xz/z-1} = \sum_{l=0}^{\infty} L_l(x) z^l \quad |z| \leq 1, \tag{C.13}$$

and

$$\int_0^{\infty} e^{-st} t^{\beta} L_n^{\alpha}(t) dt = \frac{\Gamma(\beta + 1) \Gamma(\alpha + n + 1)}{n! \Gamma(\alpha + 1)} s^{-\beta-1} F\left(-n, \beta + 1; \alpha + 1, \frac{1}{s}\right), \tag{C.14}$$

---

<sup>1</sup>I thank C. Chandler for reminding me this trick.

$F$  being the hypergeometric function such that

$$F(a, b; c; z) = \sum_{n=0}^{\infty} \frac{(a)_n (b)_n}{(c)_n} \frac{z^n}{n!}, \quad (\text{C.15})$$

and  $(a)_n = a(a+1)(a+2)\dots(a+n-1)$  is the Pochhammer symbol. Note that if  $a$  is a negative integer,  $(a)_n = 0$  for  $n > |a|$  and the hypergeometric series terminates.

Then,

$$\begin{aligned} \sum_{l=0}^{\infty} I_{kl}^{(1/2)} z^l &= \int_0^{\infty} e^{-x} \sqrt{x} L_k(x) (1-z)^{-1} e^{xz/z-1} dx \\ &= s \int_0^{\infty} e^{-sx} \sqrt{x} L_k(x) dx \quad s = 1/(1-z) \\ &= s \left[ \frac{\Gamma(3/2) \Gamma(k+1)}{k! \Gamma(1)} \right] s^{-3/2} F\left(-k, \frac{3}{2}; 1; \frac{1}{s}\right) \\ &= \frac{\sqrt{\pi}}{2} \sum_{t=0}^k \frac{(-k)_t (3/2)_t}{(1)_t} \frac{1}{t!} (1-z)^{t+1/2} \\ &= \frac{\sqrt{\pi}}{2} \sum_{l=0}^{\infty} \sum_{t=0}^k \frac{(-1)^l}{l!} \frac{(-k)_t (3/2)_t}{(t!)^2} \left(t + \frac{1}{2}\right)_l z^l, \end{aligned} \quad (\text{C.16})$$

whereby

$$I_{kl}^{(1/2)} = \frac{\sqrt{\pi}}{2} \frac{(-1)^l}{l!} \sum_{t=0}^k \frac{(-k)_t (3/2)_t}{(t!)^2} \left(t + \frac{1}{2}\right)_l, \quad (\text{C.17})$$

and  $(a)_{\underline{n}} = a(a-1)(a-2)\dots(a-n+1)$  is the ‘falling factorial’. Using the following identities for the Pochhammer symbols

$$(x)_{\underline{n}} = (-1)^n (-x)_n, \quad (\text{C.18a})$$

$$(-x)_n = (-1)^n (x-n+1)_n, \quad (\text{C.18b})$$

$$(x)_n = \Gamma(x+n)/\Gamma(x), \quad (\text{C.18c})$$

we have

$$\begin{aligned}
 I_{kl}^{(1/2)} &= \frac{(-1)^l}{l!} \sum_{t=0}^k \binom{k}{t} \frac{[\Gamma(t + 3/2)]^2}{t! \Gamma(t - l + 3/2)} \\
 &= \frac{\pi}{4} \frac{(-1)^l}{\Gamma[\frac{3}{2} - l] l!} {}_3F_2 \left( \frac{3}{2}, \frac{3}{2}, -k; 1, \frac{3}{2} - l; 1 \right).
 \end{aligned} \tag{C.19}$$

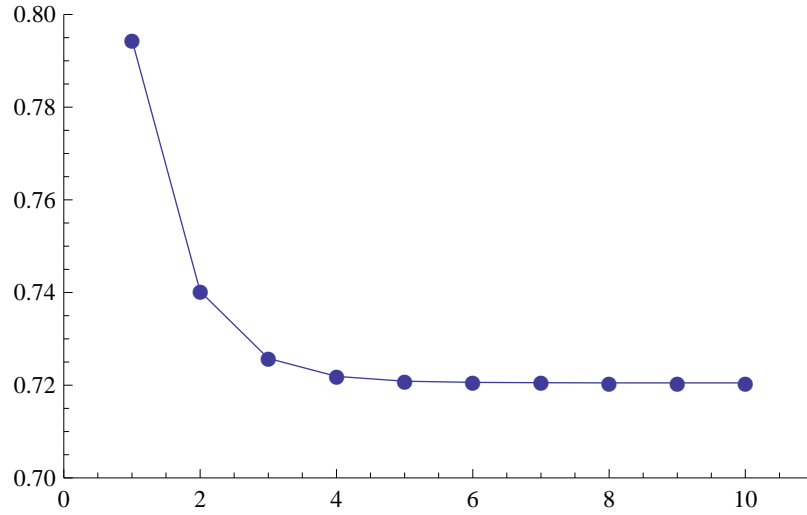


Figure C.1: The value of the normalized negativity  $\langle \mathcal{N} \rangle / 2^{n/2}$  of a random (Haar-distributed) pure state

To get the final expression for the negativity in Eq C.12, we substitute the expression for the integrals from Eq C.19. The expressions are not very illuminating, and for the lack of an asymptotic expression, we plot the numerical value in Fig C.1. As we see, the negativity also scales exponentially with the system size in the asymptotic limit. In fact, it goes as a constant multiple (0.720507) of the maximum possible negativity, just as the Schmidt rank of the DQC1 circuit that has a random unitary in it.

## References

- [1] D. Aharonov, V. F. R. Jones, and Z. Landau. A polynomial quantum algorithm for approximating the Jones polynomial. In *STOC*, page 427, 2006.
- [2] A. Ambainis, L. J. Schulman, and U. V. Vazirani. Computing with highly mixed states. In *STOC*, page 697, 2000.
- [3] S. Arnborg, D. G. Corneil, and A. Proskurowski. Complexity of finding embeddings in a  $k$ -tree. *SIAM Journal on Algebraic and Discrete Methods*, 8:277, 1987.
- [4] S. Beigi and P. W. Shor. On the complexity of computing zero-error and Holevo capacity of quantum channels. *arXiv:0709.2090*, 2007.
- [5] C. H. Bennett and G. Brassard. Quantum cryptography: Public key distribution and coin tossing. *Proceedings of IEEE International Conference on Computers, Systems and Signal Processing, New York*, page 175, 1984.
- [6] C. H. Bennett, D. P. DiVincenzo, C. A. Fuchs, T. Mor, E. Rains, P. W. Shor, J. A. Smolin, and W. K. Wootters. Quantum nonlocality without entanglement. *Phys. Rev. A*, 59:1070, 1999.
- [7] R. Bhatia. *Matrix Analysis*. Springer-Verlag, New York, 1997.
- [8] S. Boixo and R. Somma. Parameter estimation with mixed state quantum computation. *Phys. Rev. A*, 77:052320, 2008.
- [9] S. L. Braunstein, C. M. Caves, R. Jozsa, N. Linden, S. Popescu, and R. Schack. Separability of very noisy mixed states and implications for nmr quantum computing. *Phys. Rev. Lett.*, 83:1054, 1999.
- [10] S. Bravyi and A. Kitaev. Universal quantum computation with ideal Clifford gates and noisy ancillas. *Phys. Rev. A*, 71:022316, 2005.

- [11] N. Brunner, N. Gisin, and V. Scarani. Entanglement and non-locality are different resources. *New J. Phys.*, 7:88, 2005.
- [12] N. J. Cerf and C. Adami. Quantum extension of conditional probability. *Phys. Rev. A*, 60:893, 1999.
- [13] J. Conway. *A Course in Functional Analysis*. Springer-Verlag, New York, 1990.
- [14] C. Cormick, E. F. Galvao, D. Gottesman, J. P. Paz, and A. O. Pittenger. Classicality in discrete Wigner functions. *Phys. Rev. A*, 73:012301, 2006.
- [15] T. S. Cubitt, F. Verstraete, W. Dür, and J. I. Cirac. Separable states can be used to distribute entanglement. *Phys. Rev. Lett.*, 91:037902, 2003.
- [16] G. M. D'Ariano, P. L. Presti, and P. Perinotti. Classical randomness in quantum measurements. *J. Phys. A: Math. Gen.*, 38:5979, 2005.
- [17] A. Datta, S. T. Flammia, and C. M. Caves. Entanglement and the power of one qubit. *Phys. Rev. A*, 72:042316, 2005.
- [18] A. Datta and G. Vidal. Role of entanglement and correlations in mixed-state quantum computation. *Phys. Rev. A*, 75:042310, 2007.
- [19] C. M. Dawson, H. L. Haselgrove, A. P. Hines, D. Mortimer, M. A. Nielsen, and T. J. Osborne. Quantum computing and polynomial equations over the finite field  $\mathbb{Z}_2$ . *Quantum Inf. Comput.*, 5:102, 2005.
- [20] M. Van den Nest, W. Dür, G. Vidal, and H. J. Briegel. Classical simulation versus universality in measurement-based quantum computation. *Phys. Rev. A*, 75:012337, 2006.
- [21] P. Diaconis. Patterns in eigenvalues: The 70<sup>th</sup> Josiah Willard Gibbs lecture. *Bull. Amer. Math. Soc.*, 40:155, 2003.
- [22] D. DiVincenzo. The physical implementation of quantum computation. *Fortschr. Phys.*, 48:771, 2000.
- [23] A. C. Doherty, P. A. Parrilo, and F. M. Spedalieri. Complete family of separability criteria. *Phys. Rev. A*, 69:022308, February 2004.
- [24] W. Dür, J. I. Cirac, and R. Tarrach. Separability and distillability of multiparticle quantum systems. *Phys. Rev. Lett.*, 83:3562, 1999.
- [25] A. Ehrenfeucht and M. Karpinski. The computational complexity of (XOR, AND)- counting problems. *International Computer Science Institute, Berkeley, CA*, (available online at <http://www.citeseer.com>):Technical Report tr-90-033, 1990.

- [26] A. Ekert and R. Jozsa. Quantum computation and shor's factoring algorithm. *Rev. Mod. Phys.*, 68:733, 1996.
- [27] A. Ekert and R. Jozsa. Quantum algorithms: Entanglement-enhanced information processing and discussion. *Philos. Trans. R. Soc. London A*, 356:1769–1782, 1998.
- [28] J. Emerson, E. Livine, and S. Lloyd. Convergence conditions for random quantum circuits. *Phys. Rev. A*, 72:060302, 2005.
- [29] J. Emerson, S. Lloyd, D. Poulin, and D. Cory. Estimation of the local density of states on a quantum computer. *Phys. Rev. A*, 69:050305, 2004.
- [30] J. Emerson, Y. S. Weinstein, M. Saraceno, S. Lloyd, and D. G. Cory. Pseudo-random unitary operators for quantum information processing. *Science*, 302:2098, 2003.
- [31] M. H. Freedman, A. Kitaev, M. Larsen, and Z. Wang. Topological quantum computation- mathematical challenges of the 21st century. *Bull. Amer. Math. Soc.*, 40:31, 2003.
- [32] M. H. Freedman, A. Kitaev, and Z. Wang. Simulation of topological field theories by quantum computers. *Commun. Math. Phys.*, 227:587, 2002.
- [33] M. H. Freedman, M. Larsen, and Z. Wang. A modular functor which is universal for quantum computation. *Commun. Math. Phys.*, 227:605, 2002.
- [34] E. F. Galvao. Discrete Wigner functions and quantum computational speedup. *Phys. Rev. A*, 71:042302, 2005.
- [35] K. S. Gibbons, M. J. Hoffman, and W. K. Wootters. Discrete phase space based on finite fields. *Phys. Rev. A.*, 70:062101, 2004.
- [36] I. S. Gradshteyn and I. M. Ryzhik. *Table of Integrals, Series and Products*. Academic Press, New York, 1980.
- [37] B. Groisman, S. Popescu, and A. Winter. Quantum, classical, and total amount of correlations in a quantum state. *Phys. Rev. A.*, 72:032317, 2005.
- [38] L. Gurvits. Classical deterministic complexity of edmonds' problem and quantum entanglement. In *STOC*, pages 10–19, 2003.
- [39] L. Gurvits and H. Barnum. Separable balls around the maximally mixed multipartite quantum states. *Phys. Rev. A.*, 68:042312, 2003.
- [40] L. Gurvits and H. Barnum. Better bound on the exponent of the radius of the multipartite separable ball. *Phys. Rev. A.*, 72:032322, 2005.

- [41] S. Hamieh, R. Kobes, and H. Zaraket. Positive-operator-valued measure optimization of classical correlations. *Phys. Rev. A*, 70:052325–6, 2004.
- [42] P. Hayden, R. Jozsa, D. Petz, and A. Winter. Structure of states which satisfy strong subadditivity of quantum entropy with equality. *Commun. Math. Phys.*, 246, 2004.
- [43] P. Hayden, D.W. Leung, and A. Winter. Aspects of generic entanglement. *Commun. Math. Phys.*, 265, 2006.
- [44] L. Henderson and V. Vedral. Classical, quantum and total correlations. *J. Phys. A: Math. Gen.*, 34:6899, 2001.
- [45] M. Horodecki, P. Horodecki, and R. Horodecki. Separability of mixed states: Necessary and sufficient conditions. *Phys. Lett. A.*, 223, 1996.
- [46] M. Horodecki, P. Horodecki, R. Horodecki, J. Oppenheim, A. Sen(De), U. Sen, and B. Synak-Radtke. Local versus nonlocal information in quantum-information theory: Formalism and phenomena. *Phys. Rev. A*, 71:062307, 2005.
- [47] P. Horodecki. Separability criterion and inseparable mixed states with positive partial transposition. *Phys. Lett. A*, 232:333, 1997.
- [48] R. Horodecki, P. Horodecki, M. Horodecki, and K. Horodecki. Quantum entanglement. *arXiv:0702225*, 2007.
- [49] J. A. Jones. NMR quantum computation. *Prog. Nucl. Magn. Reson. Spectrosc.*, 38, 2001.
- [50] V. F. R. Jones. On knot invariants related to some statistical mechanics models. *Pacific Journal of Mathematics*, 137, 1989.
- [51] S. Jordan and P. W. Shor. Estimating jones polynomials is a complete problem for one clean qubit. *Quantum Inf. Comput.*, 8:681, 2008.
- [52] R. Jozsa and N. Linden. On the role of entanglement in quantum-computational speed-up. *Proc. Roy. Soc. A*, 459:2011–2032, 2003.
- [53] V. M. Kendon and W. J. Munro. Entanglement and its role in shor’s algorithm. *Quantum Inform. Comput.*, 6:630–640, 2006.
- [54] D. Kenigsberg, T. Mor, and G. Ratsaby. Quantum advantage without entanglement. *Quantum Inform. Comput.*, page 606, 2006.
- [55] E. Knill and R. Laflamme. Power of one bit of quantum information. *Phys. Rev. Lett.*, 81:5672, 1998.



- [56] E. Knill and R. Laflamme. Quantum computing and quadratically signed weight enumerators. *Information Processing Letters*, 79:173, 2001.
- [57] R. Laflamme, D. G. Cory, C. Negrevegne, and L. Viola. Nmr quantum information processing and entanglement. *Quantum Inf. Comput.*, 2:166, 2002.
- [58] S. Lee, D. P. Chi, S. D. Oh, and J. Kim. Convex-roof extended negativity as an entanglement measure for bipartite quantum systems. *Phys. Rev. A*, 68:062304, 2003.
- [59] D. A. Lidar. On the quantum computational complexity of the ising spin glass partition function and of knot invariants. *New Journal of Physics*, 6:167, 2004.
- [60] I. L. Markov and Y.-Y Shi. Simulating quantum computation by contracting tensor networks. *arXiv:0511069*, 2005.
- [61] L. Masanes. All bipartite entangled states are useful for information processing. *Phys. Rev. Lett.*, 96:150501, 2006.
- [62] M. A. Nielsen and I. L. Chuang. *Quantum Computation and Quantum Information*. Cambridge Univ. Press, 2000.
- [63] H. Ollivier and W. H. Zurek. Quantum discord: A measure of the quantumness of correlations. *Phys. Rev. Lett.*, 88:017901, 2002.
- [64] A. Peres. Separability criterion for density matrices. *Phys. Rev. Lett.*, 77:1413, 1996.
- [65] M. B. Plenio. The logarithmic negativity: A full entanglement monotone that is not convex. *Phys. Rev. Lett.*, 95:090503, 2005.
- [66] D. Poulin, R. Blume-Kohout, R. Laflamme, and H. Ollivier. Exponential speedup with a single bit of quantum information: Measuring the average fidelity decay. *Phys. Rev. Lett.*, 92:177906, 2004.
- [67] D. Poulin, R. Laflamme, G. J. Milburn, and J. P. Paz. Testing integrability with a single bit of quantum information. *Phys. Rev. A*, 68:022302, 2003.
- [68] M. Poźniak, K. Życzkowski, and M. Kús. Composed ensembles of random unitary matrices. *J. Phys. A: Math. Gen.*, 31, 1998.
- [69] E. Schrödinger. Die gegenwärtige situation in der quantenmechanik. *Naturwissenschaften*, 23:807, 1935.
- [70] N. Schuch, M. M. Wolf, F. Verstraete, and J. I. Cirac. Computational complexity of projected entangled pair states. *Phys. Rev. Lett.*, 98:140506, 2007.

- [71] L. J. Schulman and U. V. Vazirani. Molecular scale heat engines and scalable quantum computation. In *STOC*, page 322, 1999.
- [72] A. J. Scott and C. M. Caves. Entangling power of the quantum baker's map. *J. Phys. A: Math. Gen.*, 36:9553, 2003.
- [73] S. Sen. Average entropy of a quantum subsystem. *Phys. Rev. Lett.*, 77:1, 1996.
- [74] D. Shepherd. Computing with unitaries and one pure qubit. *arXiv:quant-ph/0608132*, 2006.
- [75] Y.-Y. Shi, L.-M. Duan, and G. Vidal. Classical simulation of quantum many-body systems with a tree tensor network. *Phys. Rev. A*, 74:022320, 2006.
- [76] S.Luo. Using measurement-induced disturbance to characterize correlations as classical or quantum. *Phys. Rev. A*, 77:022301, 2008.
- [77] G. Vidal. Efficient classical simulation of slightly entangled quantum computations. *Phys. Rev. Lett.*, 91:147902, 2003.
- [78] G. Vidal, D. Jonathan, and M. A. Nielsen. Approximate transformations and robust manipulation of bipartite pure-state entanglement. *Phys. Rev. A*, 62:012304, 2000.
- [79] G. Vidal, J. I. Latorre, E. Rico, and A. Kitaev. Entanglement in quantum critical phenomena. *Phys. Rev. Lett.*, 90:227902, 2003.
- [80] G. Vidal and R. Werner. Computable measure of entanglement. *Phys. Rev. A.*, 65:032314, 2002.
- [81] D. J. A. Welsh. *Complexity: Knots, Colorings and Counting*. London Mathematical Society Lecture Note Series 186. Cambridge Univ. Press, 1993.
- [82] P. Wocjan and J. Yard. The jones polynomial: Quantum algorithms and applications in quantum complexity theory. *Quantum Inf. Comput.*, 8:147, 2008.
- [83] J. A. Wyler. Rasputin, science, and the transmogrification of destiny. *Gen. Relativ. Gravit.*, 5:175, 1974.
- [84] W. H. Zurek. Quantum discord and Maxwell's demons. *Phys. Rev. A*, 67:012320, 2003.
- [85] M. Zwolak and G. Vidal. Mixed-state dynamics in one-dimensional quantum lattice systems: A time-dependent superoperator renormalization algorithm. *Phys. Rev. Lett.*, 93:207205, 2004.